



Oscillatory Coupling between Basal Ganglia, Cortex and Muscle in Parkinson's Disease

Inaugural-Dissertation

zur Erlangung des Doktorgrades
der Mathematisch-Naturwissenschaftlichen Fakultät
der Heinrich-Heine-Universität Düsseldorf

vorgelegt von

Jan Hirschmann

aus Göttingen

Düsseldorf, Februar 2014

Aus dem Institut für Klinische Neurowissenschaften
und Medizinische Psychologie
der Heinrich-Heine-Universität Düsseldorf

Gedruckt mit der Genehmigung der
Mathematisch-Naturwissenschaftlichen Fakultät der
Heinrich-Heine-Universität Düsseldorf

Referent: Prof. Dr. Alfons Schnitzler

Korreferent: Prof. Dr. Tobias Kalenscher

Tag der mündlichen Prüfung: 10.12.2013

TABLE OF CONTENTS

GLOSSARY	5
ZUSAMMENFASSUNG	6
SUMMARY	8
1 INTRODUCTION	11
1.1 Non-invasive measurement of neuronal oscillations	11
1.2 Analysis of neuronal oscillations	12
1.2.1 Spectral analysis	12
1.2.2 Source reconstruction	13
1.3 The basal ganglia	14
1.3.1 Anatomy	14
1.3.2 Function.....	17
1.4 Parkinson's disease	17
1.4.1 Symptoms	18
1.4.2 Pathogenesis	18
1.4.3 Pathophysiology according to the classical rate model.....	19
1.4.4 Treatment.....	20
1.5 Oscillations in Parkinson's disease	22
1.5.1 Alpha oscillations.....	22
1.5.2 Beta oscillations	23
1.5.3 Gamma and high frequency oscillations	23
2 AIMS	25
3 PARADIGM	26
4 STUDY 1: Distinct oscillatory STN-cortical loops revealed by simultaneous MEG and local field potential recordings in patients with Parkinson's disease	27
4.1 Methods	28
4.2 Results	28

4.2.1	Distribution of STN-cortical coherence across brain areas	28
4.2.2	Distribution of STN-STG and STN-M1 coherence across electrode contacts	29
4.3	Discussion	29
4.4	Conclusions	30
5	STUDY 2: Differential modulation of STN-cortical and cortico-muscular coherence by movement and levodopa in Parkinson's disease	30
5.1	Methods	31
5.2	Results.....	32
5.2.1	Effects of movement and medication.....	32
5.2.2	Correlation with clinical parameters	32
5.3	Discussion	32
5.4	Conclusions	34
6	STUDY 3: A direct relationship between oscillatory STN-cortex coupling and rest tremor in Parkinson's disease	35
6.1	Methods	36
6.2	Results.....	36
6.2.1	Sensor level	36
6.2.2	Source level	36
6.3	Discussion	37
6.4	Conclusions	38
7	GENERAL DISCUSSION	38
8	OUTLOOK.....	39
9	REFERENCES.....	41
10	ERKLÄRUNG.....	48
11	DANKSAGUNG.....	49
12	APPENDIX	50

Glossary

EEG	electroencephalography
MEG	magnetoencephalography
SQUID	superconductive quantum interference device
LCMV	linear constraint minimum variance
DICS	dynamic imaging of coherent sources
M1	primary motor cortex
GPe	external segment of the globus pallidus
GPi	internal segment of the globus pallidus
STN	subthalamic nucleus
SNc	substantia nigra pars compacta
SNr	substantia nigra pars reticulata
GABA	γ -aminobutyric acid
PD	Parkinson's disease
MPTP	1-methyl-4-phenyl-1,2,3,6-tetrahydropyridine
6-OHDA	6-hydroxydopamine
L-DOPA	L-3,4-dihydroxyphenylalanine; also known as levodopa
DBS	deep brain stimulation
LFP	local field potential
EMG	electromyography
UPDRS	unified Parkinson's disease rating scale
STG	superior temporal gyrus
ROI	region of interest
PMC	premotor cortex
PPC	posterior parietal cortex

Zusammenfassung

Morbus Parkinson ist eine progressive, neurodegenerative Erkrankung des zentralen Nervensystems, deren Symptome unter anderem mit der tiefen Hirnstimulation behandelt werden. Die dafür notwendigen chirurgischen Eingriffe ermöglichen es, Hirnaktivität der Basalganglien in Form lokaler Feldpotentiale (LFPs) aufzuzeichnen. Zahlreiche Studien, die sich mit der Analyse von LFPs beschäftigt haben, lieferten Hinweise darauf, dass neuronale, oszillatorische Aktivität bei Parkinson-Patienten pathologisch verändert ist. Zudem konnte gezeigt werden, dass neuronale Oszillationen nicht nur lokal sondern auch interregional synchronisiert sind. So sind beispielsweise Beta Oszillationen (13-35 Hz) im Nucleus subthalamicus (STN) und Cortex kohärent.

Diese Doktorarbeit befasste sich mit lokaler und interregionaler neuronaler Synchronisation bei Parkinson-Patienten. Im Mittelpunkt stand die Charakterisierung der oszillatorischen Kopplung zwischen STN, Cortex und Muskel.

Basierend auf einem einheitlichen Paradigma wurden drei Studien durchgeführt. In allen Studien wurden LFP Messungen im STN, Magnetenzephalographie (MEG) und Elektromyographie simultan durchgeführt. Akinetisch-rigide (Studien 1 und 2) und tremor-dominante Parkinson-Patienten (Studie 3) wurden in Ruhe, während der Ausführung einer Halteaufgabe (Elevation des Unterarms) und während der Ausführung einer Bewegungsaufgabe (repetitives Öffnen und Schließen der Faust) untersucht. Die Messungen wurden zunächst nach Entzug dopaminergischer Medikation durchgeführt und nach Verabreichung von Levodopa wiederholt. Die Quantifizierung von lokaler Synchronisation erfolgte durch Berechnung von Power. Die Quantifizierung von interregionaler oszillatorischer Kopplung erfolgte durch Berechnung von Kohärenz.

Studie 1 beschäftigte sich mit der räumlichen Verteilung von STN-cortikaler Kohärenz im Ruhezustand. Diese erwies sich als frequenzabhängig. Im Alpha-Band (8-12 Hz) war der STN vornehmlich an temporale Areale gekoppelt, insbesondere an den Gyrus temporalis superior (STG). Im Beta-Band hingegen zeigten der primäre motorische (M1), der primäre somatosensorische und der prämotorische Cortex die stärkste Kohärenz. Räumliche Kohärenzmaxima waren nahezu ausschließlich ipsilateral zum STN lokalisiert. Eine nähere Betrachtung der einzelnen Elektrodenkontakte im STN ergab, dass die Alpha-Kopplung zum STG an allen Kontakten zu beobachten war,

während die Beta-Kopplung zu M1 auf einen oder zwei Kontakte beschränkt war. Diese Ergebnisse zeigen, dass nur ein eingegrenzter Bereich innerhalb oder im Umfeld des STN synchron mit M1 oszilliert. Die Organisation der anatomischen Verbindungen zwischen M1 und STN lässt vermuten, dass es sich hierbei um den dorsolateralen Teil des STN handelt. Neben der Charakterisierung der frequenzabhängigen Verteilung von STN-cortikaler Kohärenz demonstrierte Studie 1 die Möglichkeit, oszillatorische Kopplungen mittels simultaner LFP-MEG Messungen zu untersuchen.

Studie 2 befasste sich mit der Modulation von STN-cortikaler und cortiko-muskulärer Kohärenz durch Bewegung und Medikation. Es wurde gezeigt, dass Alpha- und Beta-Kohärenz zwischen M1 und dem Extensor-Muskel des Unterarms durch Bewegung im Vergleich zur Halteaufgabe reduziert wird. Levodopa zeigte keine Wirkung auf die cortiko-muskuläre Kohärenz. Allerdings führte die Medikation zu einer Reduktion der Beta-Kohärenz zwischen M1 und STN. Diese korrelierte wider Erwarten nicht mit der klinischen Verbesserung der Beweglichkeit. Stattdessen wurde eine negative Korrelation zwischen Beta-Kohärenz und Unterbeweglichkeit festgestellt, d.h. Patienten mit einer stärkeren Kohärenz waren besser beweglich als Patienten mit einer schwächeren Kohärenz. Studie 2 zeigt, dass STN-cortikale und cortiko-muskuläre Kohärenz unabhängig voneinander moduliert werden können. Die negative Korrelation zwischen Beta-Kohärenz und Unterbeweglichkeit lässt Zweifel an der weit verbreiteten Annahme aufkommen, dass starke Beta-Kohärenz zwischen STN und M1 einen pathologischen Mechanismus der Parkinson-Erkrankung darstellt.

Ziel von Studie 3 war es, mögliche Veränderungen der STN-cortikalen und cortico-muskulären Kohärenz zu ermitteln, die mit dem Einsetzen des Parkinson-typischen Ruhetremors einhergehen. Die Ergebnisse zeigen, dass die neuronale Synchronisation in der Tremor-Frequenz und der doppelten Tremor-Frequenz ansteigt sobald der Tremor auftritt. Ein Anstieg konnte für Power im STN sowie für die oszillatorische Kopplung zwischen STN, Cortex und Muskel nachgewiesen werden. Eine Analyse auf Quell-Ebene offenbarte, dass M1, der prämotorische Cortex sowie der posteriore Parietallappen während des Tremors eine erhöhte Kohärenz mit den Unterarmmuskeln aufweisen und zudem untereinander synchronisiert sind. Studie 3 belegt, dass oszillatorische Kopplung in der Tremor-Frequenz ein neuronales Korrelat des Ruhetremors ist.

Die im Rahmen der Dissertation durchgeführten Studien zeigen, dass oszillatorische Kopplung zwischen STN, Cortex und Muskel durch Bewegung, dopaminerge Medikation und Tremor moduliert wird und mit Beweglichkeit korreliert. Diese Ergebnisse verdeutlichen die wichtige Rolle von synchronen Oszillationen in der Pathophysiologie von Morbus Parkinson und ermöglichen eine Zuordnung von Synchronisationsprozessen und Symptomen, die möglicherweise für eine gezielte, therapeutische Manipulation von pathologischen Oszillationen relevant werden könnte.

Summary

Parkinson's disease (PD) is a progressive, neurodegenerative disease of the central nervous system which is treated, amongst other therapeutic interventions, by deep brain stimulation (DBS). The surgical procedure for DBS provides the unique opportunity to record local field potentials (LFPs) from the human basal ganglia. Numerous studies investigating LFPs found indications for pathological alterations of synchronous oscillations in PD. These studies also showed that synchronization occurs locally as well as between distant brain regions. For example, it was demonstrated that LFPs recorded from the subthalamic nucleus (STN) are coherent with cortical oscillations in the beta band (13- 35 Hz).

This thesis investigated local and interregional synchrony in PD. Its major aim was to characterize oscillatory coupling between STN, cortex and muscle.

Three studies were performed which were all based on the same experimental paradigm. In all studies, STN LFPs, the magnetoencephalogram (MEG) and the electromyogram of forearm muscles were recorded simultaneously. Akinetic-rigid (studies 1 and 2) and tremor-dominant patients (study 3) were recorded at rest, during a static motor task (forearm elevation) and during repetitive movement (opening and closing of the fist). Measurements took place after withdrawal of dopaminergic medication and were repeated following administration of levodopa. Local synchrony was quantified by power and interregional oscillatory coupling was quantified by coherence.

Study 1 investigated the spatial distribution of STN-cortical coherence at rest. Interestingly, the distribution was found to be frequency-dependent. STN alpha (8-12

Hz) oscillations were predominantly coherent with oscillations in temporal areas. In particular, there was strong alpha coherence with superior temporal gyrus (STG). In the beta band, however, coherence was strongest with primary motor cortex (M1), primary somatosensory cortex and premotor cortex. The vast majority of spatial coherence maxima were located ipsilateral to the STN. Inspection of the distribution of coherence across STN electrode contacts revealed that alpha band coupling to STG was distributed homogeneously across contacts. In contrast, beta band coupling to M1 was usually restricted to one or two contacts. The results suggest that beta synchrony with M1 is confined to a circumscribed area within or near the STN. Given the organization of anatomical connections between M1 and STN, it is reasonable to assume that beta band coupling is restricted to the dorsolateral portion of the STN. Apart from characterizing the frequency-dependent distribution of STN-cortical coherence, study 1 demonstrated that simultaneous LFP-MEG recordings are a powerful tool for studying oscillatory coupling in PD.

Study 2 assessed modulations of STN-cortical and cortico-muscular coherence by movement and dopaminergic medication. It showed that coherence between M1 and the forearm extensor muscle is reduced by repetitive movement compared to static contraction in the alpha and beta band. Levodopa did not affect cortico-muscular coherence but led to a reduction of beta coherence between M1 and STN. Surprisingly, this reduction did not correlate with the improvement of motor symptoms. However, there was a negative correlation between beta coherence and akinesia in the OFF state, i.e. patients with strong coherence showed better motor performance than patients with weak coherence. Study 2 demonstrates that STN-cortical and cortico-muscular coherence can be modulated independently. The negative correlation between beta coherence and akinesia challenges the widespread belief that strong STN-cortical beta coherence reflects a pathological mechanism.

Study 3 aimed at characterizing the changes in STN-cortical and cortico-muscular coherence associated with the manifestation of parkinsonian rest tremor. It was found that neuronal synchrony at tremor frequency and double tremor frequency increases when tremor emerges. Increases were observed for STN power and oscillatory coupling between STN, cortex and muscle. Source level analysis revealed that M1, premotor cortex and posterior parietal cortex show increased coherence with forearm muscles during tremor and are synchronized with each other at tremor frequency and its first

upper harmonic. Study 3 demonstrates that oscillatory coupling at tremor frequency is a genuine neural correlate of rest tremor in PD.

The presented studies reveal modulations of oscillatory coupling by movement, dopaminergic medication and tremor. Further, they demonstrate that coupling is correlated with motor performance. In summary, the results emphasize the pivotal role of synchronous oscillations in PD pathophysiology and provide insights into the association between neuronal synchronization and PD symptoms. These insights might become relevant for therapeutic manipulation of pathological oscillatory processes.

1 Introduction

Neuronal oscillations are periodic fluctuations of membrane or extracellular potentials which can be measured at several scales. Ever since Hans Berger recorded oscillations non-invasively in humans for the first time (Berger, 1929), they attracted attention in the scientific community. Today, it is clear that neuronal oscillations are directly related to behavior (Buzsaki, 2006). Moreover, there is good evidence that they are pathologically altered in several neurological disorders. In particular, altered oscillatory activity was found to be a hallmark of Parkinson's disease (PD). The following introduction will provide an overview of how neuronal oscillations are measured and analyzed, describe PD on the symptom and the neurophysiological level and will finally present the current knowledge on the intricate relationship between neuronal oscillations and PD symptoms.

1.1 Non-invasive measurement of neuronal oscillations

One of the main reasons for the tremendous interest in neuronal oscillations is that they can be measured non-invasively in humans. Therefore, they can be related to complex behaviors. Traditionally, studies on neuronal oscillations divide the spectrum into five frequency bands: theta (<4 Hz), delta (4-7 Hz), alpha (8-12 Hz), beta (13-30 Hz) and gamma (>30 Hz). Importantly, these different frequency bands have been associated with different perceptual, motor and cognitive functions. Non-invasive recordings of oscillatory activity can be performed using electroencephalography (EEG) or magnetoencephalography (MEG).

In EEG, surface electrodes are attached to the skull to monitor changes in electric potentials over time. MEG is similar in principle but measures the magnetic rather than the electric field (reviewed in Hämäläinen et al., 1993). Since the magnetic fields resulting from brain activity are very small, their detection requires extremely sensitive sensors called superconductive quantum interference devices (SQUIDs). The small amplitude of brain signals further implies that they are masked by ambient fields such as the earth's steady field or the fields produced by muscle contraction. In fact, the latter surmount brain magnetic fields by several orders of magnitude. Thus, MEG is conducted within a shielded room that blocks external magnetic fields by virtue of its material (mu-metal) and by active cancellation in custom-made circuits. In addition, special types of

sensors are used to minimize interference. So-called gradiometers are designed to measure spatial field gradients rather than the fields *per se*, leading to decreased sensitivity to distant sources. Finally, several online and offline processing tools are available to suppress interference.

Both EEG and MEG measure spatial sums of signals produced in the brain such as synaptic currents, action potentials, calcium spikes or intrinsic membrane responses (reviewed in Buzsáki et al., 2012). Detection by EEG and MEG requires that several thousand events occur simultaneously. Moreover, individual contributions must not cancel. Whether cancellation occurs depends on timing and geometry. For example, radial currents produce almost no detectable signal in MEG due to magnetic field cancellation. Thus, MEG is mainly sensitive to tangential sources.

1.2 Analysis of neuronal oscillations

Oscillatory brain activity measured by MEG is typically first analyzed on the sensor level in order to identify the frequencies and/or time points relevant to the experimental task. However, these may also be defined *a priori*. Following frequency and/or epoch selection, activity can be localized in order to identify the brain areas that give rise to the effects observed on the sensor level.

1.2.1 Spectral analysis

Since neuronal oscillations are periodic, they can be decomposed into a sum of sine waves by means of Fourier transformation which yields phase and amplitude as a function of frequency. As electrophysiological recordings are finite, the latter are estimates rather than the true Fourier coefficients of the underlying process. A range of interesting parameters can be derived from these coefficients.

Spectral power is by far the most frequently analyzed parameter. It is defined as the squared amplitude at a given frequency, i.e. it quantifies signal energy. Changes in power across experimental conditions are usually interpreted as changes in the degree of synchronization within the recorded population of neurons, but could also indicate a change in the number of neurons contributing to the signal.

Coherence is a measure often employed to quantify the level of synchrony between two signals. It reflects the degree of amplitude and phase co-variation across data segments or trials. In other words, it measures whether two signals tend to keep a fixed phase difference and a fixed amplitude product over time. Coherence values range between zero (independent) and one (completely synchronous). Since a value of zero requires a perfectly symmetric distribution of individual phase differences, it is never measured in practice. Thus, coherence is biased towards non-zero values and the bias increases as the amount of available data segments decreases (Maris et al., 2007). Therefore, a comparison of coherence across experimental conditions is only sensible if the number of data segments is approximately equal for all conditions.

Coherence between signals from two distant brain areas indicates that rhythmic activity in these areas is coordinated in time. Therefore, coherence is often considered a measure of functional connectivity (reviewed in Varela et al., 2001). It was proposed that a neuronal population A may regulate its impact on a second population B by timing its input relative to intrinsic membrane potential oscillations in B (Fries, 2005). In this context, the term “impact” describes the ability of A to trigger action potentials in B . For example, the impact would be maximal if A 's input arrives when B happens to be maximally depolarized. Such coordinated, rhythmic input would result in high coherence.

1.2.2 Source reconstruction

A fundamental challenge in the analysis of EEG and MEG signals is to identify the sources of activity. This challenge is usually referred to as the “inverse problem”. To solve the inverse problem, one typically first solves the so-called “forward problem”. The forward problem is solved for each location of interest separately. For location j , the solution is a model that quantifies what sensor measurement would result from a current of unit amplitude at location j . The solution to the inverse problem is the inverse of the forward model, i.e. it maps sensor measurements to source activity. Due to the enormous number of possible sources and the limited number of sensors there is in principle too little information to reconstruct the origin of a given sensor measurement. Thus, the inverse problem can only be solved by making assumptions which guarantee the existence of a unique solution. There are various algorithms which solve the inverse

problem by making assumptions such as minimum norm, least-squares or beamforming approaches.

Beamforming is a source localization method which sequentially scans a predefined set of locations to obtain point-by-point estimates of source activity (reviewed in Hillebrand et al., 2005). The estimates are computed as weighted sums of the sensor data:

$$y(j) = w_1(j)x_1 + w_2(j)x_2 + \dots + w_N(j)x_N$$

y is the activity estimate for location j , x_i is the i th sensor recording, w_i is the weight for this sensor and N is the number of sensors.

The studies presented in this thesis make use of two kinds of beamformers. One of these operates on time domain data and is known as linear constraint minimum variance (LCMV) beamformer (Van Veen and Buckley, 1988). The other is called Dynamic Imaging of Coherent Sources (DICS; Gross et al., 2001) and operates on frequency domain data. The idea behind both algorithms is the same: they aim at minimizing interference. This is achieved by choosing the weights w such that the output y is as small as possible, with the crucial constraint that activity from location j must not be modified in any way. In consequence, the only remaining part of the signal that can be minimized is interfering activity from other locations. The optimal weights can be found analytically with the help of common concepts in optimization. In this work, beamforming was primarily used to estimate coherence between cortical areas and the basal ganglia.

1.3 The basal ganglia

The basal ganglia are a core element of the motor system. Alterations in basal ganglia activity patterns, especially in oscillatory activity, can be observed in several neurological disorders. In particular, such alterations are known to occur in PD.

1.3.1 Anatomy

The term “basal ganglia” refers to a group of interconnected subcortical nuclei which receive input from the cortex and project back to the cortex via polysynaptic pathways. Thus, cortex and basal ganglia form a loop. One outstanding characteristic of this loop is that the functional organization of the cortex is roughly maintained. Inputs of different

modality, e.g. from motor and limbic cortical areas, as well as inputs related to different body parts remain anatomically segregated throughout the loop (Alexander et al., 1986). Another striking feature of the basal ganglia-cortical loop is strong convergence within the modality-specific sub-circuits. For example, each striatal neuron in the somatomotor circuit receives several thousand cortical inputs (Kincaid et al., 1998). These may come from supplementary, premotor or primary motor cortex (M1) or from somatosensory areas.

The anatomy of the basal ganglia is illustrated schematically in Fig. 1. The basal ganglia consist of the striatum, the external and internal segment of the globus pallidus (GPe and GPi), the subthalamic nucleus (STN) and the compact and reticular compartment of the substantia nigra (SNc and SNr). The striatum is the main input structure of the basal ganglia (reviewed in Gerfen and Bolam, 2010). It receives afferents from all parts of the cortex and from the thalamus. Input is provided to medium spiny projection neurons which make up about 95% of all striatal neurons. Medium spiny neurons use γ -aminobutyric acid (GABA) as neurotransmitter and have a low spontaneous firing rate. Their activity is modulated by cholinergic striatal interneurons, serotonergic input from the raphe nuclei and dopaminergic input from SNc.

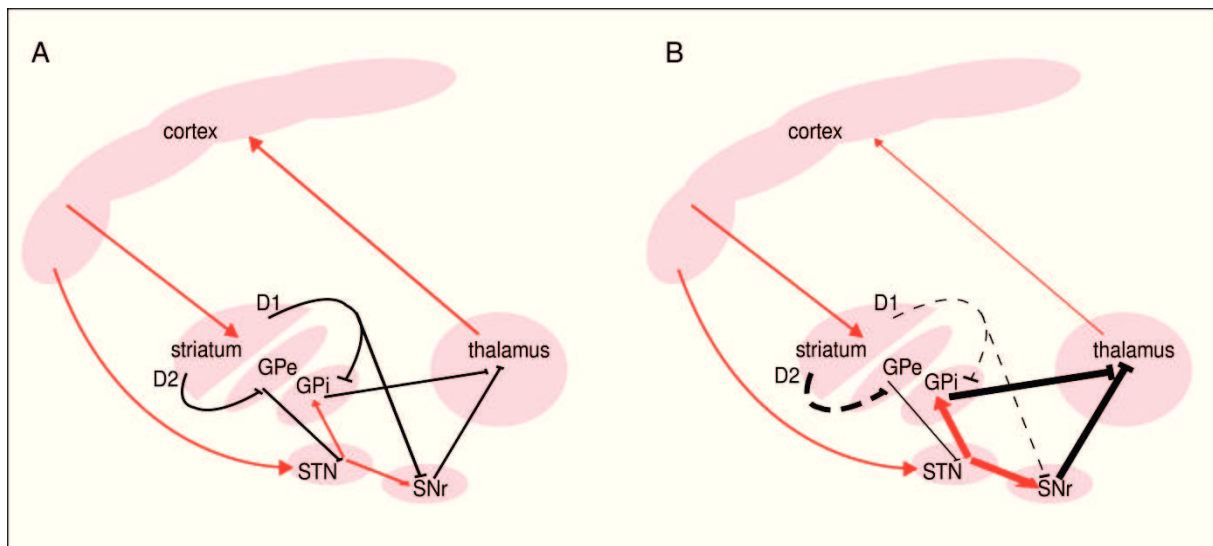


Fig 1: The functional anatomy of the basal ganglia.

A) The basal ganglia in healthy subjects. The cortex provides input to the striatum. Striatal output reaches GPi and SNr via direct projections and indirectly via GPe and STN. GPi and SNr inhibit the thalamus which projects back to the cortex.

B) The basal ganglia in Parkinson's disease according to the classical rate model (Albin et al., 1989; DeLong, 1990). Reduced activity in the direct pathway leads to decreased inhibition of GPi and SNr. Increased activity in the indirect pathway leads to increased excitation of GPi and SNr. Both result in increased inhibition of the thalamus and decreased feedback to the cortex. Red lines indicate excitatory connections whereas black lines indicate inhibitory connections. Line thickness marks relative activity. Dotted lines indicate a change due to dopamine depletion. For the direct pathway, dopamine depletion leads to a reduction of striatal output. For the indirect pathway, dopamine depletion leads to an increase of striatal output. This difference is due to expression of different dopamine receptor types.

Striatal output reaches the output nuclei of the basal ganglia, GPi and SNr, either directly or indirectly via GPe and STN. While activity in the direct pathway inhibits the output structures, activity in the indirect pathway exerts excitatory influence. Excitation is achieved by inhibition of the GPe and subsequent disinhibition of the STN which is the only glutamatergic nucleus in the loop. When disinhibited, the STN drives GPi and SNr. The STN also receives direct cortical afferents via the so-called hyperdirect pathway (Nambu et al., 1996).

GPi and SNr contain GABAergic neurons projecting to the thalamus which closes the loop by providing input to cortex and striatum. Other basal ganglia output targets are the superior colliculus and the pedunculopontine nucleus. Importantly, the ultimate outcome of cortical input to the basal ganglia is either an increase (indirect pathway) or a decrease (direct pathway) of thalamic inhibition, i.e. a regulation of feedback.

1.3.2 Function

Currently, the function of the basal ganglia is not fully understood. Many theories have been proposed but none of them satisfactorily explains all of the experimental findings. It is undisputed that the basal ganglia can strongly influence motor behavior. Abnormal basal ganglia activity patterns are observed in several movement disorders such as Parkinson's disease, Huntington's disease, dystonia or Tourette's syndrome (reviewed in Wichmann and Dostrovsky, 2011). Furthermore, the basal ganglia are known to be involved in many different types of learning and in habit formation (reviewed in Ashby et al., 2010). Other non-motor functions are known to exist but have rarely been investigated. For example, the basal ganglia were found to be involved in emotional tone processing (Pell and Leonard, 2003) and in processing of motivational value (Levy and Dubois, 2006).

With regard to motor control, suggested functions include online error correction, gain control, the retention of over-trained motor skills and action selection. Especially the latter hypothesis is well-known and still supported by numerous researchers (Mink, 1996). However, it is seriously challenged by the finding that the earliest changes in GPi firing rate occur at the time of the earliest agonist muscle activity, i.e. too late for action selection (Turner and Anderson, 1997).

Recent studies in non-human primates aimed at identifying basal ganglia motor functions by inactivating the GPi, i.e. by blocking basal ganglia output (Desmurget and Turner, 2008, 2010). GPi inactivation resulted in slowed and undershooting movements but did not impair reaction time, online movement correction or the execution of over-trained sequences. In summary, current research supports the hypothesis that the basal ganglia are involved in setting the gain of movement. However, a general consensus has not been reached and further research is necessary.

1.4 Parkinson's disease

PD is a progressive, neurodegenerative disorder which was first described by James Parkinson in 1817. Due to its relatively high prevalence (1.6% of people older than 65; Rijk et al., 1997) it has a considerable and growing impact on society. Thus, understanding PD is one of the major challenges to modern neurological research.

1.4.1 Symptoms

The main symptoms of PD are akinesia (poverty of movement), bradykinesia (slowness of movement), rigidity (muscle stiffness) and rest tremor (reviewed in Lang and Lozano, 1998a, 1998b). In addition, patients often develop further motor impairments such as postural instability or gait disturbances. Non-motor symptoms such as dementia or depression are also common, especially in late stages of the disease. PD mainly affects the elderly and age is the only risk factor consistently identified in epidemiological studies.

PD can be subdivided into two types: the akinetic-rigid subtype with no or little tremor but markedly slowed movement and the tremor-dominant subtype showing strong rest tremor but little akinesia and rigidity (reviewed in Helmich et al., 2012). The distinction is well-established and based on both subjective classification and automated statistical cluster analysis of clinical data (Lewis et al., 2005). Compared to the akinetic-rigid subtype, the tremor-dominant subtype is characterized by relatively mild impairments at disease onset and slow disease progression in the first years following diagnosis. However, late stage symptoms such as falls occur after similar disease duration in both subtypes, indicating that disease progression in tremor-dominant patients accelerates in later stages (Selikhova et al., 2009).

1.4.2 Pathogenesis

Most PD symptoms are consequences of a progressive loss of dopaminergic neurons in SNc and other midbrain nuclei. Despite decades of intensive research, the cause of cell death remains unknown. Therefore, the large majority of patients are classified as suffering from idiopathic PD (of unknown origin). However, some hereditary forms exist and a number of risk genes have been identified (reviewed in Obeso et al., 2010).

One of these risk genes is *SNCA* which codes for the presynaptic protein α -synuclein. In PD patients, α -synuclein forms intracellular aggregates together with other proteins. These aggregates are called Lewy bodies. Investigation of the distribution of Lewy bodies at different symptomatic stages revealed a progressive spread from the brainstem towards cortical areas (Braak et al., 2003). This and other studies showed that a number of areas other than SNc are affected in PD, some of them much earlier.

Interestingly, the earliest Lewy bodies are found in the dorsal XI/X motor nucleus of the glossopharyngeal and vagal nerves and in the olfactory bulb, in line with the parasympathetic and olfactory symptoms that often precede motor impairments by several years. Thus, PD comprises predominantly, but not exclusively, motor symptoms which emerge years after progressive cell death has begun in a number of brain areas.

There are two forms of human parkinsonism which are known to be caused by environmental factors: delayed-onset parkinsonism following encephalitis lethargica and intoxication with 1-methyl-4-phenyl-1,2,3,6-tetrahydropyridine (MPTP). MPTP is sometimes accidentally consumed by heroin addicts and can result in severe akinesia and rest tremor. As monkeys show a similar response, MPTP is used to create primate models of PD. Rodents are much less susceptible to the substance but develop motor symptoms reminiscent of PD after cerebral injection of 6-hydroxydopamine (6-OHDA), a toxic dopamine receptor agonist.

1.4.3 Pathophysiology according to the classical rate model

The classical rate model of PD pathophysiology proposes an imbalance between the direct and the indirect pathway within the basal ganglia-cortical loop (Albin et al., 1989; DeLong, 1990). In this model, pathological alterations are exclusively caused by a lack of dopamine in the striatum.

Dopamine depletion has opposite effects on the direct and the indirect pathway. The difference is due to expression of different dopamine receptor types. Striatal neurons projecting to GPi (direct pathway) predominantly express D1 dopamine receptors (Gerfen et al., 1990). Upon dopamine binding, medium spiny neurons expressing D1 receptors increase their firing rate, resulting in disinhibition of the thalamus (see section 1.2.1). When dopamine is lacking, disinhibition decreases and the thalamus becomes less active, leading to decreased activity in cortical motor areas and thereby to akinesia (Fig. 1B).

Striatal neurons in the indirect pathway predominantly express D2 receptors. In contrast to D1 receptors, activation of D2 receptors leads to inhibition. As depicted in Fig. 1, inhibition of striatal neurons projecting to GPe results in STN inhibition. In PD,

dopamine levels are reduced so that the STN is less inhibited and therefore drives GPi. In turn, GPi excessively inhibits the thalamus.

In summary, the classical rate model proposes that PD is characterized by too little activity in the direct pathway and too much activity in the indirect pathway. Notably, a recent optogenetic study in which the pathways were stimulated selectively supported this basic hypothesis (Kravitz et al., 2010). The model explains a number of observations. For example, activity in cortical motor areas was found to be reduced in non-medicated PD patients compared to the medicated state (Jenkins et al., 1992). Moreover, lesions of STN (Bergman et al., 1990) and GPi (Lozano et al., 1995) alleviate PD motor symptoms, as predicted by the model. However, the model also has its shortcomings. First, it is incomplete. For example, it does not incorporate the hyperdirect pathway or projections from various subcortical nuclei back to the striatum. Second, some of its predictions are wrong. For example, firing rate changes in GPi following dopamine depletion are rather small, casting doubt on the hypothesis that GPi excessively inhibits the thalamus in PD (e.g. Wichmann et al., 1999). Moreover, GPi lesions do not produce the predicted result. According to the model, GPi lesions should elicit dyskinesias (involuntary choreoathetotic movements) since the thalamus is not inhibited anymore. In reality, GPi lesions abolish dyskinesias in PD patients (Laitinen et al., 1992).

1.4.4 Treatment

To date, PD can neither be cured nor can its progression be stopped. However, its symptoms can be treated by either pharmacological or surgical intervention. L-3,4-dihydroxyphenylalanine, called levodopa or L-DOPA, is the most effective drug for PD treatment. Unlike dopamine, levodopa can pass the blood-brain barrier and thus reaches its target tissue after oral intake. In the brain, it is metabolized to dopamine and compensates for the lack of nigral dopamine. The treatment effects are highly reliable so that a positive response to levodopa is used as a criterion for diagnosis of PD.

While levodopa successfully restores motor capabilities, its long-term application is associated with side effects. After several years, patients often require a higher dosage to reach the same effect (“wearing-off”), experience unpredictable transitions between akinetic and mobile states (“ON-OFF fluctuations”) and exhibit dyskinesias. Especially

the latter can heavily impair motor performance. Therefore, levodopa-induced dyskinesias are a common motivation for considering alternative therapeutic options such as deep brain stimulation (DBS).

DBS effectively alleviates PD motor symptoms and usually allows for a substantial dose reduction of anti-parkinsonian medication (Limousin et al., 1998). In DBS, electrodes are implanted into the target area where they deliver current pulses which are generated by a subcutaneous stimulator. For treatment of PD, either STN or GPi are targeted. Typically, the STN is stimulated with a frequency of 130 Hz.

While its clinical benefit is undisputed, the mechanisms of DBS are still under debate (reviewed in Kringelbach et al., 2007). Since the outcomes of STN DBS and STN lesions are similar, DBS is often interpreted as a “functional lesion”. The term is suggestive of an inhibitory effect and, indeed, several studies found that DBS leads to a lasting reduction in the firing rate of local STN neurons (e.g. Beurrier et al., 2001). However, local neurons are not the only neural elements exposed to the electric field. Passing axons, for example, are stimulated, too. Due to their low chronaxie value, they are assumed to be the elements primarily activated by DBS. Depending on distance and orientation with respect to the stimulation contacts, DBS triggers action potentials in some axons but not in others. These may travel either towards the synaptic terminals (orthodromic activation) or towards the soma (antidromic activation). The observed effects of orthodromic activation naturally depend on the types (excitatory or inhibitory) and the number of synapses separating stimulation target and the site of measurement.

Given the wide range of possible effects and their dependence on the exact electrode placement, it is not surprising that electrophysiological studies have not yet provided a conclusive characterization of the mechanism underlying DBS. Interestingly, a recent optogenetic study proposed that out of the manifold of effects it is stimulation of cortical STN afferents which causes clinical improvement (Gradinaru et al., 2009).

1.5 Oscillations in Parkinson's disease

Implantation of DBS electrodes provides the unique opportunity to directly measure neuronal activity from the human basal ganglia. Such recordings can either be performed during surgery or in the interval between electrode and stimulator implantation. If the surgeon uses microelectrodes to locate the target, extracellular recordings from individual neurons can be obtained during surgery. In most studies, however, the DBS electrodes are used for recordings. Due to their large contacts, DBS electrodes record local field potentials (LFPs) rather than single cell activity. LFPs represent the spatial average of electric fields over several hundred micrometers (Katzner et al., 2009) and are believed to predominantly represent synaptic currents rather than action potentials (reviewed in Buzsáki et al., 2012).

In both human PD patients and animal models of PD, LFP recordings revealed prominent oscillatory activity in the basal ganglia. These discoveries led to a shift of attention away from firing rates and towards rhythmic activity.

1.5.1 Alpha oscillations

Following treatment with MPTP, some monkey species develop strong alpha oscillations in the basal ganglia (Bergman et al., 1994). The peak frequency of these oscillations is usually twice the frequency of the MPTP-induced tremor. Thus, alpha oscillations are believed to be related to tremor. In PD patients, similar tremor-related alpha oscillations were observed in GPi (Hutchison et al., 1997) and STN (Levy et al., 2000). These oscillations were coherent with tremor recordings from the muscle obtained by electromyography (EMG), supporting their possible involvement in tremor generation. Before this thesis was conducted, however, it was not known whether alpha oscillations are directly related to the presence and/or severity of tremor.

In addition to their role in tremor, alpha oscillations in the basal ganglia are modulated by voluntary movement. Recordings from the STN of PD patients demonstrated a reduction of alpha power which starts 2 s prior to movement and continues during movement execution (Oswal et al., 2012).

1.5.2 Beta oscillations

Recordings from the human STN and GPi revealed strong beta oscillations in PD patients. Beta power was found to be reduced by both levodopa administration (Brown et al., 2001) and by DBS (Eusebio et al., 2011). Moreover, the levodopa-induced reduction of beta power was reported to correlate with the concurrent reduction of akinesia and rigidity (Kühn et al., 2006). In addition, stimulation in the beta band was found to slow movement. Slowing was achieved both by STN DBS (Chen et al., 2007) and transcranial alternating current stimulation over motor cortex (Pogosyan et al., 2009). Together, these findings led to the hypothesis that beta oscillations are pathologically enhanced in PD. In addition, it was suggested that pathological hyper-synchrony causes akinesia and rigidity (Brown, 2007). A potential mechanism was suggested based on computational studies (Bar-Gad et al., 2003): enhanced synchrony might interfere with de-correlation of cortical input in the basal ganglia and thereby impair information compression (Hammond et al., 2007).

The idea of pathological hyper-synchrony in the beta band is popular in the field and has inspired numerous experiments. However, it has also been criticized. While it is generally agreed that STN beta power is a biomarker for akinesia, some studies cast doubt on the causal role of beta oscillations. The reported effect sizes for symptom worsening through stimulation at beta frequencies were small (Chen et al., 2007; Pogosyan et al., 2009). Moreover, the effect could not be reproduced in a recent animal experiment (Syed et al., 2012). Finally, akinesia was found to emerge before enhanced beta oscillations appeared in non-human primates (Leblois et al., 2007).

1.5.3 Gamma and high frequency oscillations

Gamma oscillations were proposed to have a “prokinetic” function and to be the functional counterpart of beta oscillations. In contrast to STN beta power, STN gamma power increases following levodopa administration, both at rest and during movement execution (Williams et al., 2002; Litvak et al., 2012). Moreover, beta and gamma oscillations show antagonistic modulations during movement (Fig. 2). While beta power is reduced prior to and during movement, STN gamma power and STN-M1 gamma coherence increase at movement onset (Cassidy et al., 2002; Litvak et al., 2012).

Recently, a fourth frequency band attracted attention: high frequency oscillations (HFOs; >200 Hz) were observed in the STN of medicated PD patients (Foffani et al., 2003). HFOs were found to be phase-amplitude coupled to STN beta oscillations in a dopamine-dependent fashion (López-Azcárate et al., 2010). Off medication, there was strong beta-HFO coupling and little HFO amplitude modulation by movement. On medication, cross-frequency coupling was reduced and HFO amplitude was strongly modulated during movement. In consequence, it was proposed that beta oscillations impair physiological HFO modulation through cross-frequency coupling. Another study confirmed the phase-amplitude coupling between beta oscillations and HFOs and investigated the clinical relevance of HFOs (Özkurt et al., 2011). The authors proposed a subdivision of the HFO band into a fast and a slow HFO band and showed that the ratio between fast and slow HFO power is reliably increased by levodopa administration.

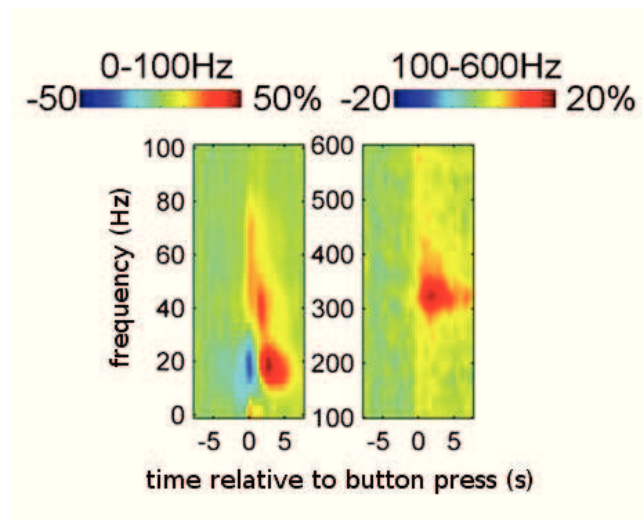


Fig 2: Movement-induced power changes in the STN of Parkinson patients.

Left: The figure illustrates the antagonistic relationship between beta and gamma oscillations in the STN. Beta power is suppressed relative to baseline immediately before and during a button press. Accordingly, beta oscillations are sometimes referred to as “antikinetic” oscillations. Following movement execution, beta power increases (beta rebound) and then returns to baseline. In contrast, gamma power increases at movement onset and immediately returns to baseline. Thus, gamma oscillations are often considered “prokinetic”. **Right:** Like gamma oscillations, high frequency oscillations increase in power at movement onset. The increase is sustained for a longer period than for gamma oscillations. Colors indicate percent change relative to baseline (-8 to -5 s). Adapted from Litvak et al. (2012).

2 Aims

The vast majority of studies on oscillations in PD dealt with synchrony within the STN. Given the network structure of the motor system, however, it seems unlikely that behaviorally relevant oscillatory activity is restricted to a single nucleus. In fact, previous studies demonstrated that STN oscillations are coherent with oscillations in other parts of the basal ganglia-cortical loop, such as the GPi (Brown et al., 2001). Importantly, they were also found to be coherent with cortical oscillations (Williams et al., 2002). However, the exact cortical areas coupled to the STN were not known. Likewise, it was unclear whether and how STN-cortical coherence is modulated by movement, levodopa administration and tremor.

In order to answer these open questions, the current thesis investigated coherence between STN, cortex and muscle under various experimental conditions and in different patient cohorts. The overall aim was to characterize synchronous oscillations in PD on the network level. Specifically, the studies aimed at:

- Study 1:** Identifying the cortical areas coupled to the STN at rest. In particular, it was investigated whether the spatial pattern of STN-cortical coherence is different for different frequency bands.
- Study 2:** Investigating the effect of movement and levodopa administration on STN-cortical coherence. Furthermore, modulations of STN-cortical coherence were compared to modulations of cortico-muscular coherence in order to assess possible dependencies between these two couplings.
- Study 3:** Describing the relationship between coherence and the manifestation of rest tremor. Specifically, the study aimed at clarifying whether coherence at tremor frequency increases when rest tremor emerges spontaneously.

3 Paradigm

All three studies presented in this thesis made use of essentially the same experimental setup and design. Three types of signals were recorded simultaneously: LFPs from the STN, MEG and the EMG of forearm muscles. The LFP signal was recorded by two bilaterally implanted DBS electrodes which were used for recording rather than stimulation. Each DBS electrode had four contacts (0-3; 0 most ventral, 3 most dorsal). The MEG signal was recorded by a 306-channel, whole-head MEG system. EMG was recorded by surface electrodes over the *extensor digitorum communis* and *flexor digitorum superficialis* muscles. Recordings were performed in the interval between electrode and stimulator implantation. Importantly, deep brain electrodes were connected to the amplifiers integrated in the MEG system by non-magnetic extension leads so that the severe artifacts described in previous LFP-MEG studies were avoided (Litvak et al., 2010).

The experiment consisted of two blocks. The first block was recorded after withdrawal of dopaminergic medication (OFF). The second block was recorded after levodopa administration (ON). Each block was preceded by a clinical rating of motor symptom severity using the motor score of the Movement Disorder Society Unified Parkinson's Disease Rating Scale (MDS UPDRS III). Within each block, two recordings were performed (Fig. 3). Both of these consisted of a 5 min rest period (REST) followed by one of two motor tasks. The tasks were performed with the symptom-dominant hand. In the first task (HOLD), subjects were asked to elevate their forearm to about 45° and to spread their fingers. The elbow was leaning on a table in front of them. In the second task (MOVE), subjects were instructed to open and close their fist repetitively. The forearm was elevated as in the HOLD condition. Movements were self-paced and performed with a frequency of approximately 1 Hz. Each motor task was interleaved by pauses in order to avoid muscle fatigue. More specifically, epochs of task execution of 1 min duration and pauses of 1 min duration alternated for 9 minutes in total (Fig. 3).

The studies differed with respect to the epochs that were analyzed and with respect to patient cohort. Study 1 investigated oscillatory coupling in the REST OFF condition and included akinetic-rigid PD patients. Study 2 assessed oscillatory coupling during motor task performance in the same patients (plus two additional subjects) in OFF and ON.

Study 3 focused on the same epoch as study 1 but included tremor-dominant PD patients.

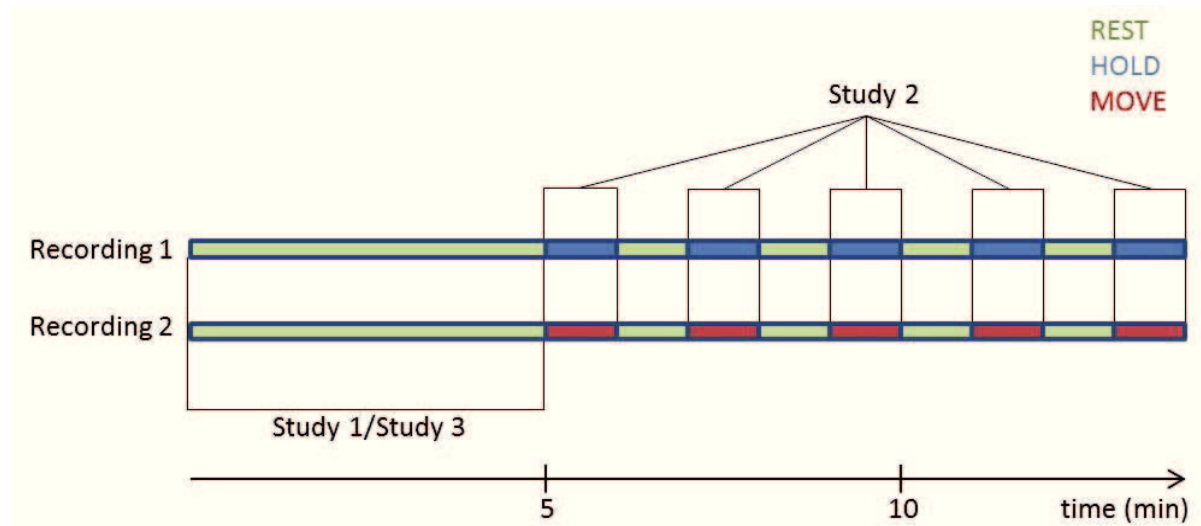


Fig. 3: Schematic time line for one block of simultaneous LFP-MEG recordings.

A block (either OFF or ON) consisted of two recordings which were performed in succession, but are depicted as parallel lines for illustration purposes. Each recording contained a 5 min rest period (REST) followed by a motor task. The task was either to elevate the forearm to 45° and to keep this position (HOLD) or to open and close the fist repeatedly with approximately 1 Hz (MOVE). Epochs of task execution were interleaved by 1 min pauses in order to avoid muscle fatigue.

In studies 1 and 3, the REST OFF period was analyzed. Study 2 focused on the periods of motor task performance in medication OFF and ON.

4 Study 1: Distinct oscillatory STN-cortical loops revealed by simultaneous MEG and local field potential recordings in patients with Parkinson's disease

Study 1 (Appendix 1) investigated coherence between STN and cortex. STN-cortical coherence is an especially interesting parameter as the cortex was shown to drive STN oscillations in the beta band (Williams et al., 2002; Lalo et al., 2008; Litvak et al., 2011). Therefore, it is often speculated that pathologically enhanced beta activity originates in the cortex. When study 1 was performed, it was known that there is significant coherence between STN and cortex (Williams et al., 2002; Fogelson et al., 2006).

However, it was unclear exactly which cortical areas are involved in this coupling and whether different cortical areas are coupled to the STN at different frequencies. Study 1 aimed at answering these open questions.

An earlier EEG study had already found first indications for a frequency-specific spatial distribution of STN-cortical coherence (Fogelson et al., 2006). However, this study was restricted to the sensor level because post-surgical dressing precluded measurements with more than a few EEG electrodes. In consequence, source localization was not feasible. Study 1 mapped STN-cortical coherence on the source level using MEG which allows for high density measurements even in the presence of surgical dressing.

4.1 Methods

Nine PD patients of the akinetic-rigid subtype participated in the study. Patients with tremor were not included since tremor is associated with strong alpha oscillations which potentially mask resting state alpha oscillations (Timmermann et al., 2003). One patient was excluded due to extensive head movement artifacts. STN LFPs, MEG and forearm EMG were recorded simultaneously. The study investigated the REST OFF condition (see Fig. 3). Four frequency bands were investigated: alpha (7-12 Hz), low beta (13-20 Hz), high beta (21-35 Hz) and gamma (70-90 Hz). For each frequency band, patient and electrode contact, the frequency with maximum coherence between STN LFPs and the MEG signal was determined automatically on the sensor level. DICS (Gross et al., 2001) was then applied for this frequency to localize coherence.

4.2 Results

4.2.1 Distribution of STN-cortical coherence across brain areas

All subjects showed significant coherence peaks in the alpha and beta band. Except for one case, gamma band coherence was not observed. Alpha coherence localized to a number of brain areas ipsilateral to the STN (Fig. 6 of Appendix 1). Although there was no significant overlap of alpha sources across subjects, a cluster of sources was observed in temporal cortex, in particular in superior temporal gyrus (STG). In contrast, beta sources consistently localized to medial sensorimotor and premotor areas ipsilateral to the STN.

4.2.2 Distribution of STN-STG and STN-M1 coherence across electrode contacts

In a subsequent analysis step, M1 and STG were defined as regions of interest (ROIs) and the distribution of STN-ROI coherence across STN electrode contacts was evaluated. STN-STG coherence peaked in the alpha band. The distribution of alpha peaks across contacts was not significantly different from a uniform distribution (Fig. 7 of Appendix 1), indicating that STG oscillations are coherent with a subcortical alpha source with large spatial extent. In contrast, STN-M1 coherence peaked in the beta band and beta peaks were usually observed for only one or two contacts, i.e. STN-M1 beta coherence was focal within the area recorded by the electrode.

4.3 Discussion

Study 1 showed that the spatial distribution of cerebral coherence with STN LFPs is frequency-dependent. STN alpha oscillations were coherent with oscillatory activity in temporal areas whereas STN beta oscillations were coherent with oscillations in sensorimotor and premotor cortex. Thus, different spectral components of the same subcortical signal coupled to different cortical areas. Notably, the frequency-dependent spatial pattern found in study 1 was confirmed by an independent study which also investigated STN-cortical coherence in PD patients (Litvak et al., 2011).

The function of the separation of couplings in the frequency domain remains unclear. One possibility is that inputs from M1 and inputs from STG are distinguished in the STN based on the frequency of the incoming signal. This strategy is known as multiplexing in communications engineering and usually serves to avoid interference between signals which are transmitted via the same physical channel (Weinstein and Ebert, 1971).

The observation of strong beta coherence between STN and motor cortex is plausible with regard to anatomy. The STN receives polysynaptic input from ipsilateral motor cortex via the indirect pathway and projects back to motor cortex via the thalamus (see chapter 2.1). Moreover, it receives monosynaptic cortical input via the hyperdirect pathway. A recent study aimed at imaging the hyperdirect pathway in humans by diffusion tensor imaging (Whitmer et al., 2012). The authors reported that the pathway originates in medial motor cortex, i.e. at a location comparable to the site of maximum beta coherence observed in the present study. They placed several strip electrodes onto

the cortical surface and found that beta coherence with STN was elevated in those contacts which covered the previously identified origin of the alleged hyperdirect pathway. Thus, intracranial recordings confirmed the results obtained in this study and suggest that the STN-cortical beta coherence reported here reflects direct motor cortical input to the STN. This interpretation tallies with the focal spatial distribution of STN-M1 beta coherence across electrode contacts. Both motor cortex and STN are somatotopically organized and any given cortical motor area projects precisely to its counterpart STN region (Nambu et al., 1996). Thus, any area in motor cortex is expected to be coupled to a limited portion of the STN rather than the whole nucleus.

The anatomical basis and the possible function are less clear for STN-STG alpha band coupling. A recent MEG-LFP study confirmed its existence and found it to be modulated by movement and dopaminergic medication (Oswal et al., 2012). Since STN-STG alpha coherence was not affected by the specific type of motor task, it was hypothesized that the coupling reflects a default functional interaction which needs to be transiently terminated before and during any kind of movement.

4.4 Conclusions

The spatial distribution of STN-cortical coherence in PD patients is frequency-dependent. There is a beta and an alpha pattern. The beta pattern represents functional connectivity between STN and cortical motor areas which might be facilitated by the hyperdirect pathway. The alpha pattern represents functional connectivity between STN and temporal areas. Its function and anatomical basis need further investigation.

5 Study 2: Differential modulation of STN-cortical and cortico-muscular coherence by movement and levodopa in Parkinson's disease

The aim of study 2 (Appendix 2) was to explore the effects of movement and dopaminergic medication on the oscillatory network identified in study 1. The experiment was designed to test hypotheses put forward by Peter Brown and colleagues who suggested that pathological hyper-synchrony in the beta band causes the slowing of movement in PD (Brown, 2007). Furthermore, it built on interpretations by Engel and Fries who consider beta oscillations a neural correlate of maintaining the status quo

(Engel and Fries, 2010). Based on these ideas, it was hypothesized that administration of levodopa will reduce beta coherence along with restoring motor capabilities. Moreover, movement was expected to decrease beta coherence, as movement implies a change in motor state.

The relationship between STN-cortical and cortico-muscular beta coherence was of particular interest. Given the generality of the hypotheses outlined above, one would expect beta band coupling to show the same responses everywhere in the motor system. Thus, experimental manipulations such as motor task execution or levodopa administration should elicit the same changes in STN-cortical and cortico-muscular beta coherence. However, it was reported previously that medication affects these two couplings differentially. Administration of levodopa was found to decrease STN-cortical beta coherence (Williams et al., 2002; Sharott et al., 2005) but to increase cortico-muscular beta coherence (Salenius et al., 2002). Thus, there are indications that STN-cortical and cortico-muscular beta coherence are independent to some degree. However, the levodopa-induced decrease in STN-cortical beta coherence is not a consistent finding. It was observed in some studies (Williams et al., 2002; Sharott et al., 2005) but not in others (Lalo et al., 2008; Litvak et al., 2011). In summary, the available data on the relationship between STN-cortical and cortico-muscular coherence is inconclusive. One reason for the divergent results could be that they were obtained in different patient cohorts. In order to perform a direct comparison, STN-cortical and cortico-muscular coherence were measured in the same patients in study 2.

5.1 Methods

10 PD patients of the akinetic-rigid subtype participated in the study. STN LFPs, MEG and forearm EMG were recorded simultaneously. Subjects performed two motor tasks in succession (see section 3): continuous elevation of the forearm (HOLD) and repetitive opening and closing of the fist (MOVE). Both tasks were performed once after withdrawal of anti-parkinsonian medication (OFF) and once after administration of levodopa (ON).

Coherence with STN LFPs and EMG was computed for two cortical regions of interest (ROIs). These were chosen as the coherence group maxima identified in study 1, i.e. M1 and STG. Coherence was analyzed in three frequency bands: alpha (8-12 Hz), beta (13-

35 Hz), and gamma (60-90 Hz). Effects of movement (factor levels: HOLD and MOVE) and medication (factor levels: ON and OFF) on coherence were tested by repeated measures analysis of variance. To investigate a potential relationship between coherence and PD symptoms, coherence was correlated with UPDRS akinesia and rigidity sub-scores.

5.2 Results

5.2.1 Effects of movement and medication

Coherence with M1 but not with STG was responsive to movement and medication. Interestingly, STN-M1 and M1-muscular coherence were modulated differentially (Fig. 1 of Appendix 2). M1-muscular coherence was decreased by repetitive movement compared to static contraction in the alpha and beta band. However, it was not modulated by levodopa administration. In contrast, STN-M1 beta coherence was decreased by levodopa administration but not significantly altered by movement.

5.2.2 Correlation with clinical parameters

Surprisingly, the dopamine-induced decrease in STN-M1 beta coherence was not correlated with the decrease in akinesia and rigidity scores. However, absolute STN-M1 beta coherence and akinesia/rigidity UPDRS scores were negatively correlated in the OFF state, i.e. the subjects with the strongest coherence had the least akinesia (Fig. 5 of Appendix 2). The correlation was specific to the beta frequency band and the OFF state, but unspecific with regard to motor task. A qualitatively similar result was obtained for M1-muscular beta coherence, suggesting inter-dependence between STN-M1 and M1-muscular coupling. Indeed, STN-cortical and cortico-muscular beta coherence were positively correlated in all experimental conditions, except for HOLD ON (Fig. S5 of Appendix 2).

5.3 Discussion

Study 2 revealed that STN-cortical and cortico-muscular coherence are differentially modulated by movement and medication, suggesting that they represent two partly independent functional loops. Please note, however, they are not entirely independent.

In most of the experimental conditions, they were positively correlated. The current results rather suggest that the two couplings respond differentially to levodopa but are closely related otherwise.

Previous studies investigating the effect of movement on M1-muscular (Kilner et al., 2000) and STN-M1 coherence (Litvak et al., 2012) found similar modulations. Both couplings showed a gamma increase at movement onset and a beta rebound following movement termination. Likewise, the current study found mean STN-cortical beta coherence to be reduced in the MOVE compared to the HOLD condition, but the reduction was less pronounced than for cortico-muscular coherence and not significant. Thus, it seems reasonable to assume that movement modulates STN-cortical and cortico-muscular coherence in a similar way. However, the modulation of cortico-muscular beta coherence appears to be stronger.

In contrast to movement, levodopa administration clearly had different effects on cortico-muscular and STN-cortical coupling. It reduced STN-cortical beta coherence but did not affect cortico-muscular beta coherence. The levodopa-induced reduction of STN-cortical beta coherence is in line with the concept of pathological hyper-synchrony in the motor system of PD patients (Brown, 2007). However, the negative correlation with akinesia and rigidity scores speaks against this hypothesis. Rather than being associated with akinesia, strong beta coherence appears to reflect relatively good mobility in the dopamine-depleted state.

There are two possible explanations for the obtained results: STN-cortical beta coherence might reflect a compensatory process which promotes movement in the OFF state but becomes oblivious when normal basal ganglia functionality is restored by levodopa administration. This interpretation would explain why the negative correlation with akinesia and rigidity was not observed in medication ON.

Alternatively, it is conceivable that STN-cortical beta coherence, as opposed to STN beta power, is required for normal motor function and is abnormally reduced in PD patients. The additional reduction induced by levodopa administration might be a side-effect of medication. It could result from the strong reduction of STN beta power and the resulting drop in signal-to-noise ratio.

A recent measurement performed in our laboratory supports the notion of different roles of STN beta power and STN-cortical beta coherence in PD pathophysiology (unpublished data). A patient with obsessive compulsive disorder (OCD) was implanted with bilateral electrodes for STN DBS and measured with the same experimental setup as used in this thesis. The experiment provided the unique opportunity to compare PD patients to a control subject free of motor impairments. Interestingly, this patient's STN-cortical beta coherence was very similar to coherence in PD patients, both with respect to the spatial distribution and with respect to coupling strength. In contrast, STN beta power was markedly lower than in any of the PD patients. In summary, these results suggest that the spatial pattern of STN-cortical beta coherence observed in PD patients is of physiological nature. Moreover, PD patients seem to exhibit strong STN beta power but normal to weak STN-cortical beta coherence, indicating that beta power and beta coherence are functionally different. These conclusions should be treated with caution, however, since the variability across individuals without movement disorder remains unknown.

5.4 Conclusions

Overall, study 2 suggests that oscillatory coupling in the beta band does not respond in a homogeneous fashion everywhere in the motor system. STN-cortical beta coherence was reduced by levodopa administration while cortico-muscular beta coherence was not affected. Furthermore, the negative correlation between beta coherence and akinesia demonstrates that beta band synchrony within the motor system does not impair movement execution in general. In contrast to local beta synchrony within the STN, inter-regional beta synchrony between STN and M1 is associated with comparably good motor performance in the dopamine-depleted state.

6 Study 3: A direct relationship between oscillatory STN-cortex coupling and rest tremor in Parkinson's disease

Besides akinesia and rigidity, tremor is one of the most eminent and frequent symptoms in PD. Classical parkinsonian tremor has a frequency of 3-7 Hz, occurs at rest and is attenuated at movement onset (reviewed in Deuschl et al., 2000). When patients settle to a new static position, the tremor typically reappears within a few seconds. At rest, tremor is usually not continuously present but intermitted by spontaneous pauses.

In the 1990s, it was debated whether tremor is caused by central or peripheral mechanisms such as spinal reflex arcs or mechanical resonances. During the last two decades, evidence for central oscillatory mechanisms has accumulated (reviewed in McAuley and Marsden, 2000; Schnitzler and Gross, 2005; Schnitzler et al., 2006). Electrophysiological studies revealed neuronal oscillations in STN, GPi and thalamus which were coherent with EMG recordings at tremor frequency and its first upper harmonic (e.g. Hurtado et al., 2005; Reck et al., 2009). A more extended tremor network including subcortical and cortical areas was identified by Timmermann et al. (2003) who localized cerebro-muscular coherence using MEG. The same network was later found to underlie voluntary tremor in healthy subjects (Pollok et al., 2004). Thus, there is evidence for pathological synchronization between several cortical and subcortical areas and tremulous muscles in parkinsonian rest tremor.

While power and coherence peaks at tremor frequency are good indications for central mechanisms in tremor generation, matching frequency alone does not imply correlation between neuronal oscillations and tremor manifestation – let alone a causal relationship. Theoretically, neuronal oscillations and tremor might be independent. In fact, rhythmic bursting at 5 Hz has been observed in the STN of tremor-free patients (Magariños-Ascone et al., 2000). Study 3 (Appendix 3) aimed at providing evidence for a direct relationship between coherence and tremor manifestation. In other words, it investigated whether coherence at tremor frequency is indeed a neural correlate of rest tremor. In contrast to previous studies, it compared tremor epochs to tremor-free epochs within subjects to clarify i) whether coherence increases when tremor emerges and ii) whether coherence is correlated with tremor amplitude.

6.1 Methods

11 tremor-dominant PD patients participated in the study. STN LFPs, MEG and forearm EMG were recorded simultaneously. The study compared epochs with spontaneous rest tremor in the upper limb to tremor-free epochs in the REST OFF condition (Fig. 3). STN power, MEG power, STN-cortical coherence, cortico-muscular coherence and STN-muscular coherence were estimated on the sensor level. MEG channels of interest were selected *a priori* such that they covered motor and premotor areas contralateral to the tremulous limb. This selection was refined individually based on maximal sensor power at tremor frequency (conditions pooled). Similarly, LFP and EMG channel selection was based on maximal coherence at tremor frequency with the MEG sensors of interest. Following sensor level analysis, coherence changes induced by tremor were localized using DICS (Gross et al., 2001). Cortico-cortical source level coupling was investigated by analysis of coherence and the imaginary part of coherency, a coupling measure insensitive to volume conduction (Nolte et al., 2004).

6.2 Results

6.2.1 Sensor level

A time-resolved analysis of spectral power revealed that STN oscillations at individual tremor frequency increase in amplitude when tremor emerges (Fig. 2 of Appendix 3). In addition, cortical power decreased in the beta band following tremor onset. STN-cortical, cortico-muscular and STN-muscular coherence were found to be higher during tremor than during tremor-free epochs specifically at tremor frequency (Fig. 3 of Appendix 3). The tremor-induced change in STN-cortical coupling was positively correlated with the change in EMG power.

6.2.2 Source level

Analysis of source level coherence at tremor frequency revealed significant changes in cortico-muscular but not in STN-cortical coherence. Tremor-induced increases were observed in M1, premotor cortex (PMC) and posterior parietal cortex (PPC) contralateral to the tremulous limb (Fig. 4 of Appendix 3). These cortical areas were found to be themselves coupled at tremor frequency and double tremor frequency. Like

cortico-muscular coupling, cortico-cortical coupling increased during tremor. Importantly, analysis of the imaginary part of coherency showed that cortico-cortical coupling was not a trivial consequence of volume conduction.

6.3 Discussion

Study 3 demonstrated that oscillatory coupling within the sensorimotor system increases during tremor. Moreover, it reproduced core elements of the previously described tremor network. Like study 3, earlier studies reported tremor-related coherence in M1, PMC and PPC (Timmermann et al., 2003; Pollok et al., 2004; Muthuraman et al., 2012). Compared to these works, study 3 made use of a more stringent methodology. The analysis included statistical tests at the group level and controlled for multiple comparisons. Furthermore, it made use of a coupling measure which is insensitive to trivial couplings resulting from volume conduction. Thus, it provided a reliable description of the tremor network.

Naturally, increased reliability comes at the cost of decreased sensitivity. Study 3 did not detect tremor-induced coherence changes in thalamus or cerebellum although both are likely involved in tremor generation (Helmich et al., 2011; Mure et al., 2011). Moreover, it did not detect an increase in STN-cortical coherence on the source level even though it was observable on the sensor level. Most likely, recording times were too short to localize this effect.

Study 3 provided important insights into the role of the STN in tremor. It confirmed a single case report stating that beta power decreases as tremor becomes manifest (Wang et al., 2005). In addition, it showed that STN power at individual tremor frequency increases following tremor onset. Thus, study 3 provided an electrophysiological biomarker of tremor onset which could be used by closed-loop DBS systems to trigger stimulation (see section 8). Further, study 3 revealed that the coupling between STN and other brain areas increases during tremor. Importantly, the increase was proportional to the increase in EMG power, suggesting that the STN generates or receives oscillatory signals which directly reflect tremor amplitude.

6.4 Conclusions

Study 3 established that STN, primary motor cortex, premotor cortex and posterior parietal cortex are part of the tremor network. Furthermore, it demonstrated that coherence within this network increases during tremor. In conclusion, the results suggest that oscillatory coupling at tremor frequency is indeed a neural correlate of parkinsonian rest tremor.

7 General discussion

This thesis aimed at investigating synchronous oscillations in PD on the network level by scanning the brain for coherence with STN LFPs and muscle activity, and by characterizing changes in coherence due to movement, dopaminergic medication and tremor. Moreover, it explored the relationship between neuronal oscillations and PD symptoms.

The overall impact was twofold: First, the studies substantially advanced the establishment of simultaneous MEG-LFP recordings as a tool for investigating functional connectivity in PD (reviewed in Schnitzler and Hirschmann, 2012; Appendix 4). The technique was introduced not more than three years ago (Litvak et al., 2010). Due to the requirements with regard to hardware and patient access, it is available in just a few centers worldwide. Thus, the studies presented here can be understood as a proof of principle, demonstrating the usefulness and feasibility of the approach.

Second, the thesis contributed significantly to the characterization of oscillatory coupling in PD. In addition to revealing the frequency-dependent spatial distribution of coherence between STN and cortex (Study 1), it confirmed some common ideas about the role of neuronal oscillations in PD and motor control in general. In line with the hypothesis that beta oscillations signal maintenance of the status quo (Engel and Fries, 2010), beta coherence between motor cortex and muscle was found to be suppressed during repetitive movement compared to static contraction (study 2). Moreover, tremor manifestation was found to be associated with an increase in coherence at tremor frequency in a distributed sensorimotor network (study 3), supporting the hypothesis that pathologically enhanced neuronal synchronization underlies parkinsonian rest tremor (Schnitzler et al., 2006). However, not all of the results are in line with the idea of

pathological hyper-synchrony. STN-cortical beta coherence was negatively correlated with akinesia and rigidity UPDRS sub-scores (study 2), suggesting that it counteracts rather than promotes the slowing of movement. Currently, there are no other publications to confirm or disconfirm this observation. Thus, future studies are needed to clarify whether STN-cortical beta coherence reflects a pathological or a physiological mechanism. Confirmation of the physiological or compensatory function suggested by study 2 would imply that STN beta power and STN-cortical beta coherence reflect fundamentally different processes.

In summary, this thesis made valuable contributions to research on PD pathophysiology. It showed that coherent oscillations are modulated during movement, respond to medication and correlate with clinical symptoms. These findings substantiate the role of oscillatory coupling in PD.

8 Outlook

The above discussion about the function of STN-cortical beta coherence highlights a fundamental challenge to clinical electrophysiology: biomarkers need to be separated from physiological mechanisms and causes need to be separated from consequences of the disease. Distinguishing biomarkers from physiological mechanisms is especially challenging in invasive patient studies as healthy controls are lacking. At best, recordings from PD patients can be compared to recordings from patients with unrelated diseases. In most cases, however, inference on pathological relevance is based on treatment ON vs. treatment OFF contrasts or experiments in animal models. Both approaches bear obvious caveats: pharmacological as well as surgical treatment does not only have clinical, but also electrophysiological side-effects. In consequence, changes observed in the treatment ON condition might be unrelated to the treatment-induced improvement of symptoms. With regard to animal models, interpretational difficulties arise from symptomatic, electrophysiological and anatomical differences between PD patients and MPTP-treated monkeys and 6OHDA-treated rodents, respectively (Betarbet et al., 2002).

In the future, PD research will need to identify reliable, electrophysiological biomarkers of PD in humans and clarify whether these are causal or correlative. In particular, it is important to know if hyper-synchrony may indeed cause motor impairments. Apart

from entrainment of neuronal oscillations by periodic brain stimulation, such as DBS at beta frequencies, one approach could be to monitor oscillations for longer periods of time. Longitudinal studies can answer an important question: What comes first, symptoms or synchronization?

So far, longitudinal electrophysiological studies are rare and restricted to animal models of PD. Interestingly, the available data suggest that beta synchrony and motor symptoms do not develop in parallel, indicating that beta oscillations might not cause motor symptoms (Leblois et al., 2007; Degos et al., 2009; Dejean et al., 2012). Future studies need to elaborate on the temporal evolution of electrophysiological hallmarks and relate it to disease progression. In patients, this will be possible in the near future. The new generation of DBS devices will be able to record data from deep brain electrodes and transmit them via radio communication (Santa et al., 2008). Thus, physical access to the electrodes will no longer be needed for deep brain recordings and the long-term dynamics of oscillations can be investigated in humans.

Apart from radio communication, the new generation of DBS systems will most likely be able to register brain activity and to flexibly react to changes in electrophysiological parameters. A recent animal study provided first evidence that closed-loop stimulation triggered by endogenous brain activity provides better symptom alleviation than conventional DBS (Rosin et al., 2011). Since closed-loop systems are not continuously active, they are expected to reduce the occurrence of side-effects and to provide more efficient battery usage. One of the challenges in the development of closed-loop systems is the identification of appropriate control parameters. This thesis suggests that neuronal oscillations might be a good candidate. More specifically, improved tremor alleviation might be achieved by applying DBS whenever STN power increases at double the tremor frequency and decreases in the beta band. Ideally, stimulation would be tailored to obtain destructive interference with the endogenous tremor rhythm (Brittain et al., 2013). Moreover, the current thesis indicates that resting state STN beta power, but not STN-cortical beta coherence, is a promising candidate parameter which could be used for triggering high frequency DBS in patients suffering from akinesia.

9 References

- Albin, R.L., Young, A.B., and Penney, J.B. (1989). The functional anatomy of basal ganglia disorders. *Trends in Neurosciences* 12, 366–375.
- Alexander, G.E., DeLong, M.R., and Strick, P.L. (1986). Parallel Organization of Functionally Segregated Circuits Linking Basal Ganglia and Cortex. *Annual Review of Neuroscience* 9, 357–381.
- Ashby, F.G., Turner, B.O., and Horvitz, J.C. (2010). Cortical and basal ganglia contributions to habit learning and automaticity. *Trends in Cognitive Sciences* 14, 208–215.
- Bar-Gad, I., Morris, G., and Bergman, H. (2003). Information processing, dimensionality reduction and reinforcement learning in the basal ganglia. *Progress in Neurobiology* 71, 439–473.
- Berger, P.D.H. (1929). Über das Elektrenkephalogramm des Menschen. *Archiv f. Psychiatrie* 87, 527–570.
- Bergman, H., Wichmann, T., and DeLong, M.R. (1990). Reversal of experimental parkinsonism by lesions of the subthalamic nucleus. *Science* 249, 1436–1438.
- Bergman, H., Wichmann, T., Karmon, B., and DeLong, M.R. (1994). The primate subthalamic nucleus. II. Neuronal activity in the MPTP model of parkinsonism. *J Neurophysiol* 72, 507–520.
- Betarbet, R., Sherer, T.B., and Greenamyre, J.T. (2002). Animal models of Parkinson's disease. *BioEssays* 24, 308–318.
- Beurrier, C., Bioulac, B., Audin, J., and Hammond, C. (2001). High-Frequency Stimulation Produces a Transient Blockade of Voltage-Gated Currents in Subthalamic Neurons. *J Neurophysiol* 85, 1351–1356.
- Braak, H., Tredici, K.D., Rüb, U., de Vos, R.A., Jansen Steur, E.N., and Braak, E. (2003). Staging of brain pathology related to sporadic Parkinson's disease. *Neurobiology of Aging* 24, 197–211.
- Brittain, J., Probert-Smith, P., Aziz, T., and Brown, P. (2013). Tremor suppression by rhythmic transcranial current stimulation. *Curr. Biol.* 23, 436–440.
- Brown, P. (2007). Abnormal oscillatory synchronisation in the motor system leads to impaired movement. *Curr. Opin. Neurobiol.* 17, 656–664.
- Brown, P., Oliviero, A., Mazzone, P., Insola, A., Tonali, P., and Di Lazzaro, V. (2001). Dopamine dependency of oscillations between subthalamic nucleus and pallidum in Parkinson's disease. *J. Neurosci.* 21, 1033–1038.
- Buzsáki, G. (2006). *Rhythms of the Brain* (Oxford University Press).
- Buzsáki, G., Anastassiou, C.A., and Koch, C. (2012). The origin of extracellular fields and currents — EEG, ECoG, LFP and spikes. *Nature Reviews Neuroscience* 13, 407–420.

- Cassidy, M., Mazzone, P., Oliviero, A., Insola, A., Tonali, P., Di Lazzaro, V., and Brown, P. (2002). Movement-related changes in synchronization in the human basal ganglia. *Brain* *125*, 1235–1246.
- Chen, C.C., Litvak, V., Gilbertson, T., Kühn, A., Lu, C.S., Lee, S.T., Tsai, C.H., Tisch, S., Limousin, P., Hariz, M., et al. (2007). Excessive synchronization of basal ganglia neurons at 20 Hz slows movement in Parkinson's disease. *Experimental Neurology* *205*, 214–221.
- Degos, B., Deniau, J.-M., Chavez, M., and Maurice, N. (2009). Chronic but not Acute Dopaminergic Transmission Interruption Promotes a Progressive Increase in Cortical Beta Frequency Synchronization: Relationships to Vigilance State and Akinesia. *Cereb. Cortex* *19*, 1616–1630.
- Dejean, C., Nadjar, A., Le Moine, C., Bioulac, B., Gross, C.E., and Boraud, T. (2012). Evolution of the dynamic properties of the cortex-basal ganglia network after dopaminergic depletion in rats. *Neurobiol. Dis.* *46*, 402–413.
- DeLong, M.R. (1990). Primate models of movement disorders of basal ganglia origin. *Trends in Neurosciences* *13*, 281–285.
- Desmurget, M., and Turner, R.S. (2008). Testing Basal Ganglia Motor Functions Through Reversible Inactivations in the Posterior Internal Globus Pallidus. *J Neurophysiol* *99*, 1057–1076.
- Desmurget, M., and Turner, R.S. (2010). Motor Sequences and the Basal Ganglia: Kinematics, Not Habits. *J. Neurosci.* *30*, 7685–7690.
- Deuschl, G., Raethjen, J., Baron, R., Lindemann, M., Wilms, H., and Krack, P. (2000). The pathophysiology of parkinsonian tremor: a review. *J. Neurol.* *247 Suppl 5*, V33–48.
- Engel, A.K., and Fries, P. (2010). Beta-band oscillations--signalling the status quo? *Curr. Opin. Neurobiol.* *20*, 156–165.
- Eusebio, A., Thevathasan, W., Doyle Gaynor, L., Pogosyan, A., Bye, E., Foltynie, T., Zrinzo, L., Ashkan, K., Aziz, T., and Brown, P. (2011). Deep brain stimulation can suppress pathological synchronisation in parkinsonian patients. *J. Neurol. Neurosurg. Psychiatr.* *82*, 569–573.
- Foffani, G., Priori, A., Egidi, M., Rampini, P., Tamma, F., Caputo, E., Moxon, K.A., Cerutti, S., and Barbieri, S. (2003). 300-Hz subthalamic oscillations in Parkinson's disease. *Brain* *126*, 2153–2163.
- Fogelson, N., Williams, D., Tijssen, M., van Bruggen, G., Speelman, H., and Brown, P. (2006). Different functional loops between cerebral cortex and the subthalamic area in Parkinson's disease. *Cereb. Cortex* *16*, 64–75.
- Fries, P. (2005). A mechanism for cognitive dynamics: neuronal communication through neuronal coherence. *Trends in Cognitive Sciences* *9*, 474–480.
- Gerfen, C., Engber, T., Mahan, L., Susel, Z., Chase, T., Monsma, F., and Sibley, D. (1990). D1 and D2 dopamine receptor-regulated gene expression of striatonigral and striatopallidal neurons. *Science* *250*, 1429–1432.

- Gerfen, C.R., and Bolam, J.P. (2010). The Neuroanatomical Organization of the Basal Ganglia. In *Handbook of Basal Ganglia Structure and Function*, H. Steiner, and K.Y. Tseng, eds. (Academic Press), pp. 3–28.
- Gradinaru, V., Mogri, M., Thompson, K.R., Henderson, J.M., and Deisseroth, K. (2009). Optical Deconstruction of Parkinsonian Neural Circuitry. *Science* 324, 354–359.
- Gross, J., Kujala, J., Hamalainen, M., Timmermann, L., Schnitzler, A., and Salmelin, R. (2001). Dynamic imaging of coherent sources: Studying neural interactions in the human brain. *Proc. Natl. Acad. Sci. U.S.A* 98, 694–699.
- Hämäläinen, M., Hari, R., Ilmoniemi, R.J., Knuutila, J., and Lounasmaa, O.V. (1993). Magnetoencephalography—theory, instrumentation, and applications to noninvasive studies of the working human brain. *Rev. Mod. Phys.* 65, 413–497.
- Hammond, C., Bergman, H., and Brown, P. (2007). Pathological synchronization in Parkinson's disease: networks, models and treatments. *Trends Neurosci.* 30, 357–364.
- Helmich, R.C., Hallett, M., Deuschl, G., Toni, I., and Bloem, B.R. (2012). Cerebral causes and consequences of parkinsonian resting tremor: a tale of two circuits? *Brain* 135, 3206–3226.
- Helmich, R.C., Janssen, M.J.R., Oyen, W.J.G., Bloem, B.R., and Toni, I. (2011). Pallidal dysfunction drives a cerebellothalamic circuit into Parkinson tremor. *Annals of Neurology* 69, 269–281.
- Hillebrand, A., Singh, K.D., Holliday, I.E., Furlong, P.L., and Barnes, G.R. (2005). A new approach to neuroimaging with magnetoencephalography. *Hum Brain Mapp* 25, 199–211.
- Hutchison, W.D., Lozano, A.M., Tasker, R.R., Lang, A.E., and Dostrovsky, J.O. (1997). Identification and characterization of neurons with tremor-frequency activity in human globus pallidus. *Exp Brain Res* 113, 557–563.
- Jenkins, I.H., Fernandez, W., Playford, E.D., Lees, A.J., Frackowiak, R.S.J., Passingham, R.E., and Brooks, D.J. (1992). Impaired activation of the supplementary motor area in Parkinson's disease is reversed when akinesia is treated with apomorphine. *Annals of Neurology* 32, 749–757.
- Katzner, S., Nauhaus, I., Benucci, A., Bonin, V., Ringach, D.L., and Carandini, M. (2009). Local Origin of Field Potentials in Visual Cortex. *Neuron* 61, 35–41.
- Kilner, J.M., Baker, S.N., Salenius, S., Hari, R., and Lemon, R.N. (2000). Human cortical muscle coherence is directly related to specific motor parameters. *J. Neurosci.* 20, 8838–8845.
- Kincaid, A.E., Zheng, T., and Wilson, C.J. (1998). Connectivity and Convergence of Single Corticostriatal Axons. *J. Neurosci.* 18, 4722–4731.
- Kravitz, A.V., Freeze, B.S., Parker, P.R.L., Kay, K., Thwin, M.T., Deisseroth, K., and Kreitzer, A.C. (2010). Regulation of parkinsonian motor behaviours by optogenetic control of basal ganglia circuitry. *Nature* 466, 622–626.

- Kringelbach, M.L., Jenkinson, N., Owen, S.L.F., and Aziz, T.Z. (2007). Translational principles of deep brain stimulation. *Nature Reviews Neuroscience* 8, 623–635.
- Kühn, A.A., Kupsch, A., Schneider, G.-H., and Brown, P. (2006). Reduction in subthalamic 8-35 Hz oscillatory activity correlates with clinical improvement in Parkinson's disease. *Eur. J. Neurosci.* 23, 1956–1960.
- Laitinen, L.V., Bergenheim, A.T., and Hariz, M.I. (1992). Leksell's posteroventral pallidotomy in the treatment of Parkinson's disease. *J. Neurosurg.* 76, 53–61.
- Lalo, E., Thobois, S., Sharott, A., Polo, G., Mertens, P., Pogosyan, A., and Brown, P. (2008). Patterns of bidirectional communication between cortex and basal ganglia during movement in patients with Parkinson disease. *J. Neurosci.* 28, 3008–3016.
- Leblois, A., Meissner, W., Bioulac, B., Gross, C.E., Hansel, D., and Boraud, T. (2007). Late emergence of synchronized oscillatory activity in the pallidum during progressive parkinsonism. *European Journal of Neuroscience* 26, 1701–1713.
- Levy, R., and Dubois, B. (2006). Apathy and the Functional Anatomy of the Prefrontal Cortex–Basal Ganglia Circuits. *Cereb. Cortex* 16, 916–928.
- Levy, R., Hutchison, W.D., Lozano, A.M., and Dostrovsky, J.O. (2000). High-frequency Synchronization of Neuronal Activity in the Subthalamic Nucleus of Parkinsonian Patients with Limb Tremor. *J. Neurosci.* 20, 7766–7775.
- Lewis, S.J.G., Foltynie, T., Blackwell, A.D., Robbins, T.W., Owen, A.M., and Barker, R.A. (2005). Heterogeneity of Parkinson's disease in the early clinical stages using a data driven approach. *J. Neurol. Neurosurg. Psychiatr.* 76, 343–348.
- Limousin, P., Krack, P., Pollak, P., Benazzouz, A., Ardouin, C., Hoffmann, D., and Benabid, A.-L. (1998). Electrical Stimulation of the Subthalamic Nucleus in Advanced Parkinson's Disease. *New England Journal of Medicine* 339, 1105–1111.
- Litvak, V., Eusebio, A., Jha, A., Oostenveld, R., Barnes, G., Foltynie, T., Limousin, P., Zrinzo, L., Hariz, M., Friston, K., et al. (2012). Movement-Related Changes in Local and Long-Range Synchronization in Parkinson's Disease Revealed by Simultaneous Magnetoencephalography and Intracranial Recordings. *J. Neurosci.* 32, 10541–10553.
- Litvak, V., Eusebio, A., Jha, A., Oostenveld, R., Barnes, G.R., Penny, W.D., Zrinzo, L., Hariz, M.I., Limousin, P., Friston, K.J., et al. (2010). Optimized beamforming for simultaneous MEG and intracranial local field potential recordings in deep brain stimulation patients. *Neuroimage* 50, 1578–1588.
- Litvak, V., Jha, A., Eusebio, A., Oostenveld, R., Foltynie, T., Limousin, P., Zrinzo, L., Hariz, M.I., Friston, K., and Brown, P. (2011). Resting oscillatory cortico-subthalamic connectivity in patients with Parkinson's disease. *Brain* 134, 359–374.
- López-Azcárate, J., Tainta, M., Rodríguez-Oroz, M.C., Valencia, M., González, R., Guridi, J., Iriarte, J., Obeso, J.A., Artieda, J., and Alegre, M. (2010). Coupling between Beta and High-Frequency Activity in the Human Subthalamic Nucleus May Be a Pathophysiological Mechanism in Parkinson's Disease. *J. Neurosci.* 30, 6667–6677.

- Lozano, A., Lang, A., Galvez-Jimenez, N., Miyasaki, J., Duff, J., Hutchison, W., and Dostrovsky, J. (1995). Effect of GPi pallidotomy on motor function in Parkinson's disease. *The Lancet* *346*, 1383–1387.
- Magariños-Ascone, C.M., Figueiras-Mendez, R., Riva-Meana, C., and Córdoba-Fernández, A. (2000). Subthalamic neuron activity related to tremor and movement in Parkinson's disease. *European Journal of Neuroscience* *12*, 2597–2607.
- Maris, E., Schoffelen, J.-M., and Fries, P. (2007). Nonparametric statistical testing of coherence differences. *Journal of Neuroscience Methods* *163*, 161–175.
- McAuley, J.H., and Marsden, C.D. (2000). Physiological and pathological tremors and rhythmic central motor control. *Brain* *123 (Pt 8)*, 1545–1567.
- Mink, J.W. (1996). The basal ganglia: focused selection and inhibition of competing motor programs. *Prog. Neurobiol.* *50*, 381–425.
- Mure, H., Hirano, S., Tang, C.C., Isaias, I.U., Antonini, A., Ma, Y., Dhawan, V., and Eidelberg, D. (2011). Parkinson's disease tremor-related metabolic network: Characterization, progression, and treatment effects. *NeuroImage* *54*, 1244–1253.
- Muthuraman, M., Heute, U., Arning, K., Anwar, A.R., Elble, R.J., Deuschl, G., and Raethjen, J. (2012). Oscillating central motor networks in pathological tremors and voluntary movements. What makes the difference? *NeuroImage* *60*, 1331–1339.
- Nambu, A., Takada, M., Inase, M., and Tokuno, H. (1996). Dual somatotopical representations in the primate subthalamic nucleus: evidence for ordered but reversed body-map transformations from the primary motor cortex and the supplementary motor area. *J. Neurosci.* *16*, 2671–2683.
- Nolte, G., Bai, O., Wheaton, L., Mari, Z., Vorbach, S., and Hallett, M. (2004). Identifying true brain interaction from EEG data using the imaginary part of coherency. *Clin Neurophysiol* *115*, 2292–2307.
- Obeso, J.A., Rodriguez-Oroz, M.C., Goetz, C.G., Marin, C., Kordower, J.H., Rodriguez, M., Hirsch, E.C., Farrer, M., Schapira, A.H.V., and Halliday, G. (2010). Missing pieces in the Parkinson's disease puzzle. *Nature Medicine* *16*, 653–661.
- Oswal, A., Brown, P., and Litvak, V. (2012). Movement related dynamics of subthalamo-cortical alpha connectivity in Parkinson's disease. *Neuroimage* *70C*, 132–142.
- Özkurt, T.E., Butz, M., Homburger, M., Elben, S., Vesper, J., Wojtecki, L., and Schnitzler, A. (2011). High frequency oscillations in the subthalamic nucleus: a neurophysiological marker of the motor state in Parkinson's disease. *Exp. Neurol.* *229*, 324–331.
- Pell, M.D., and Leonard, C.L. (2003). Processing emotional tone from speech in Parkinson's disease: A role for the basal ganglia. *Cognitive, Affective, & Behavioral Neuroscience* *3*, 275–288.
- Pogosyan, A., Gaynor, L.D., Eusebio, A., and Brown, P. (2009). Boosting Cortical Activity at Beta-Band Frequencies Slows Movement in Humans. *Current Biology* *19*, 1637–1641.

- Pollok, B., Gross, J., Dirks, M., Timmermann, L., and Schnitzler, A. (2004). The cerebral oscillatory network of voluntary tremor. *J. Physiol. (Lond.)* 554, 871–878.
- Rosin, B., Slovik, M., Mitelman, R., Rivlin-Etzion, M., Haber, S.N., Israel, Z., Vaadia, E., and Bergman, H. (2011). Closed-Loop Deep Brain Stimulation Is Superior in Ameliorating Parkinsonism. *Neuron* 72, 370–384.
- Salenius, S., Avikainen, S., Kaakkola, S., Hari, R., and Brown, P. (2002). Defective cortical drive to muscle in Parkinson's disease and its improvement with levodopa. *Brain* 125, 491–500.
- Santa, W., Jensen, R., Miesel, K., Carlson, D., Avestruz, A., Molnar, G., and Denison, T. (2008). Radios for the brain? a practical micropower sensing and algorithm architecture for neurostimulators. In *IEEE International Symposium on Circuits and Systems, 2008. ISCAS 2008*, pp. 348–351.
- Schnitzler, A., and Gross, J. (2005). Normal and pathological oscillatory communication in the brain. *Nat. Rev. Neurosci.* 6, 285–296.
- Schnitzler, A., and Hirschmann, J. (2012). Magnetoencephalography and neuromodulation. *Int. Rev. Neurobiol.* 107, 121–136.
- Schnitzler, A., Timmermann, L., and Gross, J. (2006). Physiological and pathological oscillatory networks in the human motor system. *J. Physiol. Paris* 99, 3–7.
- Selikhova, M., Williams, D.R., Kempster, P.A., Holton, J.L., Revesz, T., and Lees, A.J. (2009). A clinico-pathological study of subtypes in Parkinson's disease. *Brain* 132, 2947–2957.
- Sharott, A., Magill, P.J., Harnack, D., Kupsch, A., Meissner, W., and Brown, P. (2005). Dopamine depletion increases the power and coherence of beta-oscillations in the cerebral cortex and subthalamic nucleus of the awake rat. *Eur. J. Neurosci.* 21, 1413–1422.
- Syed, E.C.J., Benazzouz, A., Taillade, M., Baufreton, J., Champeaux, K., Falgairolle, M., Bioulac, B., Gross, C.E., and Boraud, T. (2012). Oscillatory entrainment of subthalamic nucleus neurons and behavioural consequences in rodents and primates. *European Journal of Neuroscience* 36, 3246–3257.
- Timmermann, L., Gross, J., Dirks, M., Volkmann, J., Freund, H.-J., and Schnitzler, A. (2003). The cerebral oscillatory network of parkinsonian resting tremor. *Brain* 126, 199–212.
- Turner, R.S., and Anderson, M.E. (1997). Pallidal discharge related to the kinematics of reaching movements in two dimensions. *J. Neurophysiol.* 77, 1051–1074.
- Varela, F., Lachaux, J.-P., Rodriguez, E., and Martinerie, J. (2001). The brainweb: Phase synchronization and large-scale integration. *Nat Rev Neurosci* 2, 229–239.
- Van Veen, B.D., and Buckley, K.M. (1988). Beamforming: a versatile approach to spatial filtering. *IEEE ASSP Magazine* 5, 4–24.

- Wang, S., Aziz, T.Z., Stein, J.F., and Liu, X. (2005). Time–frequency analysis of transient neuromuscular events: dynamic changes in activity of the subthalamic nucleus and forearm muscles related to the intermittent resting tremor. *Journal of Neuroscience Methods* 145, 151–158.
- Weinstein, S., and Ebert, P. (1971). Data Transmission by Frequency-Division Multiplexing Using the Discrete Fourier Transform. *IEEE Transactions on Communication Technology* 19, 628–634.
- Whitmer, D., de Solages, C., Hill, B., Yu, H., Henderson, J.M., and Bronte-Stewart, H. (2012). High frequency deep brain stimulation attenuates subthalamic and cortical rhythms in Parkinson’s disease. *Front Hum Neurosci* 6, 155.
- Wichmann, T., Bergman, H., Starr, P.A., Subramanian, T., Watts, R.L., and DeLong, M.R. (1999). Comparison of MPTP-induced changes in spontaneous neuronal discharge in the internal pallidal segment and in the substantia nigra pars reticulata in primates. *Exp Brain Res* 125, 397–409.
- Wichmann, T., and Dostrovsky, J.O. (2011). Pathological basal ganglia activity in movement disorders. *Neuroscience* 198, 232–244.
- Williams, D., Tijssen, M., Van Bruggen, G., Bosch, A., Insola, A., Di Lazzaro, V., Mazzone, P., Oliviero, A., Quartarone, A., Speelman, H., et al. (2002). Dopamine-dependent changes in the functional connectivity between basal ganglia and cerebral cortex in humans. *Brain* 125, 1558–1569.

10 Erklärung

Hiermit erkläre ich, dass ich die vorgelegte Dissertation eigenständig und ohne unerlaubte Hilfe angefertigt habe. Die Dissertation wurde in der vorliegenden oder in ähnlicher Form noch bei keiner anderen Institution eingereicht. Ich habe bisher keine erfolglosen Promotionsversuche unternommen.

Düsseldorf, den

Jan Hirschmann

11 Danksagung

Mein besonderer Dank gilt meinem Doktorvater Prof. Dr. Alfons Schnitzler für seine kontinuierliche Unterstützung, die ausgezeichnete wissenschaftliche Betreuung und seine anhaltende und ansteckende Begeisterung für dieses Forschungsprojekt.

Prof. Dr. Tobias Kalenscher danke ich herzlich für die Zweitbetreuung dieser Doktorarbeit.

Des Weiteren bin ich dem MEG-DBS Team ausgesprochen dankbar für die hervorragende Zusammenarbeit und die große Hilfsbereitschaft, die diese Gruppe auszeichnet. Dazu zählen Dr. Lars Wojtecki, Dr. Markus Butz, Dr. Tolga Özkurt, Dr. Christian Hartmann, Dipl.-Psych. Saskia Elben, Dr. Nienke Hoogenboom und cand. med. Melanie Homburger. Zudem danke ich Prof. Dr. Jan Vesper, der die Experimente von neurochirurgischer Seite stets unterstützt hat.

Ohne die Hilfsbereitschaft der Patienten, die allesamt ohne eigenen Nutzen an den teilweise langwierigen Messungen teilgenommen haben, wäre diese Arbeit nicht möglich gewesen. Herzlichen Dank!

Für das Korrekturlesen dieser Arbeit gilt mein Dank Dr. Elisabeth May, Dr. Joachim Lange und Dr. Markus Butz.

Zu guter Letzt möchte ich mich bei meinen Eltern und bei meiner Freundin Tina bedanken, mit der ich alle Höhen und Tiefen der Promotion teilen konnte.

12 Appendix

This work is based on:

Appendix 1:

Hirschmann, J., Özkurt, T.E., Butz, M., Homburger, M., Elben, S., Hartmann, C.J., Vesper, J., Wojtecki, L., and Schnitzler, A. (2011). Distinct oscillatory STN-cortical loops revealed by simultaneous MEG and local field potential recordings in patients with Parkinson's disease. *Neuroimage* 55, 1159–1168.

Impact factor (2011): 5.89

Personal contribution: 80%

Appendix 2:

Hirschmann, J., Özkurt, T.E., Butz, M., Homburger, M., Elben, S., Hartmann, C.J., Vesper, J., Wojtecki, L., and Schnitzler, A. (2013). Differential modulation of STN-cortical and cortico-muscular coherence by movement and levodopa in Parkinson's disease. *NeuroImage* 68, 203–213.

Impact factor (2011): 5.89

Personal contribution: 80%

Appendix 3:

Hirschmann, J., Hartmann, C.J., Butz, M., Hoogenboom, N., Özkurt, T.E., Elben, S., Vesper, J., Wojtecki, L., and Schnitzler, A. (2013). A direct relationship between oscillatory STN-cortex coupling and rest tremor in Parkinson's disease. *Brain* 136 (12), 3659-3670.

Impact factor (2012): 9.92

Personal contribution: 80%

Other aspects are taken from:**Appendix 4:**

Schnitzler, A., and Hirschmann, J. (2012). Magnetoencephalography and neuromodulation. *Int. Rev. Neurobiol.* 107, 121–136.

Impact factor (2011): 2.35

Personal contribution: 50%



Distinct oscillatory STN-cortical loops revealed by simultaneous MEG and local field potential recordings in patients with Parkinson's disease

J. Hirschmann^{a,b}, T.E. Özkurt^{a,b}, M. Butz^{a,b}, M. Homburger^{a,b}, S. Elben^{a,b}, C.J. Hartmann^{a,b}, J. Vesper^c, L. Wojtecki^{a,b}, A. Schnitzler^{a,b,*}

^a Institute of Clinical Neuroscience and Medical Psychology, Medical Faculty, Heinrich-Heine-University Düsseldorf, Düsseldorf, Germany

^b Department of Neurology, University Hospital Düsseldorf, Düsseldorf, Germany

^c Department of Functional Neurosurgery and Stereotaxy, University Hospital Düsseldorf, Düsseldorf, Germany

ARTICLE INFO

Article history:

Received 20 September 2010

Revised 2 November 2010

Accepted 19 November 2010

Available online 29 November 2010

Keywords:

Parkinson's disease

Magnetoencephalography

Subthalamic nucleus

Functional connectivity

Oscillations

Coherence

ABSTRACT

Neuronal oscillations are assumed to play a pivotal role in the pathophysiology of Parkinson's disease (PD). Neurons in the subthalamic nucleus (STN) generate oscillations which are coupled to rhythmic population activity both in other basal ganglia nuclei and cortical areas.

In order to localize these cortical areas, we recorded local field potentials (LFPs) and magnetoencephalography (MEG) simultaneously in PD patients undergoing surgery for deep brain stimulation (DBS). Patients were withdrawn from antiparkinsonian medication and recorded at rest. We scanned the entire brain for oscillations coherent with LFPs recorded from the STN with a frequency domain beamformer.

Coherent activity in the low (12–20 Hz) and high (20–35 Hz) beta range was found in the ipsilateral sensorimotor and the premotor cortex. Coherence in the alpha range (7–12 Hz) was observed at various locations in the ipsilateral temporal lobe. In a subset of subjects, the superior temporal gyrus consistently showed coherent alpha oscillations.

Our findings provide new insights into patterns of frequency-specific functional connectivity between basal ganglia and cortex and suggest that simultaneous inter-regional interactions may be segregated in the frequency domain. Furthermore, they demonstrate that simultaneous MEG-LFP recordings are a powerful tool to study interactions between brain areas in PD patients undergoing surgery for DBS.

© 2010 Elsevier Inc. All rights reserved.

Introduction

Recordings from the basal ganglia of patients with Parkinson's disease (PD) undergoing surgery for deep brain stimulation (DBS) revealed strong oscillatory power in the alpha (7–12 Hz) and beta (12–35 Hz) band (Brown et al., 2001; Kühn et al., 2004; Levy et al., 2002; Priori et al., 2004). Furthermore, basal ganglia oscillations were found to be coupled to oscillations in distant brain regions. By simultaneously recording electroencephalography (EEG) and local field potentials (LFPs) it was shown that oscillations recorded from the STN are coherent with oscillations in cortical areas (Cassidy et al., 2002; Fogelson et al., 2006; Lalo et al., 2008; Marsden et al., 2001; Williams et al., 2002). Much like beta power in the STN, coherence in the range from 10 to 30 Hz was found to be attenuated by movement (Cassidy et al., 2002; Lalo et al., 2008), the administration of levodopa (Lalo et al., 2008; Williams et al., 2002) and DBS (Kühn et al., 2008).

Although these findings suggest that abnormal coupling between STN and cortical oscillations may be pathophysiologically relevant,

the cortical areas engaged in this coupling have not been identified so far. Simultaneous EEG-LFP recordings provided first evidence that the distribution of coherence across cortical areas is heterogeneous and frequency-dependent (Fogelson et al., 2006; Williams et al., 2002). However, the exact topography of STN-cortical coherence remains to be determined.

In this study we utilized simultaneous magnetoencephalography (MEG)-LFP recordings to map STN-cortical coherence. In contrast to EEG, MEG allows for whole-head, post-surgical measurements and thus for source localization with high spatial resolution. Using a frequency domain beamformer (Gross et al., 2001), we localized STN-cortical coherence in eight PD patients. While the feasibility of this approach has recently been demonstrated with data from a single subject (Litvak et al., 2010), it has not been realized in a group of patients so far.

Materials and methods

Patients

Nine patients (three females) with idiopathic, akinetic-rigid PD (mean age: 64 ± 7.6 years, range: 47–75), who were clinically selected

* Corresponding author. Institute of Clinical Neuroscience and Medical Psychology, Heinrich-Heine-University Düsseldorf, Universitätsstr. 1, 40225 Düsseldorf, Germany.
E-mail address: klin.neurowiss@uni-duesseldorf.de (A. Schnitzler).

for DBS of the STN, participated in the study. One patient was excluded due to severe head movement artifacts. All patients gave written informed consent. Table 1 summarizes the clinical details.

The study was approved by the local ethics committee (study no. 3209) and is in accordance with the Declaration of Helsinki. High resolution T1-weighted magnetic resonance (MR) images were obtained from each patient prior to surgery. Antiparkinsonian medication could be substantially reduced in all but two subjects, for whom the levodopa equivalent dose (LED) stayed approximately stable. The average reduction in LED was 40% ± 26%.

Planning and implantation

All oral antiparkinsonian medication was withdrawn the evening before surgery and substituted by subcutaneous apomorphine medication using a medication pump.

Electrode implantation was performed at the Department of Stereotaxy and Functional Neurosurgery in Düsseldorf. Patients were bilaterally implanted during medication OFF.

The STN was targeted on the basis of Schaltenbrand–Wahren atlas coordinates (Schaltenbrand and Wahren, 1977), using stereotactic cranial computer tomography (CT) and high resolution MRI. We performed intra-operative microelectrode recordings using the INOMED MER system (INOMED Inc., Tenningen, Germany) to determine the STN borders and the optimal implantation area. Intraoperative recordings were performed with up to five microelectrodes. The anterior, posterior, lateral and medial microelectrodes were concentrically configured around the central electrode, each with a distance of 2 mm from the central electrode (Ben's gun system). The final placement of the DBS electrode (model 3389, Medtronic Corporation, Minneapolis, MN, USA) was based on multi-unit activity and a clinical profile of stimulation effects and side effects.

Following surgery, the locations of the four DBS electrode contacts were derived from postoperative stereotactic CT images. Fig. 1 illustrates the average position of the contacts yielding the best clinical effect when used for chronic DBS. Table S1 lists the stereotactic coordinates of all contacts for all patients.

Recordings

All recordings were performed with a 306-channel, whole-head MEG system (Elekta Oy, Helsinki, Finland). Recording sessions took place the day after electrode implantation. At this stage, the stimulator was not yet implanted so that the externalized leads of the intracranial electrodes could be connected to the EEG acquisition device of our system. We used non-magnetic extension leads (Medtronic Bakken Research Center, Maastricht, the Netherlands)

for electrode connection, thereby avoiding the strong artifact induced by ferromagnetic connectors (Litvak et al., 2010).

Administration of apomorphine was discontinued at least 2 h prior to recordings so that all patients were in a defined medication OFF during recordings. We verified the OFF state by performing ratings according to the motor section of the Unified Parkinson's Disease Rating Scale (UPDRS III; Goetz et al., 2008).

We recorded MEG, LFPs, vertical and horizontal electro-oculograms (EOGs) and the electromyogram (EMG) of the extensor and flexor muscles of both forearms simultaneously. DBS Electrode contacts were referenced against a surface electrode at the left mastoid and rearranged into a bipolar montage offline. EMG was measured with reference to surface electrodes at the forearm tendons. Sampling rate was 2 kHz. MEG signals were band-pass filtered online between 0.03 and 660 Hz. LFP and EMG signals were filtered between 0.1 and 660 Hz. Patients were recorded at rest for 5 min with no specific task, but instructed to relax and move as little as possible.

Preprocessing and artifact removal

EMG data were visually inspected and periods containing movement were discarded. A notch filter at 50 Hz was applied to MEG and LFP data to remove power line noise. The MaxFilter software (Elekta Oy, Helsinki, Finland) was used to apply signal space separation (SSS) to MEG data (Taulu and Kajola, 2005). The method served to remove interferences arising from far outside the MEG shielded room and to reconstruct data from noisy or dysfunctional channels (four channels for each patient). The algorithm performs reconstruction by interpolation, using spherical harmonic basis functions. Based on previous work on the application of SSS (Ahonen et al., 1993; Nenonen et al., 2007; Song et al., 2008; Taulu et al., 2005), we chose the expansion limits of the spherical harmonic functions as $L_{in}=8$ for the inner sources and $L_{out}=3$ for the outer sources.

Data analysis

Data were analyzed using custom-made Matlab (The Mathworks, Natick, Massachusetts, USA) scripts, most of which were based on Fieldtrip, a Matlab-based, open source analysis toolbox (<http://fieldtrip.fcdonders.nl/>). We only analyzed data recorded by the 204 planar gradiometers of the MEG system.

Coherence has been widely used to quantify similarity between neuronal oscillations and is commonly interpreted as interaction or communication between brain areas (Fries, 2005; Schnitzler and Gross, 2005). It may be understood as a measure of amplitude and phase consistency across epochs of recorded data (Maris et al., 2007). Localization of coherent sources was realized by Dynamic Imaging of Coherent Sources (DICS), a frequency domain beamforming approach

Table 1

Clinical information on subjects. UPDRS motor scores (Goetz et al., 2008; sum score: 132) were obtained the day before (column 6) and the day after surgery (column 7) to quantify the clinical effects of medication. Further UPDRS scores were obtained 3 months after surgery to quantify the clinical effect of DBS in the medication OFF (column 8). The contacts chosen for DBS in clinical tests 3 months after surgery and their stereotactic coordinates relative to the mid-commissural point are given in columns 9–12. A single number in columns 10 and 12 indicates that stimulation was monopolar, otherwise it was bipolar (+ = cathode, – = anode).

Patient	Age (years)	Sex	Disease duration (years)	Predominant side	Motor UPDRS Med-OFF preOP	Motor UPDRS Med-OFF/Med-ON postOP	Motor UPDRS DBS-OFF/DBS-ON	Stimulated contacts left	Coordinates stimulated contacts left	Stimulated contacts right	Coordinates stimulated contacts right
BH	75	f	26	Left	35	50/32	42/29	2–	[–12.5, 0.0, 1.4]	2–	[10.8, –1.7, –0.1]
HH	69	m	11	Right	33	41/33	unavailable	1–	[–14.2, –1.7, 0.01]	1–	[14.5, –0.1, 0.0]
KH	62	m	16	Right	36	44/30	52/28	1–	[–13.1, –1.1, –1.4]	1–	[13.8, –2.8, –0.9]
LW	70	m	11	Right	28	39/31	23/15	1–	[–13.1, –2.8, –2.6]	2–	[12.1, –2.0, –1.7]
PH	62	f	15	Left	43	27/21	46/37	3+	[–12.4, 0.7, 2.4]	3+	[14.1, 0.7, 2.5]
								2–	[–11.7, –0.9, 0.7]	2–	[13.4, –0.9, 0.8]
SA	72	m	16	Left	44	43/38	29/13	1–	[–12.9, 2.0, –2.3]	2–	[12.7, 4.5, –2.4]
WA	64	f	18	Left	35	24/9	34/21	2+	[–11.9, 2.1, –0.2]	2+	[14.6, 0.0, –1.9]
								1–	[–11.2, 0.4, –2.0]	1–	[13.9, –1.7, –3.7]

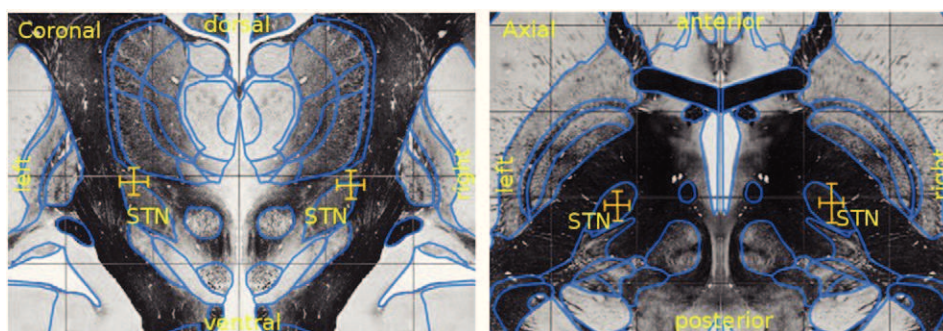


Fig. 1. Average position of the contacts showing the best clinical effect when used for chronic DBS. Stereotactic contact coordinates were normalized with respect to the distance between the anterior commissure (AC) and the posterior commissure (PC) and projected onto the Schaltenbrand–Wahren atlas (Schaltenbrand and Wahren, 1977). When stimulation was bipolar, the mean coordinates of the contact pair were used for averaging across subjects. Left: Average position of stimulated contacts (left hemisphere: $x = -12.4 \text{ mm} \pm 1.44 \text{ mm}$, $z = -0.6 \text{ mm} \pm 1.55 \text{ mm}$; right hemisphere: $x = 13 \text{ mm} \pm 1.32 \text{ mm}$, $z = -0.9 \text{ mm} \pm 1.44 \text{ mm}$) projected onto coronal slice 3 mm behind mid-commissural point (MCP). The coordinates indicate that the points are situated behind MCP (negative y, given by slice) and below MCP (negative z). Right: Average position of stimulated contacts (left hemisphere: $x = -12.4 \text{ mm} \pm 1.44 \text{ mm}$, $y = -0.7 \text{ mm} \pm 1.79 \text{ mm}$; right hemisphere: $x = 13 \text{ mm} \pm 1.32 \text{ mm}$, $y = -0.7 \text{ mm} \pm 2.35 \text{ mm}$) projected onto axial slice 1.5 below AC-PC line. Grid spacing is 9 mm; yellow crosses depict standard deviations.

(Gross et al., 2001). Activity recorded in the four LFP channels (Fig. 2A) served as the reference signals for coherence computation in a dense grid of spatial locations spanning the entire brain. Coherence was analyzed separately in four frequency bands: alpha (7–12 Hz), low beta (12–20 Hz), high beta (20–35 Hz) and gamma (70–90 Hz). Because DICS works frequency-wise, analyzing a range of frequencies for each patient and LFP channel would be extremely computationally demanding. Therefore, we estimated the frequency of strongest coherence prior to source localization based on MEG sensor data. For each patient, LFP channel and frequency band, we identified the five MEG sensors with the highest mean coherence and averaged their coherence spectra. We automatically searched the averaged spectra for the highest local maximum and chose its frequency for source localization. Fig. 2B and C illustrates the procedure.

DICS projects sensor data through a spatial filter derived from the leadfield and the cross-spectral densities (CSDs). To obtain a good estimate of the latter, they were calculated for overlapping, Hanning-tapered segments of the continuous rest data (varying between 150 and 300 s) and averaged over segments. The regularization parameter for DICS was set to 0.5% of the mean power. Frequency resolution for DICS was 3.9 Hz. Low frequency resolution was necessary to provide good CSD estimates and therewith reliable source localization.

The leadfield was calculated using a single-shell head model based on the patients' individual MRIs (Nolte, 2003). MRIs were first normalized to the T1 template brain included in SPM2 (<http://www.fil.ion.ucl.ac.uk/spm/>). The inverse of that normalization was then applied to a beamformer grid based on the template brain (Mattout et

al., 2007). As a consequence, all grid points in the warped grid corresponded to a grid point in the template grid and thus had a defined position in Montreal Neurological Institute (MNI) space. Grid spacing was 5 mm.

Since only a single spatial maximum was usually discernible in the functional images, we defined a source as the cluster of supra-threshold voxels showing maximal coherence. The threshold was defined according to Halliday et al. (1995). Sources were required to consist of eight neighboring supra-threshold voxels at least. The number 8 was chosen because simulations had shown that eight neighbors occurred rarely ($p < 0.03$) when randomly setting 5% of voxels above threshold. We note that this procedure does not provide rigorous control over the number of false positive detections but is preferable to simple thresholding. A nonparametric significance test, which effectively controls for multiple comparisons, was applied to test for the significance of coherence on the group level (see Statistics section).

For visualization, functional images were coregistered to a canonical MR image, using nasion, left and right pre-auricular point, and interpolated on the MR image. MNI coordinates of the maxima of interpolated images were identified with the help of the AFNI atlas (<http://afni.nimh.nih.gov/afni>), integrated into Fieldtrip.

Statistics

Statistical analyses were performed using Matlab. When comparing LFP-MEG coupling across subjects or frequency bands we used the

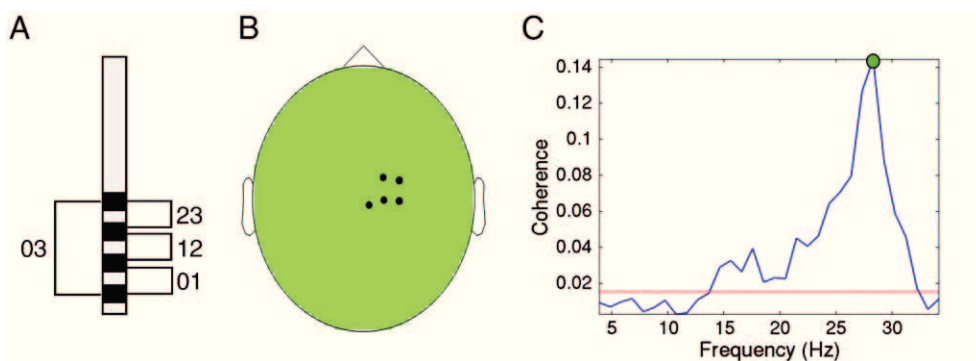


Fig. 2. Reference scheme for DBS electrodes and example for the choice of frequency. A) Schematic drawing of the DBS electrode. Electrode contacts were re-referenced offline, resulting in four bipolar LFP channels. B) The five MEG sensors with the highest average coherence in the high beta band in one exemplary subject (Patient HH, LFP channel R03). Note that the spatial neighborhood of these sensors is of physiological origin and not resulting from the application of any spatial criteria. C) Coherence averaged across the five channels depicted in B). Frequency resolution is 1 Hz. The red line depicts the significance threshold. The green dot marks the highest peak. For this particular patient (HH), LFP channel (R03) and frequency band (high beta) the frequency chosen for source localization was 28 Hz.

Fisher-transformed modulus of coherency instead of coherence (Brillinger, 1981). We will refer to this measure as z-transformed coherence.

Significance of coherence on the group level was tested by a nonparametric test (Nichols and Holmes, 2002; Schoffelen et al., 2008). The test corresponded to a one-sided, single sample *t*-test. We considered only functional images showing maximal coherence for a given subject and frequency band (grid spacing: 1 cm, frequency resolution: 1.9 Hz). First, we computed an image of z-transformed difference values for each subject ($z = \arctanh(\sqrt{\text{coh}}) - \arctanh(\sqrt{\text{threshold}})$), threshold according to Halliday et al. (1995) and averaged the difference images. We then determined the maximum of the average image, which served as the test statistic. The null hypothesis stated that the individual difference values are symmetrically distributed around zero. Under this assumption, alternative samples may be generated by flipping the sign of any subset of difference images prior to calculating the test statistic. The full permutation distribution of the test statistic was computed by flipping the sign of all possible subsets and recalculating the test statistic. The critical value was defined as the $0.05 \times N$ highest statistic of the permutation distribution, *N* being the number of permutations. Voxels showing z-values higher than the critical value were considered significant.

For the assessment of the distribution of peak coherence across electrode channels, we used a parametric test developed by Amjad et al. (1997). The significance level was Dunn–Sidak corrected for multiple comparisons.

Results

Sensor level analysis

We observed significant coherence between LFPs and MEG sensors in the alpha, low beta and high beta band in all subjects (see Fig. S2 in the supplementary material). Coherence lateralized to the ipsilateral side with respect to the STN. On average, sensors ipsilateral to the STN showed higher coherence than contralateral sensors (Fig. 3). As in the example shown in Fig. 4, coherence was usually strongest in sensors located above the paramedian central sulcus region.

Except for a single patient (patient ZE), significant coherence in the gamma band was not observed. This patient was exceptional as he had received DBS of the globus pallidus internus for several years before another pair of electrodes was implanted for STN stimulation. As coherence in the gamma band was seen only in this one instance, we did not take the gamma band into account in subsequent analysis.

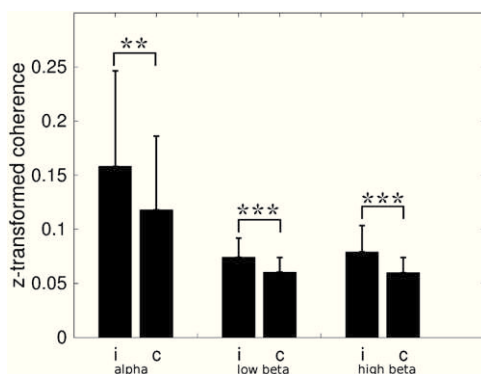


Fig. 3. Lateralization of coherence on the sensor level. z-transformed MEG–LFP coherence averaged across ipsilateral (i) and contralateral (c) MEG sensors. Values for all subjects and LFP channels were pooled. Asterisks indicate *p*-values (***p* < 0.01, ****p* < 0.001, Wilcoxon rank sum test).

Source level analysis

Characterization of coherent sources

Having identified the frequencies at which coherence was highest on the sensor level, we used DICS to localize coherent activity at these frequencies. In the following, we will use the term “source” when referring to areas of elevated STN–cortical coherence detected by the procedure outlined in Data analysis section. We identified 161 sources, thereof 53 coherent in the alpha band, 48 in the low beta band and 60 in the high beta band. Please note that with our definition a source signifies localized coherent activity with respect to a given LFP channel. In case signals of two LFP channels are similar, as it may be the case for neighboring channels, two sources of similar frequency and location may well reflect the same cerebral activity. As we accepted only one source per frequency band and LFP channel, the highest possible number of sources for a given frequency band was 64 (eight patients, eight channels).

Fig. 5 shows an alpha and a high beta source found for the same LFP channel. The example demonstrates that a single recording site in the basal ganglia may show coherence with different cortical areas at different frequencies.

We investigated whether the strength of oscillatory coupling differed across frequency bands. An analysis of variance (ANOVA) revealed that z-transformed coherence at the source maximum and mean source coherence (averaged across voxels) was similar for all frequency bands ($F_{\text{max}(2)} = 1.2$, $p_{\text{mean}} = 0.3$; $F_{\text{mean}(2)} = 2.01$, $p_{\text{mean}} = 0.14$).

Topography of coherent sources

In order to investigate frequency-dependent differences in the spatial topography of sources, we pooled all coherent sources identified for a given frequency band and determined the MNI coordinates of their maxima. The coordinates were then assigned to brain regions with the help of the AFNI atlas.

The vast majority of source maxima was located ipsilateral to the STN (alpha: 83%, low beta: 88%, high beta: 95%). As can be seen from Fig. 6, there was a clear difference between alpha and beta sources with respect to the locations of their maxima.

Alpha source maxima were mostly situated in the temporal cortex. They did not show a consistent topography when pooled over subjects and LFP channels but scattered across a large area. However, one larger cluster was found in the posterior part of the superior temporal gyrus (STG; 11 sources, 5 hemispheres, 4 subjects). For the three patients showing unilateral alpha coherence in STG, coherence was located on the left side, which was ipsilateral to the body side most affected by PD symptoms in all three cases. Alpha coherence was also found in the postcentral gyrus (PostCG; 6 sources, 3 hemispheres, 3 subjects) and precentral gyrus (PreCG; 4 sources, 4 hemispheres, 4 subjects).

Contrary to alpha sources, high beta sources clustered in one area. In seven out of eight subjects we found high beta source maxima to cluster in the ipsilateral sensorimotor cortex. The cluster encompassed PreCG (26 sources, 11 hemispheres, 6 subjects), PostCG (7 sources, 4 hemispheres, 4 subjects) and parts of Brodmann area 6 rostral to PreCG (5 sources, 3 hemispheres, 3 subjects). All source maxima in PostCG were located contralateral to the body side most affected by PD. In contrast, all source maxima in premotor areas were situated ipsilateral to the latter.

The topography of low beta sources resembled that of high beta sources, with source maxima clustering around PreCG (10 sources, 6 hemispheres, 5 subjects). We did not observe clear differences in the topographies of low and high beta source maxima within cortical motor areas. Low beta source maxima were also found in the fusiform gyrus, PostCG, the insula, the temporal lobe, the cerebellum, and the frontal lobe, but did not cluster in a specific region other than the sensorimotor cortex.

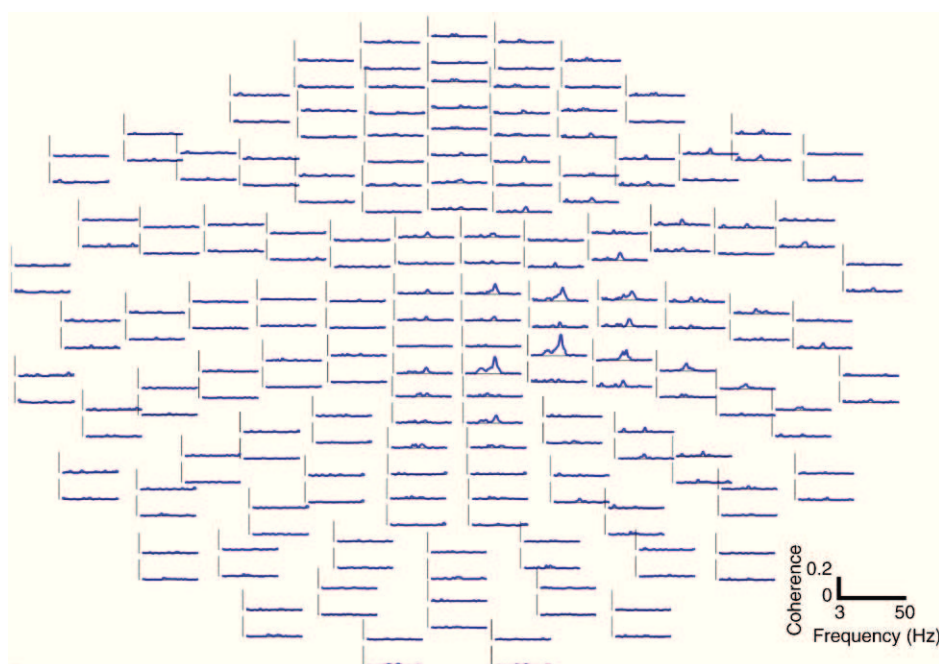


Fig. 4. Example of MEG-LFP coherence in the high beta band (Patient HH, LFP channel R03). The figure shows the coherence spectra of all planar gradiometers (array is seen from above, the subject's nose points to the top of the page). Note that coherence peaks in medial sensors, ipsilateral to the STN. Frequency resolution is 2 Hz.

A nonparametric statistical test revealed that subjects consistently showed beta coherence in the ipsilateral sensorimotor cortex. High and low beta coherence around the central sulcus was significantly higher than threshold when averaged across subjects (Fig. 6D). Coherence in the alpha band was not significant on the group level in any brain area.

Finally, we tested whether sources coherent with different LFP channels in the same frequency band differed in their x , y or z coordinates in MNI space. One-way ANOVAs did not yield any evidence for a systematic relationship between the sources' coordinates and the LFP channels sources were coherent with.

Distribution of coherence across LFP channels

The first part of the analysis revealed that beta oscillations in PreCG and alpha oscillations in STG were coherent with LFPs recorded from the STN. In the second part, we defined the spatial maxima of sources found in these areas as regions of interest (mean MNI

coordinates STG: $\pm 51, -20, 5$; PreCG: $\pm 33, -22, 57$) and computed the full coherence spectrum with all LFP channels. If several sources had been identified in the same PreCG or STG (relating to different LFP channels of the same subject), we chose the source of strongest coherence. The aim of this analysis was to investigate the spatial distribution of coherence within the area recorded by the DBS electrode.

As expected, the spectra of STG and PreCG sources showed clear differences. Fig. 7 shows an example of the distribution of alpha (Fig. 7A) and beta coherence (Fig. 7B) across LFP channels.

STG sources showed strongest coherence in the alpha band. The frequency of peak coherence was 11.3 Hz on average. In all cases, coherence with ipsilateral channels was markedly higher than with contralateral channels. When considering only ipsilateral channels, we found that the distribution of peak alpha coherence across LFP channels was not significantly different from a homogeneous distribution in any case (Table 2), suggesting that alpha oscillations

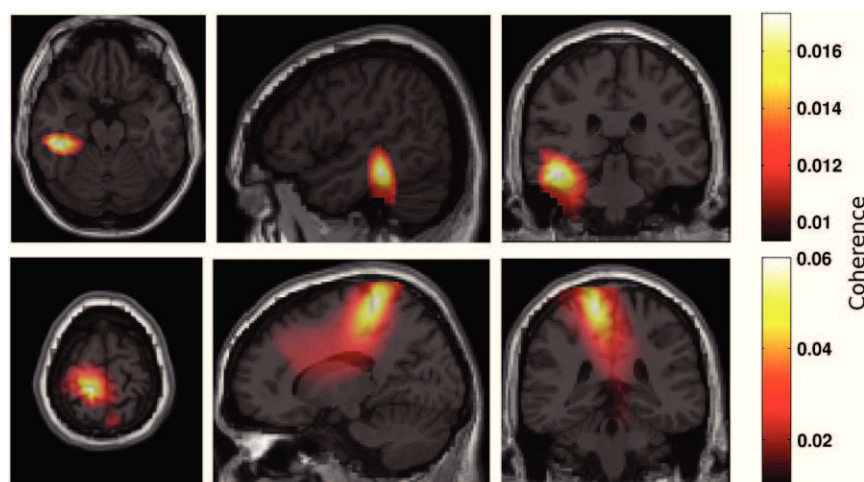


Fig. 5. An exemplary alpha (upper row) and high beta (lower row) source localized by DICS. Coherence is color-coded. Both sources are coherent with activity recorded in the same LFP channel (Patient LW, LFP channel L12), but at different frequencies (6.8 and 23.4 Hz).

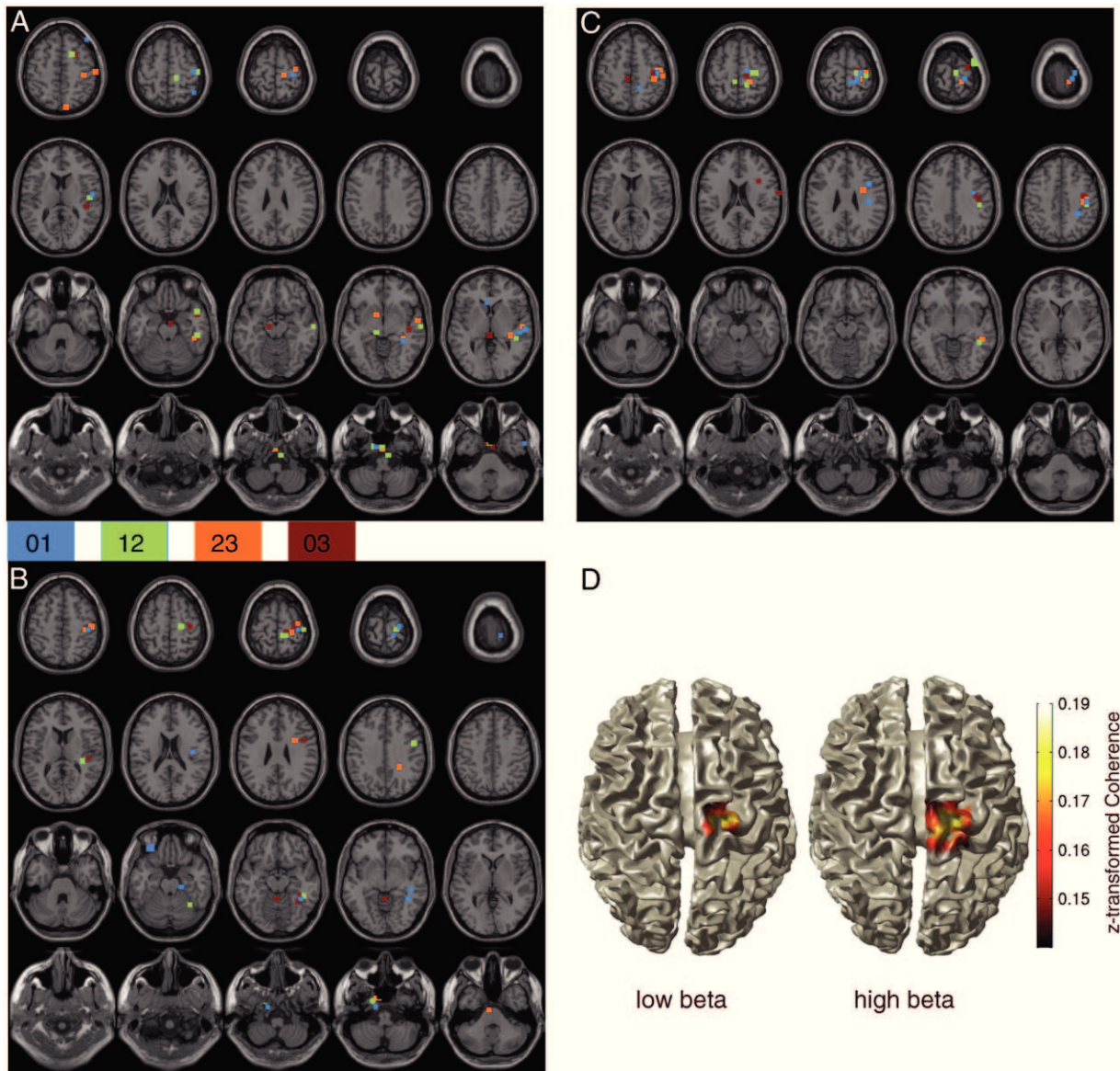


Fig. 6. Frequency-dependent differences in the topography of coherence. Colored squares represent the maxima of all alpha (A), low beta (B) and high beta (C) sources detected in this study. Maxima were enlarged for visualization and interpolated on a canonical MR image. Sources coherent to the left STN have been mirrored into the contralateral hemisphere. LFP channels with which sources were coherent are color-coded. D) z-transformed coherence averaged across subjects. Only significant values ($\alpha = 0.05$, corrected) are displayed.

in STG are coupled to more widely distributed STN alpha rhythm. Consistent with this idea, the LFP channel with the largest contact spacing (channel 03) showed the strongest coherence on average.

PreCG sources showed the highest coherence with LFP channels in the beta band. The average frequency of peak coherence was 22.6 Hz. As in the example shown in Fig. 7B, PreCG-LFP coherence was focal in most cases. The null hypothesis of equal peak beta coherence with all ipsilateral LFP channels was rejected in 7 of 12 cases. Fig. 8 shows the average distribution of peak beta coherence across LFP channels for these seven cases. On average, coherence was strongest with the ipsilateral channel 12 and weakest with channel 01. However, the difference between channels was not significant ($F_{(3)} = 1.27$, $p = 0.3$).

Discussion

This study shows that the ipsilateral sensorimotor and adjacent premotor cortex is the main source of cortical activity coherent with beta oscillations in the STN of PD patients. Moreover, it identified ipsilateral temporal areas as a source of coherent alpha activity.

Methodological considerations

Before discussing the physiological aspects of the results in detail, we will make some methodological considerations. Coherence analysis of electrophysiological recordings bears the risk to overestimate or falsely detect oscillatory coupling due to field spread (Schoffelen and Gross, 2009; Srinivasan et al., 2007; Winter et al., 2007). When the same signal is picked up at separate sites of measurement, this will lead to the detection of coherence even if the local activities at these sites are uncorrelated. There are several reasons to believe that the results reported here are not due to field spread.

First, we used beamforming to compute coherence, a technique designed to suppress signals which do not originate from the location that is being scanned (Van Veen et al., 1997). Beamforming is known to alleviate the effects of field spread (Schoffelen and Gross, 2009).

Second, we used bipolar referencing of electrode contacts, i.e. the LFP channels recorded local activity. In principle, it is conceivable that such local activity was recorded by MEG sensors as well, despite its low

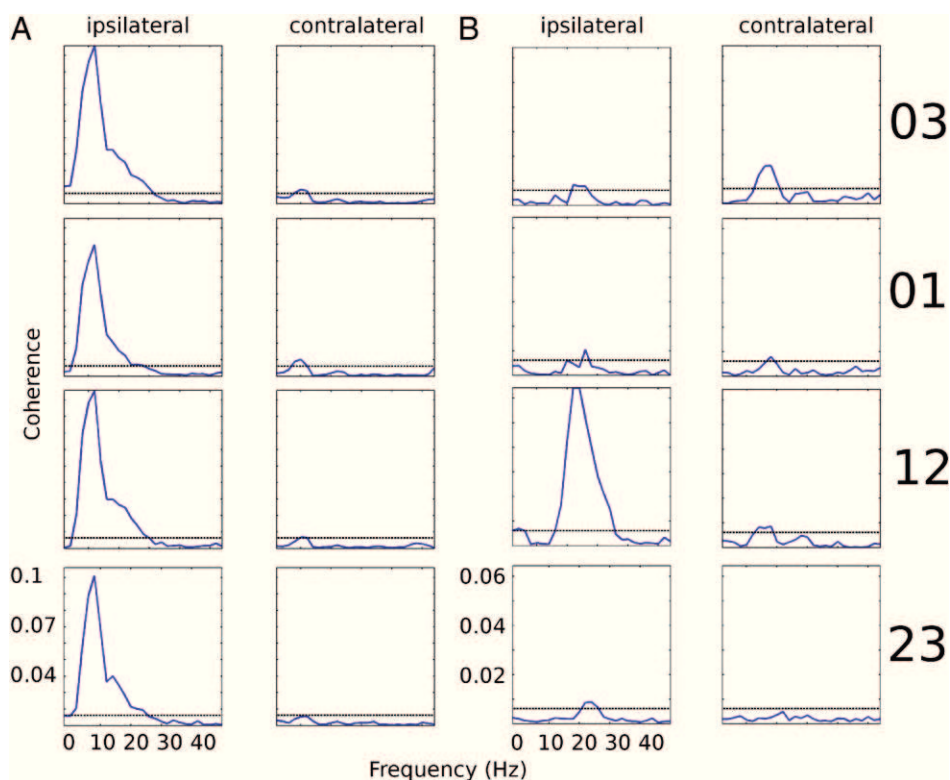


Fig. 7. Examples of the distribution of coherence across electrode contacts. The blue lines depict coherence and the dotted, black lines the significance threshold. Labels of LFP channels are shown to the right of the coherence spectra. Frequency resolution is 2 Hz, and frequency smoothing due to multi-tapering is 3.9 Hz. A) STG-LFP coherence (patient PH). Scaling is the same in all subplots. B) PreCG-LFP coherence (patient LW). Scaling is the same in all subplots. Note that the distribution of coherence across LFP channels is roughly homogeneous for STG signals, whereas it is focal for PreCG signals.

amplitude. However, signals from sources as deep as the basal ganglia would be detected by a large number of sensors and the amplitude distribution across sensors would be roughly uniform. In this case, coherent sources would be mapped to deep, central areas by beamforming. Signals reaching MEG sensors from deep areas by field spread are not expected to localize to cortical areas. Furthermore, coherence induced by field spread is not expected to be physiologically

plausible, i.e. field spread cannot explain why beta coherence is especially high in motor areas.

Apart from conduction of neuronal signals, artifacts may lead to erroneous results in connectivity analysis (Schoffelen and Gross, 2009). Artifact handling is especially challenging in simultaneous MEG-LFP recordings, as ferromagnetic components of the recording setup may severely impair data quality (Litvak et al., 2010). In this study we used exclusively non-magnetic hardware. As a result, the data quality obtained in this study was comparable to the quality obtained when the MEG signal is recorded from subjects without any implants. To improve data quality further, we removed signal

Table 2

Coherence between cortical signals and LFP channels. The fourth column contains the probabilities that peak band coherence is the same with all LFP channels. The fifth column contains the probabilities that peak band coherence is the same with all ipsilateral LFP channels. Probabilities below significance level ($\alpha=0.05$, corrected) are marked by bold print. All channels listed in the second column are ipsilateral channels.

Brain area	Channel with highest peak	Frequency of peak (Hz)	<i>p</i> value (all channels)	<i>p</i> value (ipsilateral channels)
STG	03	9.8	< 0.001	0.91
STG	03	11.7	0.14	0.47
STG	03	11.7	0.21	0.25
STG	03	11.7	0.007	0.18
STG	01	11.7	0.004	0.1
PreCG	03	13.6	< 0.001	< 0.001
PreCG	12	21.5	< 0.001	< 0.001
PreCG	23	15.6	0.03	0.016
PreCG	12	29.3	< 0.001	< 0.001
PreCG	03	23.4	< 0.001	< 0.001
PreCG	01	29.3	0.062	0.2
PreCG	03	25.3	< 0.001	0.11
PreCG	23	27.3	0.0015	0.027
PreCG	23	21.5	< 0.001	0.013
PreCG	23	19.5	< 0.001	< 0.001
PreCG	03	25.4	0.058	0.83
PreCG	03	19.5	< 0.001	< 0.001

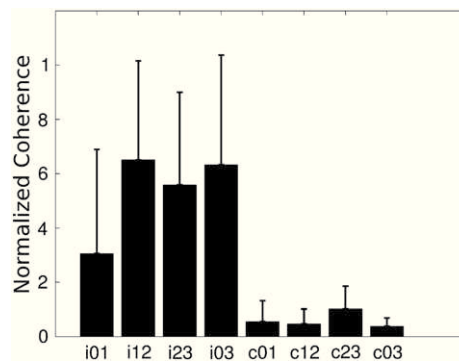


Fig. 8. Average distribution of peak beta coherence across electrode contacts (i = ipsilateral, c = contralateral). For each hemisphere, we searched the eight coherence spectra for the highest peak and determined the frequency at which it occurred. Subsequently, we normalized coherence in each channel at that frequency by dividing by the peak value. Normalized coherences were then averaged across hemispheres. Bars depict standard deviations.

components attributable to sources outside the head by the application of SSS (Taulu and Kajola, 2005).

Finally, transient tissue responses to electrode insertion, such as edema, may be a methodological concern. LFP power has been shown to be variable in the first days after surgery, and different frequency bands may be differentially affected by transient changes in the tissue (Rosa et al., 2010). Accordingly, coherence measured at later stages may in principle differ from the data presented in this study. However, we do not expect our main results to be qualitatively affected by edema, since coherent sources may remain undetected due to edema, but edema are unlikely to introduce significant coherences or a consistent remapping of coherent sources

STN-cortical coupling

Using simultaneous MEG-LFP recordings in PD patients, we found cortical activity to be coherent with STN LFPs in the alpha and beta, but not in the gamma band. This finding is in agreement with simultaneous EEG-LFP recordings of PD patients in the medication OFF (Williams et al., 2002). While significant coherence in the alpha and beta band was readily observed after withdrawal of antiparkinsonian medication, coherence in the gamma band emerged only after the administration of levodopa (Lalo et al., 2008; Williams et al., 2002).

Coherence in the high beta band

Owing to the large number of sensors available in MEG recordings, we were able to localize coherent activity on the source level. We found coherent high beta activity to be generated ipsilaterally in PreCG, more rostral sites in Brodmann area 6 and in PostCG. Functionally, these areas represent the primary motor cortex (M1), the premotor cortex and the primary somatosensory cortex, respectively. We thus conclude that the area of strongest oscillatory coupling in the high beta band is the ipsilateral sensorimotor and adjacent premotor cortex.

Anatomically, a functional interaction between the motor cortex and the STN is plausible. Both primary and secondary motor cortex have abundant connections to the STN (Alexander et al., 1986; Alexander and Crutcher, 1990). Cortical inputs may reach the STN via the striatum and the external segment of the globus pallidus. Alternatively, they are transmitted without relay via the so-called hyperdirect pathway (Nambu et al., 1996). In turn, subthalamic output reaches the motor cortex via the ventrolateral thalamus (Hoover and Strick, 1999).

As both the motor cortex and the STN are somatotopically organized (Rodriguez-Oroz et al., 2001) and regions representing the same body part are anatomically connected (Miyachi et al., 2006; Nambu et al., 1996), it is conceivable that corresponding regions in the STN and the motor cortex show selective functional coupling. We assessed this question by investigating whether the position of a coherent cortical source varies systematically with the LFP channel used as reference for coherence calculation. The absence of such a relationship in our data suggests that, if selective functional coupling occurs, it may not be readily detectable in post-surgical recordings with DBS electrodes. The contacts of DBS electrodes are large compared to the scale of somatotopic representation in the STN and the direction of electrode insertion (mainly dorsoventral) does not match the direction of somatotopic representation (mainly medio-lateral). Moreover, inter-individual differences in the exact position of DBS electrodes and the presence of edema might have hindered the detection of a significant relationship.

Interhemispheric differences in STN-cortical beta coherence

Interestingly, this study reveals first indications for a hemispheric asymmetry of STN-cortical beta coherence, reminiscent of the motor symptom asymmetry typical for PD (Djaldetti et al., 2006). High beta source maxima were found in the PostCG contralateral to the body

side most affected by PD, but not in the ipsilateral PostCG. In contrast, high beta coherence in premotor areas occurred only ipsilaterally. Thus, the patterns of STN-cortical coherence may not be identical for both hemispheres. The hemisphere more affected by dopamine depletion, i.e. contralateral to the more affected body side, may show coherence with a more posterior sensorimotor area than the less affected hemisphere. Note, however, that the data presented here provide only indirect evidence, as the observed difference between hemispheres is based on an across-subject comparison.

Coherence in the low beta band

We subdivided the beta band into low and high beta since there is evidence for the existence of two functionally distinct beta rhythms in the STN (Marceglia et al., 2006; Priori et al., 2004). One may speculate that the underlying thalamo-cortical loops are spatially segregated. In this study, neither the automatic detection of maximally coherent sources nor the inspection of unprocessed functional images yielded any evidence for a difference in topography. Our results therefore suggest that the proposed difference in function relies on distinct coupling frequencies rather than on interactions with spatially distinct cortical areas. We note, however, that frequency resolution was kept rather low in this study for the sake of precise source localization. Low frequency resolution might have precluded the detection of subtle differences between the topographies of low and high beta coherence.

The occurrence of low beta sources in both motor and temporal areas suggests that defining frequency bands according to the traditional EEG literature may not lead to an optimal spatial separation of cortical coherent sources. Choosing a higher frequency as the border between the alpha and the low beta band would most probably have resulted in clearer spatial separation of sources. With a different definition of frequency bands, it is conceivable that sources coherent in the extended alpha band would localize to the temporal lobe, while sources coherent in the truncated beta band cluster in cortical motor areas.

Apart from the choice of frequency band width, non-linear correlations between alpha, low and high beta oscillations in the STN may have contributed to the co-localization of cortical coherent sources (Marceglia et al., 2006).

Distribution of beta coherence across LFP channels

Analysis of the distribution of spectral peaks across LFP channels revealed that beta coherence with PreCG was not spatially uniform but showed relative focality within the recording range of the DBS electrode. This finding is in line with reports on intra-operative LFP recordings showing that beta power depends on LFP recording site within the STN area (Kühn et al., 2005; Trottenberg et al., 2007; Weinberger et al., 2006).

Since post-surgical imaging does not allow for contact localization with mm precision, the exact site of elevated beta coherence within the STN area could not be determined. We found the LFP channel showing maximal PreCG-LFP beta coherence to vary substantially across hemispheres, most likely due to differences in electrode placement. Accordingly, there was no significant difference across LFP channels on average. However, the average distribution of beta coherence showed an increase from the ventralmost (channel 01) to more dorsal LFP channels (Fig. 8). It is therefore reasonable to assume that PreCG-LFP beta coherence is increased in the dorsal part of the STN, which constitutes the motor part of the nucleus (Rodriguez-Oroz et al., 2001). Beta power has been shown to be locally elevated in this area (Trottenberg et al., 2007).

Coherence in the alpha band

We localized coherent alpha activity in the ipsilateral temporal cortex. This new finding contradicts previous studies investigating EEG-LFP coherence, which localized alpha coherence to mesial rather

than lateral sensors (Fogelson et al., 2006; Williams et al., 2002). A reason for the divergent localizations could be that those previous studies included tremor-dominant patients while we included exclusively PD patients of the akinetic-rigid subtype. Parkinsonian rest tremor is characterized by strong coherence in the alpha range between activity in cortical motor areas, muscle activity and activity in several other brain regions, including deep, diencephalic structures (Pollok et al., 2009; Timmermann et al., 2003). Thus, alpha coherence due to tremor may have dominated the spatial patterns of STN-cortical alpha coherence described earlier. Previous studies may also have missed STN-temporal lobe coupling due the limited spatial sampling of cortical signals in post-surgical EEG recordings.

While alpha sources showed substantial spatial variability across subjects and electrode contacts, a subset of subjects consistently showed alpha coherence in the ipsilateral STG. In line with the diffuse distribution of alpha power in the subthalamic region (Kühn et al., 2005), the pattern of alpha coherence suggests that activity in STG is coherent to a rather global alpha rhythm. Thus, STG-LFP coherence does not necessarily reflect a specific interaction between STG and STN but may well relate to other basal ganglia structures.

Anatomically, an interaction between the temporal cortex and the basal ganglia could be explained by temporal projections to the ventromedial caudate nucleus (Selemon and Goldman-Rakic, 1985; Van Hoesen et al., 1981; Yeterian and Van Hoesen, 1978) or by projections from the substantia nigra pars reticulata to the inferior temporal cortex (Middleton and Strick, 1996). Functionally, STG has been ascribed a role in perception rather than action. It is involved in auditory (Buchsbaum et al., 2001; Howard et al., 2000) movement (Howard et al., 1996; Puce et al., 1998) and vestibular perception (Fasold et al., 2002; Friberg et al., 1985). Thus, it is possible that alpha coherence reflects a coupling between the temporal cortex and sensory regions of the basal ganglia nuclei (Brown et al., 1997). This hypothesis is supported by a recent study showing that auditory evoked fields can be modulated by stimulation of the STN (Airaksinen et al., 2010). Interestingly, the hypothesis implies that frequency may differentiate sensory from motor processing in STN-cortical loops. Alpha coherence between STN and cortex may reflect sensory processing in akinetic-rigid PD patients, whereas coherence in the beta band reflects motor processing. However, this interpretation remains speculative at this stage and requires further investigation.

Conclusions

By recording MEG and LFPs simultaneously we were able to precisely map frequency-dependent interactions between STN and cortex for the first time. Our study showed that STN-cortical coherence is focal in the spatial and in the frequency domain and revealed two distinct couplings between STN and cortex: One with the motor cortex in the beta frequency band and one with temporal areas in the alpha frequency band. Moreover, it further established simultaneous MEG and intracranial electrode recordings as a means to study connectivity between deep and cortical brain areas in patients.

Acknowledgments

The authors would like to express their sincere gratefulness to the patients who participated in this study. Furthermore, we are very thankful to the people of Medtronic Neuromodulation (Dr. Ali Sarem-Aslani, Mr. Paul van Venrooij, and Mr. Andreas Rolf) for technical support. In addition, we thank Mrs. E. Rädisch for assistance with MRI scans, Prof. Joachim Gross (CCNi Glasgow) for help in analysis issues and the people behind the fieldtrip project for excellent support. This study was supported by the ERANET-Neuron Grant "PhysiolDBS" (Neuron-48-013) to A.S. The funding source did not influence the collection, analysis and interpretation of data or the writing and

submission of the report. J.H. was supported by a travel grant from the Böhlinger Ingelheim Foundation (B.I.F.).

Appendix A. Supplementary data

Supplementary data to this article can be found online at doi:10.1016/j.neuroimage.2010.11.063.

References

- Ahonen, A., Hamalainen, M., Ilmoniemi, R., Kajola, M., Knuutila, J., Simola, J., Vilkmann, V., 1993. Sampling theory for neuromagnetic detector arrays. *Biomed. Eng. IEEE Trans.* 40, 859–869.
- Airaksinen, K., Mäkelä, J.P., Taulu, S., Ahonen, A., Nurminen, J., Schnitzler, A., Pekkonen, E., 2010. Effects of DBS on auditory and somatosensory processing in Parkinson's disease. *Hum. Brain Mapp.* Electronic publication ahead of print.
- Alexander, G.E., Crutcher, M.D., 1990. Functional architecture of basal ganglia circuits: neural substrates of parallel processing. *Trends Neurosci.* 13, 266–271.
- Alexander, G.E., DeLong, M.R., Strick, P.L., 1986. Parallel organization of functionally segregated circuits linking basal ganglia and cortex. *Annu. Rev. Neurosci.* 9, 357–381.
- Amjad, A.M., Halliday, D.M., Rosenberg, J.R., Conway, B.A., 1997. An extended difference of coherence test for comparing and combining several independent coherence estimates: theory and application to the study of motor units and physiological tremor. *J. Neurosci. Meth.* 73, 69–79.
- Brillinger, D.R., 1981. *Time series: data analysis and theory* (SIAM).
- Brown, L.L., Schneider, J.S., Lidsky, T.I., 1997. Sensory and cognitive functions of the basal ganglia. *Curr. Opin. Neurobiol.* 7, 157–163.
- Brown, P., Oliviero, A., Mazzone, P., Insola, A., Tonali, P., Di Lazzaro, V., 2001. Dopamine dependency of oscillations between subthalamic nucleus and pallidum in Parkinson's disease. *J. Neurosci.* 21, 1033–1038.
- Buchsbaum, B.R., Hickok, G., Humphries, C., 2001. Role of left posterior superior temporal gyrus in phonological processing for speech perception and production. *Cogn. Sci.* 25, 663–678.
- Cassidy, M., Mazzone, P., Oliviero, A., Insola, A., Tonali, P., Di Lazzaro, V., Brown, P., 2002. Movement-related changes in synchronization in the human basal ganglia. *Brain* 125, 1235–1246.
- Djalldetti, R., Ziv, I., Melamed, E., 2006. The mystery of motor asymmetry in Parkinson's disease. *Lancet Neurol.* 5, 796–802.
- Fasold, O., von Brevern, M., Kuhberg, M., Ploner, C.J., Villringer, A., Lempert, T., Wenzel, R., 2002. Human vestibular cortex as identified with caloric stimulation in functional magnetic resonance imaging. *Neuroimage* 17, 1384–1393.
- Fogelson, N., Williams, D., Tijssen, M., van Bruggen, G., Speelman, H., Brown, P., 2006. Different functional loops between cerebral cortex and the subthalamic area in Parkinson's disease. *Cereb. Cortex* 16, 64–75.
- Friberg, L., Olsen, T.S., Roland, P.E., Paulson, O.B., Lassen, N.A., 1985. Focal increase of blood flow in the cerebral cortex of man during vestibular stimulation. *Brain* 108 (Pt 3), 609–623.
- Fries, P., 2005. A mechanism for cognitive dynamics: neuronal communication through neuronal coherence. *Trends Cogn. Sci. (Regul. Ed.)* 9, 474–480.
- Goetz, C.G., Tilley, B.C., Shaftman, S.R., Stebbins, G.T., Fahn, S., Martinez-Martin, P., Poewe, W., Sampaio, C., Stern, M.B., Dodel, R., et al., 2008. Movement Disorder Society-sponsored revision of the Unified Parkinson's Disease Rating Scale (MDS-UPDRS): scale presentation and clinimetric testing results. *Mov. Disord.* 23, 2129–2170.
- Gross, J., Kujala, J., Hamalainen, M., Timmermann, L., Schnitzler, A., Salmelin, R., 2001. Dynamic imaging of coherent sources: studying neural interactions in the human brain. *Proc. Natl. Acad. Sci. U. S. A.* 98, 694–699.
- Halliday, D.M., Rosenberg, J.R., Amjad, A.M., Breeze, P., Conway, B.A., Farmer, S.F., 1995. A framework for the analysis of mixed time series/point process data—theory and application to the study of physiological tremor, single motor unit discharges and electromyograms. *Prog. Biophys. Mol. Biol.* 64, 237–278.
- Hoover, J.E., Strick, 1999. The organization of cerebellar and basal ganglia outputs to primary motor cortex as revealed by retrograde transneuronal transport of herpes simplex virus type 1. *J. Neurosci.* 19, 1446–1463.
- Howard, Brammer, M., Wright, I., Woodruff, P.W., Bullmore, E.T., Zeki, S., 1996. A direct demonstration of functional specialization within motion-related visual and auditory cortex of the human brain. *Curr. Biol.* 6, 1015–1019.
- Howard, M., Volkov, I., Mirsky, R., Garell, P., Noh, M., Granner, M., Damasio, H., Steinschneider, M., Reale, R., Hind, J., et al., 2000. Auditory cortex on the human posterior superior temporal gyrus. *J. Comp. Neurol.* 416, 79–92.
- Kühn, A.A., Williams, D., Kupsch, A., Limousin, P., Hariz, M., Schneider, G., Yarrow, K., Brown, P., 2004. Event-related beta desynchronization in human subthalamic nucleus correlates with motor performance. *Brain* 127, 735–746.
- Kühn, A.A., Trottenberg, T., Kivi, A., Kupsch, A., Schneider, G., Brown, P., 2005. The relationship between local field potential and neuronal discharge in the subthalamic nucleus of patients with Parkinson's disease. *Exp. Neurol.* 194, 212–220.
- Kühn, A.A., Kempf, F., Brücke, C., Gaynor Doyle, L., Martinez-Torres, I., Pogossyan, A., Trottenberg, T., Kupsch, A., Schneider, G., Hariz, M.I., et al., 2008. High-frequency stimulation of the subthalamic nucleus suppresses oscillatory beta activity in patients with Parkinson's disease in parallel with improvement in motor performance. *J. Neurosci.* 28, 6165–6173.

- Lalo, E., Thobois, S., Sharott, A., Polo, G., Mertens, P., Pogoyan, A., Brown, P., 2008. Patterns of bidirectional communication between cortex and basal ganglia during movement in patients with Parkinson disease. *J. Neurosci.* 28, 3008–3016.
- Levy, R., Ashby, P., Hutchison, W.D., Lang, A.E., Lozano, A.M., Dostrovsky, J.O., 2002. Dependence of subthalamic nucleus oscillations on movement and dopamine in Parkinson's disease. *Brain* 125, 1196–1209.
- Litvak, V., Eusebio, A., Jha, A., Oostenveld, R., Barnes, G.R., Penny, W.D., Zrinzo, L., Hariz, M.I., Limousin, P., Friston, K.J., et al., 2010. Optimized beamforming for simultaneous MEG and intracranial local field potential recordings in deep brain stimulation patients. *Neuroimage* 50, 1578–1588.
- Marceglia, S., Foffani, G., Bianchi, A.M., Baselli, G., Tamma, F., Egidi, M., Priori, A., 2006. Dopamine-dependent non-linear correlation between subthalamic rhythms in Parkinson's disease. *J. Physiol. Lond.* 571, 579–591.
- Maris, E., Schoffelen, J., Fries, P., 2007. Nonparametric statistical testing of coherence differences. *J. Neurosci. Meth.* 163, 161–175.
- Marsden, J.F., Limousin-Dowsey, P., Ashby, P., Pollak, P., Brown, P., 2001. Subthalamic nucleus, sensorimotor cortex and muscle interrelationships in Parkinson's disease. *Brain* 124, 378–388.
- Mattout, J., Henson, R.N., Friston, K.J., 2007. Canonical source reconstruction for MEG. *Comput. Intell. Neurosci.* 67613.
- Middleton, F.A., Strick, P.L., 1996. The temporal lobe is a target of output from the basal ganglia. *Proc. Natl. Acad. Sci. U. S. A.* 93, 8683–8687.
- Miyachi, S., Lu, X., Imanishi, M., Sawada, K., Nambu, A., Takada, M., 2006. Somatotopically arranged inputs from putamen and subthalamic nucleus to primary motor cortex. *Neurosci. Res.* 56, 300–308.
- Nambu, A., Takada, M., Inase, M., Tokuno, H., 1996. Dual somatotopical representations in the primate subthalamic nucleus: evidence for ordered but reversed body-map transformations from the primary motor cortex and the supplementary motor area. *J. Neurosci.* 16, 2671–2683.
- Nenonen, J., Taulu, S., Kajola, M., Ahonen, A., 2007. Total information extracted from MEG measurements. *Int. Congr. Ser.* 1300, 245–248.
- Nichols, T.E., Holmes, A.P., 2002. Nonparametric permutation tests for functional neuroimaging: a primer with examples. *Hum. Brain Mapp.* 15, 1–25.
- Nolte, G., 2003. The magnetic lead field theorem in the quasi-static approximation and its use for magnetoencephalography forward calculation in realistic volume conductors. *Phys. Med. Biol.* 48, 3637–3652.
- Pollok, B., Makhlofi, H., Butz, M., Gross, J., Timmermann, L., Wojtecki, L., Schnitzler, A., 2009. Levodopa affects functional brain networks in Parkinsonian resting tremor. *Mov. Disord.* 24, 91–98.
- Priori, A., Foffani, G., Pesenti, A., Tamma, F., Bianchi, A.M., Pellegrini, M., Locatelli, M., Moxon, K.A., Villani, R.M., 2004. Rhythm-specific pharmacological modulation of subthalamic activity in Parkinson's disease. *Exp. Neurol.* 189, 369–379.
- Puce, A., Allison, T., Bentin, S., Gore, J.C., McCarthy, G., 1998. Temporal cortex activation in humans viewing eye and mouth movements. *J. Neurosci.* 18, 2188–2199.
- Rodriguez-Oroz, M.C., Rodriguez, M., Guridi, J., Mewes, K., Chockkman, V., Vitek, J., DeLong, M.R., Obeso, J.A., 2001. The subthalamic nucleus in Parkinson's disease: somatotopic organization and physiological characteristics. *Brain* 124, 1777–1790.
- Rosa, M., Marceglia, S., Servello, D., Foffani, G., Rossi, L., Sassi, M., Mrakic-Sposta, S., Zangaglia, R., Pacchetti, C., Porta, M., et al., 2010. Time dependent subthalamic local field potential changes after DBS surgery in Parkinson's disease. *Exp. Neurol.* 222, 184–190.
- Schaltenbrand, G., Wahren, W., 1977. Atlas for stereotaxy of the human brain with guide to the atlas for stereotaxy of the human brain, Pkg Lslf. (Thieme).
- Schnitzler, A., Gross, J., 2005. Normal and pathological oscillatory communication in the brain. *Nat. Rev. Neurosci.* 6, 285–296.
- Schoffelen, J., Gross, 2009. Source connectivity analysis with MEG and EEG. *Hum. Brain Mapp.* 30, 1857–1865.
- Schoffelen, J., Oostenveld, R., Fries, P., 2008. Imaging the human motor system's beta-band synchronization during isometric contraction. *Neuroimage* 41, 437–447.
- Selemon, L., Goldman-Rakic, P., 1985. Longitudinal topography and interdigitation of corticostriatal projections in the rhesus monkey. *J. Neurosci.* 5, 776–794.
- Song, T., Gaa, K., Cui, L., Feffer, L., Lee, R.R., Huang, M., 2008. Evaluation of signal space separation via simulation. *Med. Biol. Eng. Comput.* 46, 923–932.
- Srinivasan, R., Winter, W.R., Ding, J., Nunez, P.L., 2007. EEG and MEG coherence: measures of functional connectivity at distinct spatial scales of neocortical dynamics. *J. Neurosci. Meth.* 166, 41–52.
- Taulu, S., Kajola, M., 2005. Presentation of electromagnetic multichannel data: the signal space separation method. *J. Appl. Phys.* 97, 124905.
- Taulu, S., Simola, J., Kajola, M., 2005. Applications of the signal space separation method. *Signal Process. IEEE Trans.* 53, 3359–3372.
- Timmermann, L., Gross, J., Dirks, M., Volkmann, J., Freund, H., Schnitzler, A., 2003. The cerebral oscillatory network of parkinsonian resting tremor. *Brain* 126, 199–212.
- Trottenberg, T., Kupsch, A., Schneider, G., Brown, P., Kühn, A.A., 2007. Frequency-dependent distribution of local field potential activity within the subthalamic nucleus in Parkinson's disease. *Exp. Neurol.* 205, 287–291.
- Van Hoesen, G.W., Yeterian, E.H., Lavizzo-Mourey, R., 1981. Widespread corticostriate projections from temporal cortex of the rhesus monkey. *J. Comp. Neurol.* 199, 205–219.
- Van Veen, B.D., van Drongelen, W., Yuchtman, M., Suzuki, A., 1997. Localization of brain electrical activity via linearly constrained minimum variance spatial filtering. *IEEE Trans. Biomed. Eng.* 44, 867–880.
- Weinberger, M., Mahant, N., Hutchison, W.D., Lozano, A.M., Moro, E., Hodaie, M., Lang, A.E., Dostrovsky, J.O., 2006. Beta oscillatory activity in the subthalamic nucleus and its relation to dopaminergic response in Parkinson's disease. *J. Neurophysiol.* 96, 3248–3256.
- Williams, D., Tijssen, M., Van Bruggen, G., Bosch, A., Insola, A., Di Lazzaro, V., Mazzone, P., Oliviero, A., Quartarone, A., Speelman, H., et al., 2002. Dopamine-dependent changes in the functional connectivity between basal ganglia and cerebral cortex in humans. *Brain* 125, 1558–1569.
- Winter, W.R., Nunez, P.L., Ding, J., Srinivasan, R., 2007. Comparison of the effect of volume conduction on EEG coherence with the effect of field spread on MEG coherence. *Stat. Med.* 26, 3946–3957.
- Yeterian, E.H., Van Hoesen, G.W., 1978. Cortico-striate projections in the rhesus monkey: the organization of certain cortico-caudate connections. *Brain Res.* 139, 43–63.

Supplementary Material

Table S1 lists the stereotactic coordinates of all contacts from all patients.

Figure S2 demonstrates that each subject showed distinct alpha and beta peaks in MEG-LFP coherence on the sensor level.

S1: Stereotactic coordinates of all DBS electrode contacts mm referenced to mid-commissural point (Schaltenbrand-Wahren coordinate system).

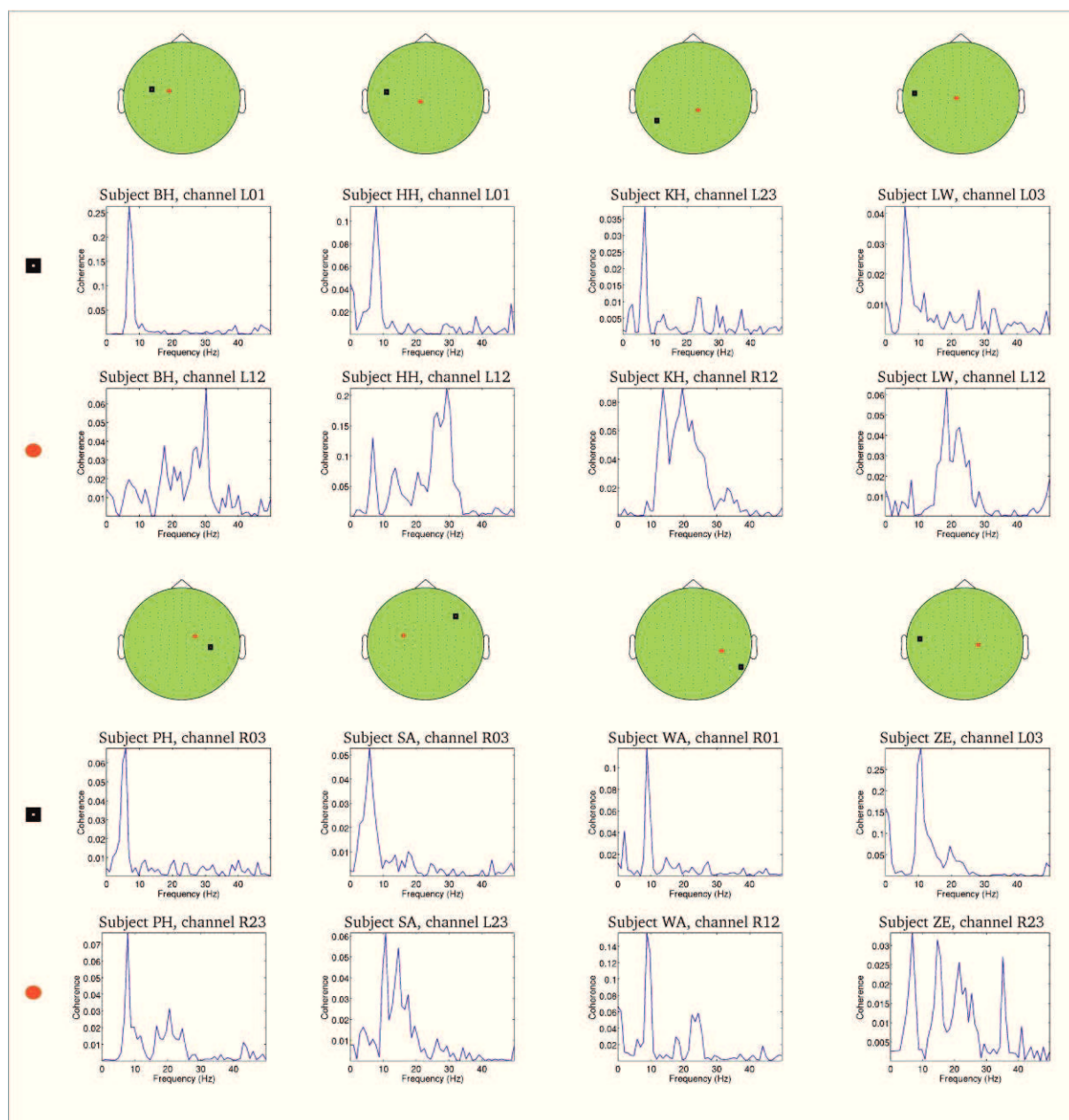
	x	y	z	x	y	z
left 0	-11.1	-3.5	-2.2	-13.6	-3.3	-1.7
left 1	-11.9	-1.7	-0.4	-14.2	-1.7	0.0
left 2	-12.6	0.0	1.4	-14.9	-0.1	1.7
left 3	-13.4	1.8	3.2	-15.6	1.6	3.4
right 0	9.3	-5.2	-3.7	13.8	-1.7	-1.7
right 1	10.1	-3.4	-1.9	14.5	-0.1	0.0
right 2	10.8	-1.7	-0.1	15.2	1.5	1.7
right 3	11.6	0.1	1.7	15.9	3.2	3.4
Patient	BH			HH		

	x	y	z	x	y	z
left 0	-12.5	-2.6	-2.9	-12.2	0.4	-3.9
left 1	-13.1	-1.1	-1.4	-12.9	2.0	-2.3
left 2	-13.7	0.4	0.2	-13.5	3.5	-0.7
left 3	-14.4	1.9	1.7	-14.2	5.1	0.9
right 0	13.2	-4.3	-2.4	11.4	1.4	-5.6
right 1	13.8	-2.8	-0.9	12.1	3.0	-4.0
right 2	14.4	-1.3	0.7	12.7	4.5	-2.4
right 3	15.1	0.2	2.2	13.4	6.1	-0.8
Patient	KH			SA		

	x	y	z	x	y	z
left 0	-8.5	-5.1	-2.6	-12.5	-4.3	-4.2
left 1	-9.1	-3.7	-1.1	-13.1	-2.8	-2.6
left 2	-9.7	-2.3	0.3	-13.8	-1.3	-1.1
left 3	-10.3	-0.9	1.8	-14.4	0.2	0.5
right 0	10.9	-4.7	-3.0	10.8	-5.0	-4.8
right 1	11.5	-3.3	-1.5	11.4	-3.5	-3.2
right 2	12.1	-1.9	-0.1	12.1	-2.0	-1.7
right 3	12.7	-0.5	1.4	12.7	-0.5	-0.1
Patient	ZE			LW		

	x	y	z	x	y	z
left 0	-10.3	-4.1	-2.6	-10.5	-1.3	-3.7
left 1	-11.0	-2.5	-0.9	-11.2	0.4	-2.0
left 2	-11.7	-0.9	0.7	-11.9	2.1	-0.2
left 3	-12.4	0.7	2.4	-12.7	3.8	1.5
right 0	12.0	-4.1	-2.5	13.2	-3.4	-5.4
right 1	12.7	-2.5	-0.8	13.9	-1.7	-3.7
right 2	13.4	-0.9	0.8	14.6	0.0	-1.9
right 3	14.1	0.7	2.5	15.4	1.7	-0.2
Patient	PH			WA		

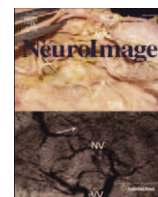
	x	y	z	x	y	z
left 0	-11.4	-3.0	-3.0	1.61	1.78	0.88
left 1	-12.1	-1.4	-1.3	1.62	1.82	0.92
left 2	-12.7	0.2	0.3	1.63	1.86	0.97
left 3	-13.4	1.8	1.9	1.64	1.91	1.03
right 0	11.8	-3.4	-3.6	1.52	2.22	1.48
right 1	12.5	-1.8	-2.0	1.51	2.23	1.47
right 2	13.2	-0.2	-0.4	1.51	2.24	1.48
right 3	13.8	1.4	1.3	1.51	2.26	1.49
Patient	average			standard deviation		



S2: Examples of MEG-LFP coherence on the sensor level. For each subject, the two coherence spectra with the most prominent peaks in the alpha and beta band, respectively, are depicted. The positions of the corresponding MEG sensors are indicated in the topographical plots of the MEG sensor array. Black squares relate to the spectra showing alpha peaks, red circles relate to the spectra showing beta peaks. The corresponding LFP channels are given above the coherence spectra.

References

Schaltenbrand, G., and Wahren, W. (1977). Atlas For Stereotaxy of The Human Brain With Guide to The Atlas For Stereotaxy of The Human Brain, Pkg Lslf. (Thieme).



Differential modulation of STN-cortical and cortico-muscular coherence by movement and levodopa in Parkinson's disease

J. Hirschmann^{a,b}, T.E. Özkurt^c, M. Butz^{a,d}, M. Homburger^{a,b}, S. Elben^{a,b}, C.J. Hartmann^{a,b}, J. Vesper^e, L. Wojtecki^{a,b}, A. Schnitzler^{a,b,*}

^a Institute of Clinical Neuroscience and Medical Psychology, Medical Faculty, Heinrich-Heine-University Düsseldorf, Düsseldorf, Germany

^b Department of Neurology, University Hospital Düsseldorf, Düsseldorf, Germany

^c Department of Health Informatics, Informatics Institute, Middle East Technical University, Ankara, Turkey

^d Sobell Department of Motor Neuroscience and Movement Disorders, Institute of Neurology, University College London, London, UK

^e Department of Functional Neurosurgery and Stereotaxy, University Hospital Düsseldorf, Düsseldorf, Germany

ARTICLE INFO

Article history:

Accepted 15 November 2012

Available online 16 December 2012

Keywords:

Parkinson's disease

Oscillations

MEG

Coherence

STN

Deep brain stimulation

ABSTRACT

Previous research suggests that oscillatory coupling between cortex, basal ganglia and muscles plays an important role in motor behavior. Furthermore, there is evidence that oscillatory coupling is altered in patients with movement disorders such as Parkinson's disease (PD).

In this study, we performed simultaneous magnetoencephalography (MEG), local field potential (LFP) and electromyogram (EMG) recordings in PD patients selected for therapeutic subthalamic nucleus (STN) stimulation. Patients were recorded (i) after withdrawal of anti-parkinsonian medication (OFF) and (ii) after levodopa administration (ON). We analyzed STN-cortical and cortico-muscular coherence during static forearm contraction and repetitive hand movement in order to evaluate modulations of coherence by movement and medication. Based on previous results from studies investigating resting state coherence in PD patients, we selected primary motor cortex (M1) and superior temporal gyrus (STG) as regions of interest.

We found beta coherence between M1 and STN to be suppressed by administration of levodopa. M1-muscular coherence was strongly reduced in the alpha and beta band during repetitive movement compared to static contraction, but was unaffected by administration of levodopa. Strong STG-STN but not STG-muscular coherence could be observed in the alpha band. Coherence with STG was modulated neither by movement nor by medication. Finally, we found both M1-STN and M1-muscular beta coherence to be negatively correlated with UPDRS akinesia and rigidity sub-scores in the OFF state.

The present study provides new insights into the functional roles of STN-cortical and cortico-muscular coherence and their relationship to PD symptoms. The results indicate that STN-cortical and cortico-muscular coupling are correlated, but can be modulated independently. Moreover, they show differences in their frequency-specific topography. We conclude that they represent partly independent sub-loops within the motor system. Given their negative correlation with akinesia, neither can be considered "antikinetic".

© 2012 Elsevier Inc. All rights reserved.

Introduction

Parkinson's disease (PD) is a neurodegenerative disorder resulting from a loss of dopaminergic neurons which leads to alterations of neural activity in the basal ganglia, thalamus and cortex (Lang and Lozano, 1998). Recent research pinpointed excessive synchronization as an electrophysiological hallmark of PD (for a review see Hammond et al., 2007). Local field potential (LFP) recordings from the subthalamic nucleus (STN) of patients undergoing surgery for deep brain stimulation (DBS) revealed strong oscillatory activity, particularly in the beta band

(13–35 Hz). STN beta oscillations were found to be reduced by application of levodopa (Brown et al., 2001; Kühn et al., 2006; Levy et al., 2002; Priori et al., 2004), movement (Cassidy et al., 2002; Kühn et al., 2004) and DBS (Eusebio et al., 2011; Giannicola et al., 2010; Kühn et al., 2008). Furthermore, it was shown that STN beta power reduction correlates with clinical improvement (Kühn et al., 2008). Given their prominence in static states, beta oscillations have been labeled "antikinetic". In turn, gamma oscillations (60–90 Hz) have been labeled "prokinetic" and are considered the functional counterpart of beta oscillations (Brown, 2003). They increase in power with both anti-parkinsonian medication and movement (Cassidy et al., 2002; Williams et al., 2002).

A similar pattern of responses is observable in other brain areas which are part of the motor network and in oscillatory coupling between areas. For example, movement reduces beta band coherence between STN and sensorimotor cortex (Lalo et al., 2008; Marsden

* Corresponding author at: Institute of Clinical Neuroscience and Medical Psychology, Heinrich-Heine-University Düsseldorf, Universitätsstr. 1, D-40225 Düsseldorf, Germany. Fax: +49 211 811 9033.

E-mail address: SchnitzA@med.uni-duesseldorf.de (A. Schnitzler).

et al., 2001b), the latter of which was reported to show enhanced beta power in PD (Pollok et al., 2012). Likewise, beta coherence between sensorimotor cortex and muscle activity is suppressed during movement (Baker et al., 1997; Kilner et al., 1999). The question arises whether these observations reflect network responses, affecting all couplings between motor areas alike, or whether oscillatory coupling may be modulated independently and specifically for any two elements of the network.

An example for independent modulations may be given by the responses of STN-cortical and cortico-muscular beta coherence to PD treatment. Cortico-muscular beta coherence was reported to be enhanced by levodopa (Salenius et al., 2002) and DBS was found to increase intermuscular beta coherence (Marsden et al., 2001a). STN-cortical beta coherence, on the other hand, was reported to be decreased by administration of levodopa (Sharott et al., 2005; Williams et al., 2002) and DBS (Kühn et al., 2008).

However, recent studies could not confirm the effect of pharmacological intervention on STN-cortical coherence. Lalo et al. (2008) investigated the direct transfer function between STN and cortex and did not detect a difference in beta band interactions after levodopa was administered. Along the same lines, Litvak et al. (2011) could not detect a decrease in beta coherence either, but reported an increase in a small area in prefrontal cortex.

In summary, the role of STN-cortical coupling in the pathophysiology of PD remains to be elucidated. Currently, it is unclear if and how it is modulated by levodopa, how such modulations relate to clinical symptoms and whether it changes independently from cortico-muscular coherence. In this study, we aimed to answer these questions by analysis of simultaneous magnetoencephalography (MEG), LFP and electromyogram (EMG) recordings. We studied STN-cortical and cortico-muscular coherence during epochs of repetitive movement and static contraction before and after the administration of levodopa. Our analyses provide a comprehensive and comparative description of STN-cortical and cortico-muscular coherence in PD patients and give new insights into their relation to clinical symptoms.

Materials and methods

Patients

10 PD patients (four female), who were clinically selected for deep brain stimulation (DBS) because of levodopa-induced fluctuations and dyskinesias, participated in this study with written informed consent. For all patients, the dominant symptoms were akinesia and rigidity. MEG and LFP data from eight of these subjects (rest condition, off medication) were analyzed in a previous study (Hirschmann et al., 2011). Table 1 summarizes the clinical details. The study was approved by the local ethics committee (study no. 3209) and is in accordance with the Declaration of Helsinki.

Surgery

The implantation of macroelectrodes was carried out at the Department of Functional Neurosurgery and Stereotaxy of the University Hospital Düsseldorf. The surgical procedures are described elsewhere (Özkurt et al., 2011). Oral anti-parkinsonian medication was withdrawn the evening before surgery and substituted by subcutaneous apomorphine medication. All but one subject were implanted with electrode model 3389 (Medtronic Inc., Minneapolis, MN, USA). Subject 9 was implanted with a DBS system by St. Jude Medical (St. Jude Medical Inc., St. Paul, MN, USA). Electrode placement was guided by intraoperative microelectrode recordings, intraoperative stimulation and clinical testing. Correct placement was confirmed by stereotactic, postsurgical computer tomography (CT). Fig. S1 of the supplementary material shows a projection of the average, normalized coordinates of the contacts used

in this study onto the *Schaltenbrand–Wahren* atlas (Schaltenbrand and Wahren, 1977).

Recordings

We simultaneously recorded MEG, LFPs from the STN, EMG of the *extensor digitorum communis* and *flexor digitorum superficialis* muscles of both upper limbs and vertical and horizontal electrooculograms (EOGs). All recordings were performed using a 306 channel, whole-head MEG system (Elekta Oy, Helsinki, Finland). The sampling rate was 2 kHz. For all but one subject (subject 10) non-magnetic extension leads were available to connect the DBS macroelectrodes to the EEG amplifier integrated into the MEG system. MEG signals were filtered online between 0.03 and 660 Hz, while LFP, EMG and EOG signals were filtered between 0.1 and 660 Hz. EMGs were referenced to surface electrodes at the muscle tendons. LFPs were referenced to a surface electrode at the left mastoid and rearranged into a bipolar montage offline. This was done by subtracting from each of the four monopolar signals the signal of its ventral neighbor channel, so that three bipolar channels per electrode were obtained

Paradigm

Recordings took place the day after surgery. Two hours before recording the apomorphine pump was switched off. The experiment had a block design. It included (i) one block off dopaminergic medication (OFF) and (ii) one block following the administration of levodopa (ON). The clinical OFF state was quantified by means of the motor score of the Movement Disorder Society Unified Parkinson's Disease Rating Scale (MDS-UPDRS III) immediately before the recording started (Goetz et al., 2008). The rating was performed by an experienced movement disorders specialist and recorded with video camera for an additional offline rating by a second rater.

The experiment started with a 5 min rest recording (REST), followed by two motor tasks. Subjects had their eyes open. In the first task (HOLD), subjects were asked to elevate one forearm to about 45° with the elbow resting on a table in front of them and to spread their fingers. In the second task (MOVE), subjects were instructed to open and close one fist. The arm was elevated to about 45°, as in the HOLD condition. Subjects were asked to perform self-paced movements with a frequency of approximately 1 Hz. Task performance was monitored online by the experimenters via a video camera and offline by visual investigation of EMG signals. In all tasks solely the symptom-dominant hand was used. Each motor task lasted 9 min: Five times 1 min of task performance interleaved by four pauses of 1 min duration. Pauses served to avoid muscle fatigue.

After completion of all three aforementioned conditions in the OFF state, levodopa was administered (Madopar LT, Roche Pharma AG, Basel, Switzerland). The doses are listed in Table 1. They were chosen to be approximately 1.5 times the pre-surgical morning dose of each individual subject to obtain a good clinical ON state. In several cases doses were adjusted by the neurologist supervising the experiment in order to minimize levodopa-induced dyskinesias, which occurred in five subjects. After waiting for ≥ 30 min, we tested upper limb rigidity and akinesia. In case an improvement was observable, another MDS UPDRS motor score was performed and videotaped to quantify the subjects' ON state and the motor tasks were repeated.

Apart from the experimenters' instructions and corrections, no visual or auditory stimuli were presented.

Data preprocessing

Data were notch filtered at 50 Hz to remove power line noise. EMGs were high-pass filtered at 10 Hz and full-wave rectified (Kilner et al., 2000). All data were down-sampled to 256 Hz and divided into half-overlapping segments of 256 samples. The 5 min block of motor

Table 1
Clinical details of patients.

Stereotactic coordinates are given in millimeters and are defined according to the *Schaltenbrand–Wahren* coordinate system. Since recordings were bipolar, the table lists the average coordinates of two neighboring contacts for each subject. n.a. = not available.

Subject	Age	Sex	Disease duration (years)	UPDRS OFF presurgical	UPDRS OFF postsurgical	UPDRS ON postsurgical	Pre-surgical medication (daily dose in mg)	Administered dose of levodopa (mg)	Coordinates of contact for LFP recordings (X Y Z)
1	68	M	11	34	43	29	Levodopa 400 Entacapone 800 Pramipexole 1.4	150	– 14.0 – 0.8 0.8
2	75	F	26	n.a.	46	19	Levodopa 800 Ropinirole 18 Rasagiline 1 Tolcapone 100	150	8.6 – 3.8 – 2.5
3	71	M	16	45	48	34	Levodopa 1000 Entacapone 1200 Amantadine 100 Ropinirole 10	200	13.1 5.3 – 1.6
4	70	M	11	34	46	17	Levodopa 825 Entacapone 1000 Pramipexole 3.15 Rasagiline 1	250	– 14.1 – 2.1 – 1.9
5	61	M	16	39	43	27	Levodopa 825 Entacapone 1000 Selegiline 10	200	– 13.3 – 1.9 – 2.2
6	62	M	21	39	61	33	Levodopa 950 Entacapone 1000 Ropinirol 24 Rasagiline 1	250	– 11.1 – 1.8 1.1
7	64	F	18	38	30	11	Levodopa 900 Amantadine 400 Pramipexole 1.4 Rasagiline 1	150	13.3 – 0.8 – 2.6
8	62	F	15	44	27	22	Levodopa 450 Pramipexole 0.54 Rasagiline 1	150	13.3 – 0.1 1.6
9	53	M	11	n.a.	30	15	Levodopa 300 Amantadine 100	300	– 12.0 – 0.6 – 4.9
10	55	F	10	44	46	13	Levodopa 800 Tolcapone 300 Rasagiline 1 Ropinirole 24	200	– 13.1 – 0.2 0.8
Mean	64.1		15.5	40	42	22		200	12.6 – 0.7 – 1.1
Std	7.0		5.2	4.4	10.3	8.3		52.7	1.7 2.4 2.1

task execution, which was interleaved by 1 min pauses, was treated as one continuous recording. Signals underwent thorough visual examination. Artifacts and bad channels were excluded from analysis. Reasons for data exclusion were postural tremor (3 subjects), difficulties in performing the required movement (2 subjects) and contamination by noise from magnetic extension leads (1 subject; see below). Preprocessing and artifact removal yielded epochs of clean data with a mean duration of 257 s per subject and motor task (range: 137–330 s). EMGs were used to identify periods of holding and moving of the hand and pauses between epochs of task execution were discarded.

Subject 10 was recorded with magnetic extension leads. MEG data for this subject were contaminated by artifacts. Thus, we applied *temporal Signal Space Separation* (tSSS) specifically on this dataset in order to suppress the magnetic artifacts (Taulu and Simola, 2006). Previously, tSSS has been used successfully to suppress magnetic artifacts occurring during combined MEG and DBS (Airaksinen et al., 2011, 2012). The limits of spherical harmonic expansion were chosen as $L_{in} = 8$ for the inner and $L_{out} = 3$ for the outer sources, as these values have been shown to be optimal in an earlier study (Taulu et al., 2005). Visual examination confirmed that tSSS resulted in acceptable data quality, except for some epochs which were discarded (mean duration of clean data per condition: 205 s).

Data analysis

Only the 204 gradiometer channels were used for the analysis of MEG signals. Data analysis was performed with *Matlab R2010* (The

Mathworks, Natick, Massachusetts, USA) and we made use of the *FieldTrip* toolbox (Oostenveld et al., 2011). ANOVAs were computed using the software package *IBM SPSS Statistics 19* (IBM Corporation, Somers, USA).

Regions of interest and channel selection

We estimated coherence between two cortical regions of interest (ROIs) and an LFP and EMG reference channel, respectively. In order not to bias statistical analysis, we did not choose ROIs and reference channels based on maxima observed in any of the two motor tasks. Instead, we used maxima occurring in the rest recordings preceding the motor tasks and excluded these recordings from subsequent analysis, i.e. rest recordings served as independent localizer sessions. Thus, we avoided the risk of selecting reference channels and ROIs in which high values occurred by chance in only one of several conditions (Saxe et al., 2006).

The spatial maxima of STN-cortical coherence at rest have been studied previously in a subset of the subjects included here (Hirschmann et al., 2011). In addition, resting state coherence in PD has been investigated in an independent study (Litvak et al., 2011). Both studies reported strong beta coherence between STN and sensorimotor areas, including primary motor cortex (M1). Alpha coherence was found predominantly with areas in the temporal lobe, in particular with superior temporal gyrus (STG). Accordingly, we chose M1 and STG as ROIs. The MNI coordinates were $\pm 33, -22, 57$ for M1 and $\pm 51, -20, 5$ for STG (Hirschmann et al., 2011). Cortico-muscular coherence was measured at the same

location so that it could be directly compared to STN-cortical coherence. The macroelectrode contact pair yielding highest beta coherence with a group of sensorimotor MEG channels at rest was chosen as the reference channel for STN-cortical coherence computations. Only contact pairs contralateral to the moved limb were considered. As reference channel for cortico-muscular coherence, we chose the EMG of the *extensor digitorum communis* muscle of the moved limb.

Spectral analysis

Estimation of spectral parameters was performed using the multitapering approach (Thomson, 1982). We studied three frequency bands: alpha (8–12 Hz), beta (13–35 Hz) and gamma (60–90 Hz). In order to obtain a single value for an entire band, we computed spectral estimates for the central frequency of each band with appropriate spectral smoothing to cover the entire band. For computation of complete spectra, we convolved data with a Hanning taper and applied Welch's method.

Source reconstruction

Estimation of power and coherence on the source level was realized by *Dynamic Imaging of Coherent Sources* (DICS; Gross et al., 2001), a frequency domain beamformer. Orientation of the reconstructed activity was defined as the orientation that maximized power. Regularization was not applied. DICS projects sensor data through a spatial filter derived from the forward model and the MEG sensor cross spectral densities. We used all artifact-free gradiometers for filter construction. The forward model was based on a realistic, single shell head model derived from individual T1-weighted structural magnetic resonance images (Nolte, 2003). The latter were obtained prior to surgery using a Magnetom Trio MRI scanner (Siemens, Erlangen, Germany) and 3D magnetization-prepared rapid gradient-echo imaging (repetition time: 2300 ms, echo time: 2.98 ms).

Analysis of effects of medication and motor task

Effects of medication and motor task were investigated by repeated measures analysis of variance (ANOVA). Coherence values were Fisher z -transformed prior to computing ANOVAs since the distribution of the transform is closer to normal than that of non-transformed coherence (Halliday et al., 1995). The number of data segments considered in statistical analysis was intra-individually balanced across experimental conditions by choosing an equally long interval from all conditions. A three-way ANOVA was performed for each frequency band. The factors were shuffling (ORIGINAL, SHUFFLED), medication (ON, OFF) and motor task (HOLD, MOVE). In the SHUFFLED condition, the signal of the reference channel was shifted forward in time by k segments (circular shift). k was a random integer between 2 and $N-1$, N being the total number of segments. True physiological effects are expected to interact with shuffling as it destroys condition specific coherence differences present in the original data. In case an effect interacted with shuffling, we performed two-way, follow-up ANOVAs for the ORIGINAL and the SHUFFLED condition separately.

Correlation between coherence and clinical symptoms

In order to investigate the relation between coherence and clinical symptoms we computed Pearson's linear correlation coefficient between Fisher z -transformed coherence values and the sum of the hemibody akinesia/rigidity UPDRS sub-scores (part 3, items 3.3b–3.8b, body side specific for the moved limb). We used the average of both ratings, i.e. the online and the offline UPDRS rating for correlation. To assure that the observed correlations were independent of clinical improvements induced by electrode implantation (stun effect) we repeated correlations using pre-surgical UPDRS scores. These were obtained

five days prior to surgery by a movement disorders specialist and were also re-rated offline. Recent pre-surgical OFF scores were unavailable for two cases (subjects 2 and 9).

Statistical tests of correlation were corrected for multiple comparisons by the Benjamini–Hochberg procedure for false discovery rate control. All p -values were adjusted.

Results

There was a main effect of shuffling on coherence for all signal pairs and frequency bands investigated ($F \geq 6.92$, $p \leq 0.03$), except for M1–STN gamma coherence ($F = 2.42$, $p = 0.16$) and STG–muscular alpha coherence ($F = 3.73$, $p = 0.09$). In the following, we will report all significant interactions with shuffling and the results of the corresponding follow-up ANOVAs. Table 2 summarizes the results of the follow-up ANOVAs for the ORIGINAL condition. The degrees of freedom were 1 (between measures) and 9 (error).

Coherence between M1 and STN

We found an interaction between shuffling and medication for M1–STN beta coherence ($F = 11.27$, $p < 0.01$). The follow-up ANOVAs revealed a significant effect of medication in the ORIGINAL ($F = 11.66$, $p < 0.01$) but not in the SHUFFLED condition ($F = 1.62$, $p = 0.24$). In the ORIGINAL condition, a statistical trend was observable for an interaction between medication and motor task ($F = 4.08$, $p = 0.07$). As shown in Fig. 1, administration of levodopa reduced mean M1–STN beta coherence. This effect was more pronounced in the HOLD than in the MOVE condition, in which beta coherence was comparably weak.

Fig. 2 illustrates the spectral changes which occurred in response to levodopa intervention in two individual subjects and the group average. The choice of displayed single subject spectra was based on similarity to group data. The strength of the dopamine-induced reduction and the exact frequencies at which it occurred were variable across subjects, so that the average spectra do not exhibit very clear differences (Figs. 2B and D). Moreover, the effect of levodopa was not limited to the beta band in all cases. Individual subjects showed an additional decrease in alpha coherence or an increase in gamma (60–90 Hz) coherence (Fig. 2A).

Coherence between M1 and muscle

In contrast to M1–STN coherence, M1–muscular coherence showed strong modulation by movement rather than medication. Shuffling interacted with motor task in the alpha ($F = 11.12$, $p < 0.01$) and beta band ($F = 17.79$, $p < 0.01$). The effect of motor task was significant in the ORIGINAL (alpha: $F = 8.41$, $p = 0.02$; beta: $F = 18.9$, $p < 0.01$) but not in the SHUFFLED condition (alpha: $F = 4.45$, $p = 0.06$; beta:

Table 2
ANOVA tables for the original data.

Effects which showed an interaction with shuffling in the foregoing three-way ANOVA are printed in italics.

	Beta coherence M1–STN		Alpha coherence M1–muscle	
	F	p	F	P
<i>Medication</i>	11.66	<0.01	Medication	1.38 0.27
<i>Motor task</i>	2.89	0.12	<i>Motor task</i>	8.41 0.02
<i>Medication * motor task</i>	4.08	0.07	<i>Medication * motor task</i>	0.01 0.94
	Gamma coherence STG–STN		Beta coherence M1–muscle	
	F	p	F	P
<i>Medication</i>	3.61	0.09	Medication	0.25 0.63
<i>Motor task</i>	1.40	0.27	<i>Motor task</i>	18.90 <0.01
<i>Medication * motor task</i>	0.48	0.51	<i>Medication * motor task</i>	0.04 0.86

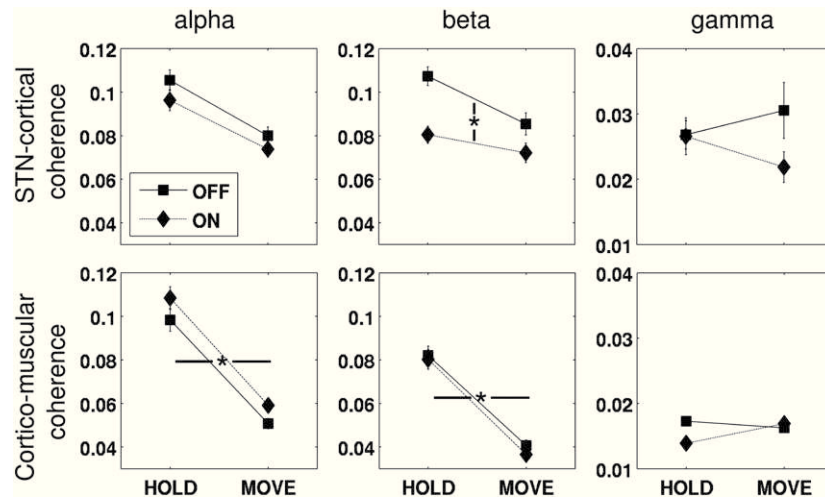


Fig. 1. Effects of levodopa and motor task on mean coherence with M1. Coherence values were z-transformed and averaged across subjects. Error bars indicate the standard error of the mean (SEM). Asterisks mark significant differences ($p < 0.05$). Please note the smaller scaling for the gamma band.

$F = 0.05$, $p = 0.83$). As depicted in Fig. 1, mean cortico-muscular alpha and beta coherence was smaller in the MOVE than in the HOLD condition.

Fig. 3 illustrates the spectral changes induced by movement in two individual subjects and the group average. The effect of motor task on M1-muscular coherence was more broad-band and more consistent across subjects than the effect of levodopa on M1-STN coherence (Figs. 3B and D). It was equally strong in the OFF and the ON state.

Coherence between STG and STN

Fig. 4 depicts the average STG-STN and STG-muscular coherence spectra. STG showed strong alpha band coherence with STN in all

experimental conditions, as evidenced by a strong main effect of shuffling ($F = 14.56$, $p < 0.01$). STG-STN coherence was neither modulated by administration of levodopa nor by motor task in any frequency band. We did find a significant interaction between shuffling and medication in the gamma band ($F = 5.80$, $p = 0.04$). However, the effect of medication was not significant in the ORIGINAL condition ($F = 3.61$, $p = 0.09$).

Coherence between STG and muscle

In contrast to STG-STN coherence, shuffling did not affect alpha coherence between STG and muscle ($F = 3.73$, $p = 0.09$), indicating

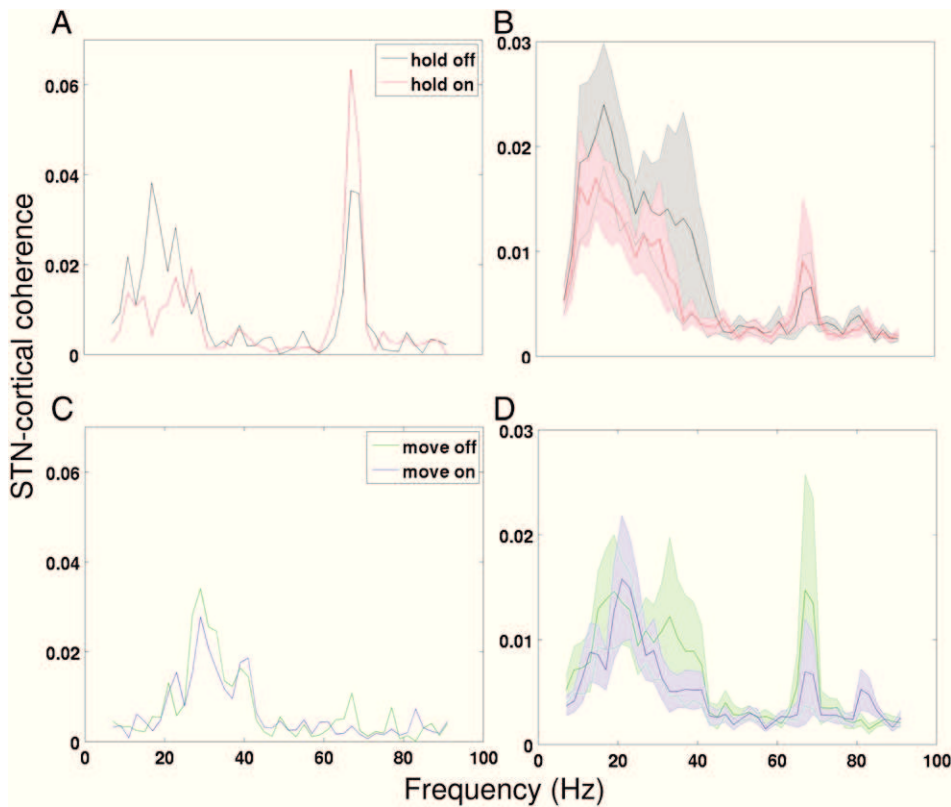


Fig. 2. Administration of levodopa reduces beta coherence between M1 and STN. A) Coherence spectra of subject 6 in the HOLD condition. Please note the gamma band increase co-occurring with a beta band decrease. B) Average coherence in the HOLD condition. Shaded areas indicate SEMs. C) Coherence spectra of subject 2 in the MOVE condition. D) Average coherence in the MOVE condition.

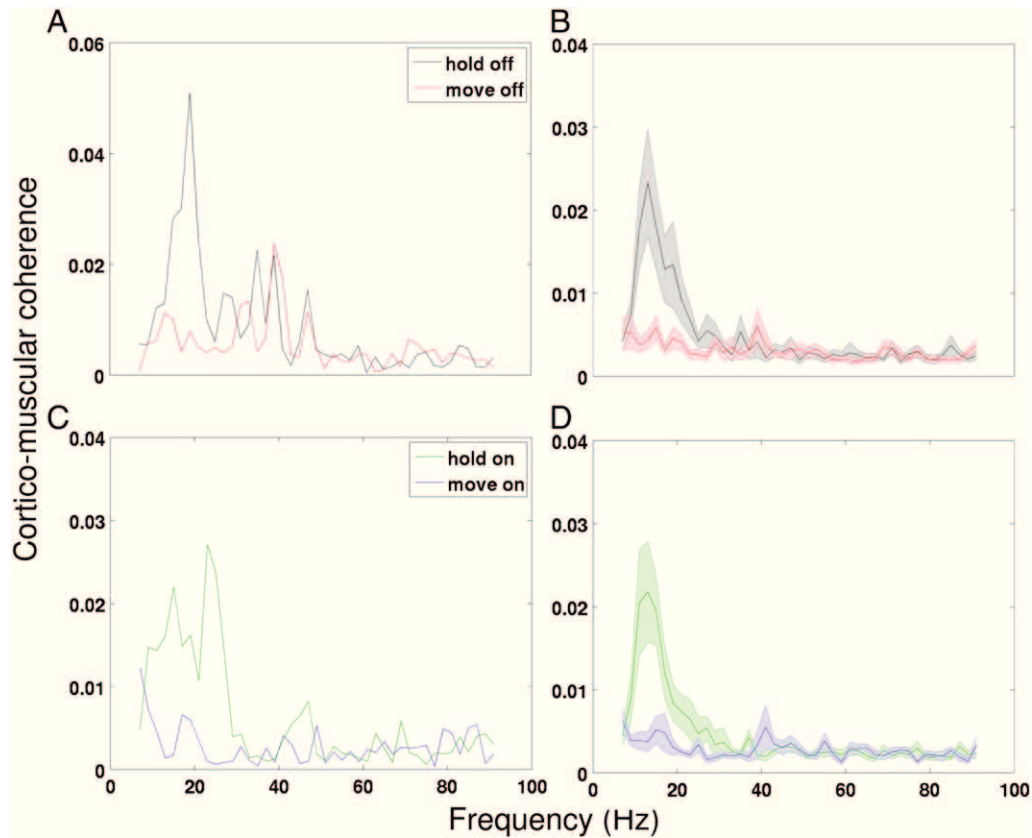


Fig. 3. Movement reduces alpha and beta coherence between M1 and muscle. A) Coherence spectra of subject 10 in medication OFF. B) Average coherence in medication OFF. Shaded areas indicate SEMs. C) Coherence spectra of subject 7 in medication ON. D) Average coherence in medication ON.

that muscle activity was not coherent with STG activity in the alpha band. While there was a main effect of shuffling when considering beta or gamma coherence, no significant interactions with shuffling were detected in any frequency band.

MEG, LFP and EMG power and STN–muscular coherence

We investigated whether modulations of power were similar to modulations of coherence. To limit the amount of statistical tests, only signals showing significant modulations of coherence in the previous analysis were considered. Fig. S2 of the supplementary material shows the condition-specific means. M1 alpha and beta power were neither affected by medication nor by motor task. STN beta power

was reduced by administration of levodopa ($F = 12.65$, $p < 0.01$) and showed a trend for reduction by movement ($F = 4.6$, $p = 0.06$). EMG alpha ($F = 6.96$, $p = 0.03$) and beta ($F = 7.09$, $p = 0.03$) power were increased during MOVE compared to HOLD.

In addition, we investigated modulations of coherence between STN and muscle. STN–muscular coherence was reduced by movement in the beta band ($F = 11.9$, $p < 0.01$) but was not affected by administration of levodopa (Fig. S3).

Correlations with UPDRS

The reduction of M1–STN beta coherence induced by levodopa did not correlate with the reduction of akinesia/rigidity hemibody UPDRS

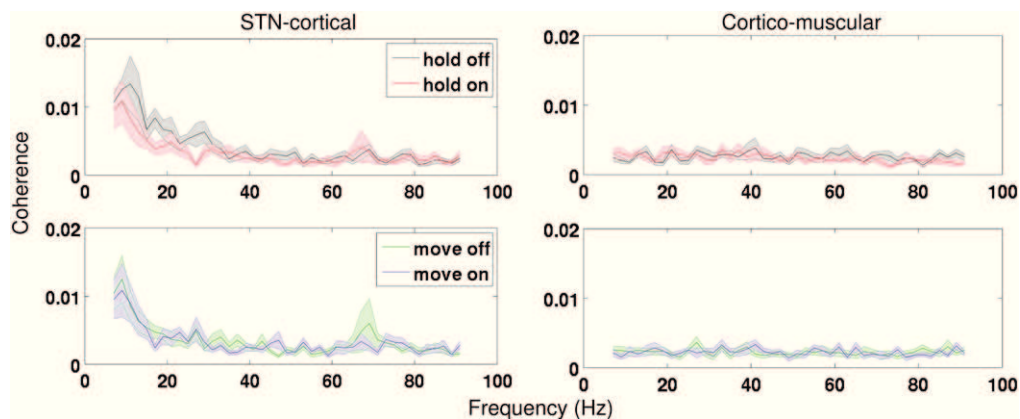


Fig. 4. STN but not muscle activity is coherent with STG. Average coherence between STG and STN (left) and STG and muscle (right). Shaded areas indicate SEMs.

score, nor did coherence and UPDRS correlate in the ON state ($|r| \leq 0.29$, $p \geq 0.52$). In the OFF state, however, M1–STN beta coherence correlated negatively with UPDRS score, i.e. the subjects with the least akinesia showed the strongest coupling. The anti-correlation was significant in the MOVE OFF condition ($r = -0.82$, $p = 0.04$) and a trend was observable in the HOLD OFF condition ($r = -0.67$, $p = 0.08$). For coherence between M1 and muscle, a similar pattern was observed ($r_{\text{HOLD_OFF}} = -0.70$, $p = 0.07$; $r_{\text{MOVE_OFF}} = -0.73$, $p = 0.06$; Fig. 5). The correlation was specific to the beta band. Neither alpha ($r_{\text{M1_STN}} = 0.01$, $p = 0.99$; $r_{\text{M1_MUSCLE}} = -0.48$, $p = 0.25$) nor gamma band coherence ($r_{\text{M1_STN}} = -0.34$, $p = 0.46$; $r_{\text{M1_MUSCLE}} = 0.00$, $p = 0.99$) showed a similar relation to UPDRS scores (Fig. 6). Furthermore, the correlation could not be attributed to changes induced by electrode implantation. Like post-surgical scores, pre-surgical OFF scores were negatively correlated with M1–STN beta coherence ($r = -0.88$, $p = 0.04$; Fig. S4).

The similarity between M1–STN and M1–muscular coherence regarding their relation to clinical symptoms suggests that they are not independent, despite their different sensitivity to movement and levodopa. Indeed, we found a positive relationship between M1–STN and M1–muscular beta coherence (Fig. S5). The latter was significant in HOLD OFF ($r = 0.80$, $p = 0.04$) and observable as a trend in MOVE OFF ($r = 0.65$, $p = 0.08$) and MOVE ON ($r = 0.72$, $p = 0.06$). Interestingly, it was much weaker in HOLD ON ($r = 0.52$, $p = 0.21$), i.e. the experimental condition in which the effect of levodopa administration on M1–STN beta coherence was strongest.

Finally, we found indications that the negative relationship between beta coherence and UPDRS scores may hold in the resting state as well (Fig. S6). However, anti-correlations were weaker in REST OFF than during task performance and did not reach significance ($r_{\text{M1_STN}} = -0.60$, $p = 0.12$; $r_{\text{M1_MUSCLE}} = -0.68$, $p = 0.07$).

Effect of spatial sampling

We investigated coherence between a reference channel and cortical ROIs which consisted of a single cortical location each. Thus, spatial sampling of the cortical signal was very sparse. Spatial under-sampling may act as confound, especially if the quality of the spatial

filter varies systematically across conditions. In order to assess the robustness of the results against changes in spatial sampling, we repeated the analysis with a different definition of the M1 ROI. Instead of a single location, we considered a 2-dimensional grid in the axial plane that was centered on the original M1 ROI (5×5 points, 5 mm spacing). Importantly, changing the ROI did not lead to any qualitative changes, neither with regard to modulation of coherence (Table S2), nor with regard to correlations with UPDRS (Fig. S7).

Discussion

In this study, we investigated modulations of oscillatory coupling between cortex, STN and muscle by movement and administration of levodopa in akinetic-rigid PD patients. We found that beta band coherence between STN and motor cortex was reduced by administration of levodopa. Alpha and beta band coherence between forearm muscle and motor cortex was strongly reduced during repetitive movement compared to static contraction but was not affected by levodopa. STN-cortical and cortico-muscular beta coherence were negatively correlated with akinesia/rigidity UPDRS scores in the OFF state.

Methodological considerations

Before discussing the results in detail, we would like to point out some methodological limitations. First, for organizational reasons subjects were recorded the day after surgery. It has been shown that electrode impedance is variable in the first days following surgery (Rosa et al., 2010). Therefore, it is conceivable that LFP signal quality and therewith coherence changed at a timescale of several days after surgery. Given the slow dynamics of impedance changes, they are, however, unlikely to have caused coherence changes across experimental conditions which occurred within minutes. Moreover, impedance changes are not expected to introduce couplings between cortex and STN, i.e. to generate false positive couplings.

Second, we estimated contact position by projecting normalized coordinates derived from post-surgical CT onto the *Schaltenbrand–Wahren* atlas. Like all other available methods, the procedure is not precise enough to know exactly whether a given contact was recording from

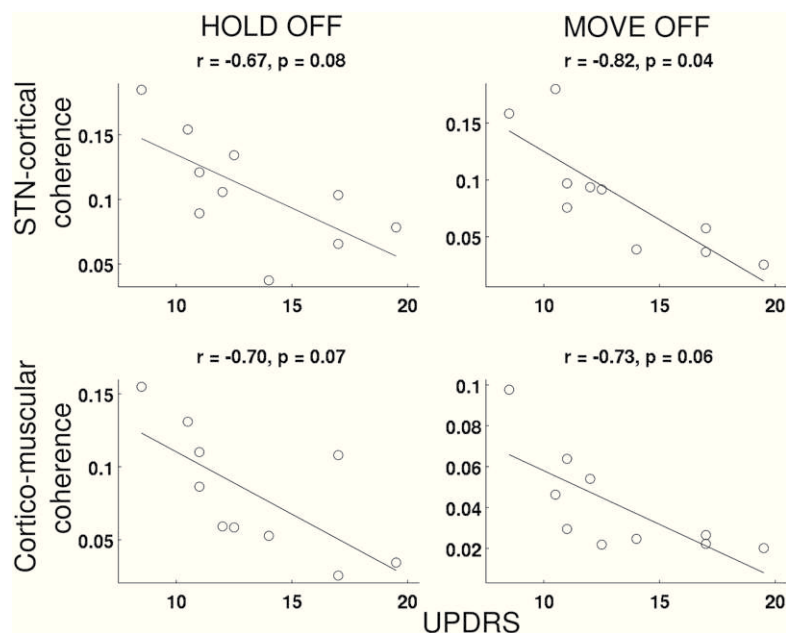


Fig. 5. M1–STN and M1–muscular beta coherence are anti-correlated with UPDRS scores in the OFF state. Beta coherence between motor cortex and STN is plotted against hemibody akinesia/rigidity UPDRS OFF score in the upper row. The lower row shows the same plots for cortico-muscular coherence. Black lines indicate the best linear fit. Pearson's correlation coefficients and the corresponding p-values are given in the figure headings.

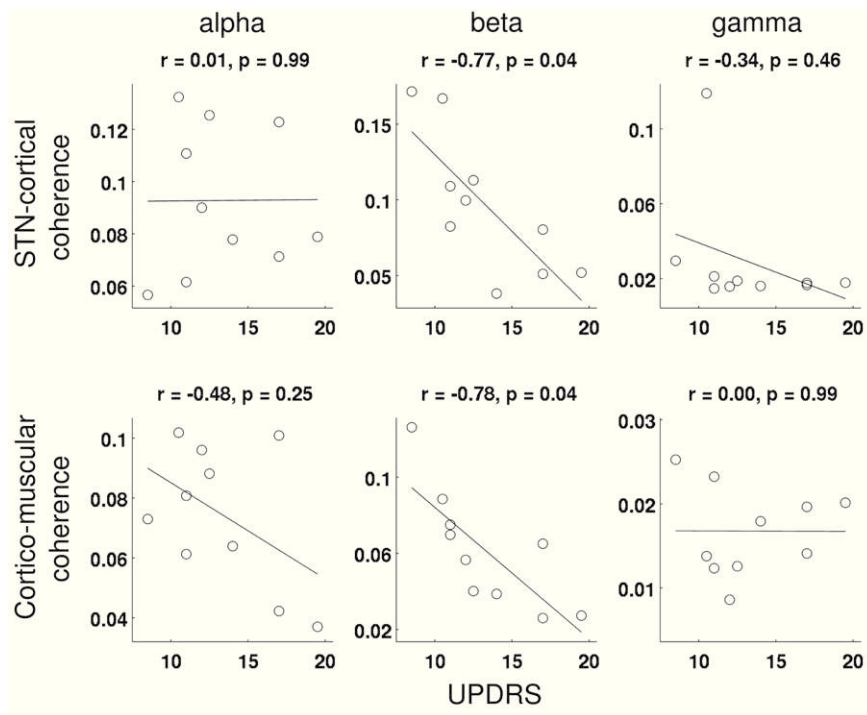


Fig. 6. The negative correlation between coherence and UPDRS scores is frequency-specific. Scatter plots show M1–STN (upper row) and M1–muscular coherence (lower row) plotted against hemibody akinesia/rigidity UPDRS OFF score. Coherence was averaged across HOLD OFF and MOVE OFF. Black lines indicate the best linear fit. Pearson's correlation coefficients and the according p-values are given in the figure headings.

the STN or nearby areas. Atlas-based localization bears the advantage of avoiding the potential risks and artifacts associated with post-surgical MR imaging and the difficulty of identifying the STN on individual MR images (O'Gorman et al., 2004; Videen et al., 2008). Strong support for contact placement in the STN comes from the observed clinical effects of stimulation and from microelectrode recordings during surgery rather than from post-surgical imaging.

Third, the influence of changes in power and therewith signal-to-noise ratio (SNR) is a fundamental problem in the analysis of coherence differences (Palva and Palva, 2012; Schoffelen and Gross, 2009). The statistical analysis of group data reduces the influence of this confound, as SNR variations need to be consistent across subjects in order to have an effect. Furthermore, comparison of coherence between different signals can help to assess the impact of power changes. In this study, STN-cortical and cortico-muscular coherence were modulated differently, although the cortical signal was identical in both cases. Thus, cortical power changes cannot explain the observed changes in coherence. Power changes in the reference channel cannot explain them either, as a power decrease (STN beta power in response to levodopa) and a power increase (EMG beta power in response to movement) were both associated with a coherence decrease. Nevertheless, influences of power changes cannot be ruled out completely.

Fourth, we made use of a block design to investigate movement effects. Thus, signals were treated as stationary although EMG, LFP and MEG signals are known to undergo movement-related changes. For example, M1 beta power is reduced prior to movement and re-emerges following movement execution (e.g. Pfurtscheller et al., 2003). In consequence, the current study cannot answer how much each aspect of temporal modulation contributed to the net effects reported here.

Finally, the possibility remains that LFP recordings contained contributions from areas other than the STN. A major contribution is unlikely, however, since bipolar referencing minimized the impact of volume conduction. The fact that we did not find coherent sources in or near the STN in a previous study (Hirschmann et al., 2011) evidences that

bipolar LFP channels record local STN activity which is not detected by MEG.

Coherence with STG

Two studies independently reported resting state alpha coherence between STN and temporal areas, such as STG (Hirschmann et al., 2011; Litvak et al., 2011). Here we show that STN but not muscle activity is coherent with STG activity in the alpha band during motor tasks. The functional significance of this coupling remains unclear. In this study, coherence was neither modulated by movement nor by administration of levodopa, suggesting that it does not play a role in the basal ganglia-cortex sensorimotor loop. It is conceivable that alpha band coherence between STN and temporal cortex is related to auditory processing (Airaksinen et al., 2011). Alternatively, one might speculate that alpha band coherence reflects attentional processes, in which alpha oscillations are thought to play an important role (Palva and Palva, 2007). In fact, there are some indications for an involvement of STG and STN in attention: in a functional MRI study designed to reveal attention networks, presentation of an alerting, visual cue activated STG and also the thalamus, which could mediate functional connectivity with STN (Fan et al., 2005). In a study investigating the neuropsychological effects of DBS it was found that, amongst other effects, STN stimulation led to a decline in selective attention (Smeding et al., 2006). Experimental manipulation of attention is required to further address the relevance of STN–STG alpha coherence in attentional processes.

Effects of motor task

We measured coherence during repetitive movement and static contraction. In line with previous literature (Baker et al., 1997; Kilner et al., 1999, 2000), movement decreased M1–muscular beta coherence compared to static contraction. M1–STN beta coherence, which has

been reported to be reduced during movement as well (Marsden et al., 2001b), did not show a main effect of motor task in this study. However, the levodopa-induced decrease in M1–STN beta coherence tended to be weaker in the MOVE than in the HOLD condition, indicating a floor effect.

In general, this study provides further evidence for a modulation of STN–cortical and cortico–muscular coupling by movement and supports the general notion that oscillatory activity in the beta band is suppressed during a change in motor state (Engel and Fries, 2010). In addition, it shows that STN–cortical and cortico–muscular coherence differ in their responsiveness to movement.

Recently, Litvak et al. (2012) investigated movement-induced changes in STN–cortical coupling in detail and found short-lived increases in the gamma band at the time of movement onset. In the present study, effects in the gamma band were not observed on the group level, most likely because their detection requires an event-related experimental design. However, clear coherence peaks in the gamma band were observed in a subset of subjects, consistent with the findings by Litvak et al. and other previous studies (Cassidy et al., 2002; Williams et al., 2002).

Effects of medication

We found that levodopa administration decreased beta coherence between STN and motor cortex. This finding is in good keeping with a study in the rat model of PD reporting that injection of the dopamine receptor agonist apomorphine reduced STN–cortical beta coherence in animals with a 6-hydroxydopamine (6-OHDA) midbrain lesion (Sharott et al., 2005). Furthermore, it is in line with a study by Williams et al. (2002), which investigated STN–cortical coherence in PD patients before and after levodopa administration and presented data evidencing a suppression of beta coherence by levodopa. The result is not in agreement, however, with two more recent studies in PD patients which did not report such an effect (Lalo et al., 2008; Litvak et al., 2011). These studies differed from the current study as they used a different coupling measure (Lalo et al., 2008), investigated rest rather than movement epochs (Litvak et al., 2011) and did not exclude tremor-dominant PD patients. In this study, we excluded tremor-dominant patients to assure that the observed changes in coherence are not confounded by changes in tremor-associated coherence (Pollok et al., 2008; Timmermann et al., 2003). Selection of tremor-free data may also explain why we could not confirm the previously reported decrease in cortico–muscular alpha coherence and concurrent increase in cortico–muscular beta coherence in response to levodopa administration (Salenius et al., 2002), as these are characteristics of tremor alleviation (Park et al., 2009; Wang et al., 2007).

Another plausible explanation why some previous studies did not find an effect of levodopa on STN–cortical beta coherence could be that the effect is mild and therefore hard to detect. In this study, we applied a methodology with strong emphasis on estimation reliability and statistical power. We combined beamforming, multitaper spectral estimation and ROI analysis. Beamforming offers protection against artifacts to some extent (Litvak et al., 2010), making source-level estimates of coherence often more reliable than sensor-level estimates. Estimation reliability was further increased by using the multitapering method, i.e. by averaging many estimates. Finally, the statistics computed from these estimates did not have to be corrected for multiple comparisons since we concentrated on only two ROIs. Thus, we were able to detect effects which are easily overlooked with less sensitive approaches.

Is strong STN–cortical beta coherence pathological?

Beta oscillations in the STN have been labeled “antikinetic” (Brown, 2003) in the sense that strong beta activity is either correlated with or causing the slowing of movement in PD. This view is supported by an impressive body of evidence (Brown, 2007). Given that the cortex was

reported to drive STN activity in the beta band (Lalo et al., 2008; Litvak et al., 2011; Williams et al., 2002), one might expect STN–cortical beta coherence to reflect this pathological drive and consider it “antikinetic” as well.

The present study casts doubt on the appropriateness of this label. The negative correlation with UPDRS scores rather suggests that strong M1–STN beta coherence may be beneficial for PD patients in the OFF state. Interestingly, the negative relationship was observed for both M1–STN and M1–muscular coherence in both motor tasks and at rest, suggesting that it holds for baseline levels of beta band coupling within a wider sensorimotor network.

The observed anti-correlation can be interpreted in two ways. One could assume that PD patients with a low UPDRS score bear more resemblance to healthy subjects with regard to STN–cortical coupling than patients with a higher score, i.e. that the observed anti-correlation can be extrapolated. In this case, one would expect healthy humans, unlike rats (Sharott et al., 2005), to show stronger M1–STN beta coherence than subjects suffering from PD. In consequence, M1–STN beta coherence would need to be considered a physiological parameter which is reduced in PD, as was proposed for M1–muscular beta coherence (Salenius et al., 2002). Hence, both couplings may reflect a pathologically reduced, system-wide beta coupling baseline which is necessary for motor control. This interpretation is in line with the observation that both measures are correlated. However, it implies that levodopa reduces a physiological coupling. A possible explanation for this seemingly paradoxical effect could be that levodopa acts not by restoring the absolute but the relative level of M1–STN beta coherence, thereby reestablishing the balance among couplings in the motor system. Another possibility is that the dopamine-induced reduction of M1–STN beta coherence is a by-product of the dopamine-induced reduction of STN beta power. This effect might create the misleading impression that the roles of beta coherence and beta power in motor control are similar, although they may actually be fundamentally different. The latter idea is supported by the observation that in some subjects M1–STN coherence and STN power peak at different frequencies within the beta band.

As an alternative to viewing strong beta coherence as a part of normal motor function, one may hypothesize that patients with a low UPDRS score are compensating better for dopamine depletion than patients with a higher score. M1–STN beta coherence may mark the ability to compensate and be actively up-regulated in PD. Compensation may become oblivious when dopamine is administered, explaining the reduction in coherence by administration of levodopa. This interpretation would also explain why a correlation between coherence and motor score was observed only in the OFF state. Supporting the idea of cortex-driven compensation, motor cortex was shown to increase its oscillatory activity in the beta band (Degos et al., 2009) and its influence on basal ganglia output structures in response to dopamine depletion in the basal ganglia (Belluscio et al., 2007; Dejean et al., 2012; Magill et al., 2001). The temporal evolution of changes in cortical beta band oscillations and cortico–basal ganglia coupling did not match the development of motor impairments, suggesting that they relate to neuronal reorganization rather than causing or reflecting PD symptoms (Degos et al., 2009; Dejean et al., 2012). It is possible that these changes serve compensation and that STN–cortical beta coherence is a marker of cortical control exerted on the STN.

Further studies are needed to test the hypotheses outlined above. A better understanding of the underlying mechanisms may require investigation of not only beta oscillations but also their cross-frequency coupling with activity in other frequency bands, such as high frequency oscillations, which attracted interest recently (López-Azcárate et al., 2010; Özkurt et al., 2011).

Conclusion

We investigated oscillatory coupling in PD patients and found that STN–cortical and cortico–muscular coherence are correlated but can

be modulated independently by levodopa, suggesting that they reflect activity in two partly independent sub-loops within the motor system. Being anti-correlated to akinesia and rigidity, they might reflect physiological or compensatory rather than pathological mechanisms.

Role of the funding source

The funding source did neither influence the study design, collection, analysis or interpretation of data nor the decision to submit the paper for publication.

Acknowledgments

The authors would like to express their sincere gratefulness to the patients who participated in this study. Furthermore, we are very thankful to Nienke Hoogenboom for helpful discussions of data analysis and to the people of Medtronic (Dr. Ali Sarem-Aslani, Mr. Paul van Venrooij, and Mr. Andreas Rolf) for technical support. In addition, we thank Mrs. E. Rädisch for assistance with MRI scans. A.S. acknowledges support by the ERANET-Neuron Grant “PhysiolDBS” (Neuron-48-013) and by the DFG (FOR1328, SCHN 592/3-1). M.B. was supported by a Marie Curie Fellowship of the EU (FP7-PEOPLE-2009-IEF-253965).

Appendix A. Supplementary data

Supplementary data to this article can be found online at <http://dx.doi.org/10.1016/j.neuroimage.2012.11.036>.

References

- Airaksinen, K., Mäkelä, J.P., Taulu, S., Ahonen, A., Nurminen, J., Schnitzler, A., Pekkonen, E., 2011. Effects of DBS on auditory and somatosensory processing in Parkinson's disease. *Hum. Brain Mapp.* 32, 1091–1099.
- Airaksinen, K., Butorina, A., Pekkonen, E., Nurminen, J., Taulu, S., Ahonen, A., Schnitzler, A., Mäkelä, J.P., 2012. Somatomotor mu rhythm amplitude correlates with rigidity during deep brain stimulation in Parkinsonian patients. *Clin. Neurophysiol.* 123 (10) (October), 2010–2017.
- Baker, S.N., Olivier, E., Lemon, R.N., 1997. Coherent oscillations in monkey motor cortex and hand muscle EMG show task-dependent modulation. *J. Physiol.* 501, 225–241.
- Belluscio, M.A., Riquelme, L.A., Murer, M.G., 2007. Striatal dysfunction increases basal ganglia output during motor cortex activation in parkinsonian rats. *Eur. J. Neurosci.* 25, 2791–2804.
- Brown, P., 2003. Oscillatory nature of human basal ganglia activity: relationship to the pathophysiology of Parkinson's disease. *Mov. Disord.* 18, 357–363.
- Brown, P., 2007. Abnormal oscillatory synchronisation in the motor system leads to impaired movement. *Curr. Opin. Neurobiol.* 17, 656–664.
- Brown, P., Oliviero, A., Mazzone, P., Insola, A., Tonali, P., Di Lazzaro, V., 2001. Dopamine dependency of oscillations between subthalamic nucleus and pallidum in Parkinson's disease. *J. Neurosci.* 21, 1033–1038.
- Cassidy, M., Mazzone, P., Oliviero, A., Insola, A., Tonali, P., Di Lazzaro, V., Brown, P., 2002. Movement-related changes in synchronization in the human basal ganglia. *Brain* 125, 1235–1246.
- Degos, B., Deniau, J.-M., Chavez, M., Maurice, N., 2009. Chronic but not acute dopaminergic transmission interruption promotes a progressive increase in cortical beta frequency synchronization: relationships to vigilance state and akinesia. *Cereb. Cortex* 19, 1616–1630.
- Dejean, C., Nadjar, A., Le Moine, C., Bioulac, B., Gross, C.E., Boraud, T., 2012. Evolution of the dynamic properties of the cortex–basal ganglia network after dopaminergic depletion in rats. *Neurobiol. Dis.* 46, 402–413.
- Engel, A.K., Fries, P., 2010. Beta-band oscillations—signalling the status quo? *Curr. Opin. Neurobiol.* 20, 156–165.
- Eusebio, A., Thevathasan, W., Doyle Gaynor, L., Pogoyan, A., Bye, E., Foltynie, T., Zrinzo, L., Ashkan, K., Aziz, T., Brown, P., 2011. Deep brain stimulation can suppress pathological synchronisation in parkinsonian patients. *J. Neurol. Neurosurg. Psychiatry* 82, 569–573.
- Fan, J., McCandliss, B.D., Fossella, J., Flombaum, J.I., Posner, M.I., 2005. The activation of attentional networks. *NeuroImage* 26, 471–479.
- Giannicola, G., Marceglia, S., Rossi, L., Mrakic-Sposta, S., Rampini, P., Tamma, F., Cogiamanian, F., Barbieri, S., Priori, A., 2010. The effects of levodopa and ongoing deep brain stimulation on subthalamic beta oscillations in Parkinson's disease. *Exp. Neurol.* 226, 120–127.
- Goetz, C.G., Tilley, B.C., Shaftman, S.R., Stebbins, G.T., Fahn, S., Martinez-Martin, P., Poewe, W., Sampaio, C., Stern, M.B., Dodel, R., et al., 2008. Movement Disorder Society-sponsored revision of the Unified Parkinson's Disease Rating Scale (MDS-UPDRS): scale presentation and clinimetric testing results. *Mov. Disord.* 23, 2129–2170.
- Gross, J., Kujala, J., Hamalainen, M., Timmermann, L., Schnitzler, A., Salmelin, R., 2001. Dynamic imaging of coherent sources: studying neural interactions in the human brain. *Proc. Natl. Acad. Sci. U. S. A.* 98, 694–699.
- Halliday, D.M., Rosenberg, J.R., Amjad, A.M., Breeze, P., Conway, B.A., Farmer, S.F., 1995. A framework for the analysis of mixed time series/point process data—theory and application to the study of physiological tremor, single motor unit discharges and electromyograms. *Prog. Biophys. Mol. Biol.* 64, 237–278.
- Hammond, C., Bergman, H., Brown, P., 2007. Pathological synchronization in Parkinson's disease: networks, models and treatments. *Trends Neurosci.* 30, 357–364.
- Hirschmann, J., Özkurt, T.E., Butz, M., Homburger, M., Elben, S., Hartmann, C.J., Vesper, J., Wojtecki, L., Schnitzler, A., 2011. Distinct oscillatory STN–cortical loops revealed by simultaneous MEG and local field potential recordings in patients with Parkinson's disease. *NeuroImage* 55, 1159–1168.
- Kilner, J.M., Baker, S.N., Salenius, S., Jousmäki, V., Hari, R., Lemon, R.N., 1999. Task-dependent modulation of 15–30 Hz coherence between rectified EMGs from human hand and forearm muscles. *J. Physiol.* 516, 559–570.
- Kilner, J.M., Baker, S.N., Salenius, S., Hari, R., Lemon, R.N., 2000. Human Cortical Muscle Coherence Is Directly Related to Specific Motor Parameters. *J. Neurosci.* 20, 8838–8845.
- Kühn, A.A., Williams, D., Kupsch, A., Limousin, P., Hariz, M., Schneider, G.-H., Yarrow, K., Brown, P., 2004. Event-related beta desynchronization in human subthalamic nucleus correlates with motor performance. *Brain* 127, 735–746.
- Kühn, A.A., Kupsch, A., Schneider, G.-H., Brown, P., 2006. Reduction in subthalamic 8–35 Hz oscillatory activity correlates with clinical improvement in Parkinson's disease. *Eur. J. Neurosci.* 23, 1956–1960.
- Kühn, A.A., Kempf, F., Brücke, C., Gaynor Doyle, L., Martinez-Torres, I., Pogoyan, A., Trottenberg, T., Kupsch, A., Schneider, G.-H., Hariz, M.I., et al., 2008. High-frequency stimulation of the subthalamic nucleus suppresses oscillatory beta activity in patients with Parkinson's disease in parallel with improvement in motor performance. *J. Neurosci.* 28, 6165–6173.
- Lalo, E., Thobois, S., Sharott, A., Polo, G., Mertens, P., Pogoyan, A., Brown, P., 2008. Patterns of bidirectional communication between cortex and basal ganglia during movement in patients with Parkinson disease. *J. Neurosci.* 28, 3008–3016.
- Lang, A.E., Lozano, A.M., 1998. Parkinson's Disease. *N. Engl. J. Med.* 339, 1130–1143.
- Levy, R., Ashby, P., Hutchison, W.D., Lang, A.E., Lozano, A.M., Dostrovsky, J.O., 2002. Dependence of subthalamic nucleus oscillations on movement and dopamine in Parkinson's disease. *Brain* 125, 1196–1209.
- Litvak, V., Eusebio, A., Jha, A., Oostenveld, R., Barnes, G.R., Penny, W.D., Zrinzo, L., Hariz, M.I., Limousin, P., Friston, K.J., et al., 2010. Optimized beamforming for simultaneous MEG and intracranial local field potential recordings in deep brain stimulation patients. *NeuroImage* 50, 1578–1588.
- Litvak, V., Jha, A., Eusebio, A., Oostenveld, R., Foltynie, T., Limousin, P., Zrinzo, L., Hariz, M.I., Friston, K., Brown, P., 2011. Resting oscillatory cortico-subthalamic connectivity in patients with Parkinson's disease. *Brain* 134, 359–374.
- Litvak, V., Eusebio, A., Jha, A., Oostenveld, R., Barnes, G., Foltynie, T., Limousin, P., Zrinzo, L., Hariz, M.I., Friston, K., et al., 2012. Movement-Related Changes in Local and Long-Range Synchronization in Parkinson's Disease Revealed by Simultaneous Magnetoencephalography and Intracranial Recordings. *J. Neurosci.* 32, 10541–10553.
- López-Azcárate, J., Tainta, M., Rodríguez-Oroz, M.C., Valencia, M., González, R., Guridi, J., Iriarte, J., Obeso, J.A., Artieda, J., Alegre, M., 2010. Coupling between Beta and High-Frequency Activity in the Human Subthalamic Nucleus May Be a Pathophysiological Mechanism in Parkinson's Disease. *J. Neurosci.* 30, 6667–6677.
- Magill, P., Bolam, J., Bevan, M., 2001. Dopamine regulates the impact of the cerebral cortex on the subthalamic nucleus–globus pallidus network. *Neuroscience* 106, 313–330.
- Marsden, J., Limousin-Dowsey, P., Fraix, V., Pollak, P., Odin, P., Brown, P., 2001a. Intermuscular coherence in Parkinson's disease: effects of subthalamic nucleus stimulation. *NeuroReport* 12, 1113–1117.
- Marsden, J.F., Limousin-Dowsey, P., Ashby, P., Pollak, P., Brown, P., 2001b. Subthalamic nucleus, sensorimotor cortex and muscle interrelationships in Parkinson's disease. *Brain* 124, 378–388.
- Nolte, G., 2003. The magnetic lead field theorem in the quasi-static approximation and its use for magnetoencephalography forward calculation in realistic volume conductors. *Phys. Med. Biol.* 48, 3637–3652.
- O'Gorman, R.L., Selway, R.P., Reid, C.J., Hotton, G.R., Hall, E., Jarosz, J.M., Polkey, C.E., Hill, D.L.G., 2004. Registered computed tomography images as an alternative to postimplantation magnetic resonance imaging in the assessment of subthalamic electrode placement. *J. Comput. Assist. Tomogr.* 28, 548–550.
- Oostenveld, R., Fries, P., Maris, E., Schoffelen, J.-M., 2011. FieldTrip: Open Source Software for Advanced Analysis of MEG, EEG, and Invasive Electrophysiological Data. *Comput. Intell. Neurosci.* 2011, 1–9.
- Özkurt, T.E., Butz, M., Homburger, M., Elben, S., Vesper, J., Wojtecki, L., Schnitzler, A., 2011. High frequency oscillations in the subthalamic nucleus: A neurophysiological marker of the motor state in Parkinson's disease. *Exp. Neurol.* 229, 324–331.
- Palva, S., Palva, J.M., 2007. New vistas for alpha-frequency band oscillations. *Trends Neurosci.* 30, 150–158.
- Palva, S., Palva, J.M., 2012. Discovering oscillatory interaction networks with M/EEG: challenges and breakthroughs. *Trends Cogn. Sci. (Regul. Ed.)* 16, 219–230.
- Park, H., Kim, J.S., Paek, S.H., Jeon, B.S., Lee, J.Y., Chung, C.K., 2009. Cortico-muscular coherence increases with tremor improvement after deep brain stimulation in Parkinson's disease. *NeuroReport* 20, 1444–1449.
- Pfurtscheller, G., Graimann, B., Huggins, J.E., Levine, S.P., Schuh, L.A., 2003. Spatiotemporal patterns of beta desynchronization and gamma synchronization in corticographic data during self-paced movement. *Clin. Neurophysiol.* 114, 1226–1236.
- Pollak, B., Makhlofi, H., Butz, M., Gross, J., Timmermann, L., Wojtecki, L., Schnitzler, A., 2008. Levodopa affects functional brain networks in parkinsonian resting tremor. *Mov. Disord.* 24, 91–98.

- Pollok, B., Krause, V., Martsch, W., Wach, C., Schnitzler, A., Südmeyer, M., 2012. Motor-cortical oscillations in early stages of Parkinson's disease. *J. Physiol.* 590, 3203–3212.
- Priori, A., Foffani, G., Pesenti, A., Tamma, F., Bianchi, A.M., Pellegrini, M., Locatelli, M., Moxon, K.A., Villani, R.M., 2004. Rhythm-specific pharmacological modulation of subthalamic activity in Parkinson's disease. *Exp. Neurol.* 189, 369–379.
- Rosa, M., Marceglia, S., Servello, D., Foffani, G., Rossi, L., Sassi, M., Mrakic-Sposta, S., Zangaglia, R., Pacchetti, C., Porta, M., et al., 2010. Time dependent subthalamic local field potential changes after DBS surgery in Parkinson's disease. *Exp. Neurol.* 222, 184–190.
- Salenius, S., Avikainen, S., Kaakkola, S., Hari, R., Brown, P., 2002. Defective cortical drive to muscle in Parkinson's disease and its improvement with levodopa. *Brain* 125, 491–500.
- Saxe, R., Brett, M., Kanwisher, N., 2006. Divide and conquer: A defense of functional localizers. *NeuroImage* 30, 1088–1096.
- Schaltenbrand, G., Wahren, W., 1977. Atlas For Stereotaxy of The Human Brain With Guide to The Atlas For Stereotaxy of The Human Brain, Pkg. Thieme.
- Schoffelen, J.-M., Gross, 2009. Source connectivity analysis with MEG and EEG. *Hum. Brain Mapp.* 30, 1857–1865.
- Sharott, A., Magill, P.J., Harnack, D., Kupsch, A., Meissner, W., Brown, P., 2005. Dopamine depletion increases the power and coherence of beta-oscillations in the cerebral cortex and subthalamic nucleus of the awake rat. *Eur. J. Neurosci.* 21, 1413–1422.
- Smeding, H.M.M., Speelman, J.D., Koning-Haanstra, M., Schuurman, P.R., Nijssen, P., van Laar, T., Schmand, B., 2006. Neuropsychological effects of bilateral STN stimulation in Parkinson disease: A controlled study. *Neurology* 66, 1830–1836.
- Taulu, S., Simola, J., 2006. Spatiotemporal signal space separation method for rejecting nearby interference in MEG measurements. *Phys. Med. Biol.* 51, 1759–1768.
- Taulu, S., Simola, J., Kajola, M., 2005. Applications of the Signal Space Separation Method. *IEEE Trans. Signal Process.* 53, 3359–3372.
- Thomson, D.J., 1982. Spectrum estimation and harmonic analysis. *Proc. IEEE* 70, 1055–1096.
- Timmermann, L., Gross, J., Dirks, M., Volkmann, J., Freund, H.-J., Schnitzler, A., 2003. The cerebral oscillatory network of parkinsonian resting tremor. *Brain* 126, 199–212.
- Videen, T.O., Campbell, M.C., Tabbal, S.D., Karimi, M., Hershey, T., Perlmutter, J.S., 2008. Validation of a fiducial-based atlas localization method for deep brain stimulation contacts in the area of the subthalamic nucleus. *J. Neurosci. Methods* 168, 275–281.
- Wang, S., Chen, Y., Ding, M., Feng, J., Stein, J.F., Aziz, T.Z., Liu, X., 2007. Revealing the dynamic causal interdependence between neural and muscular signals in Parkinsonian tremor. *J. Franklin Inst.* 344, 180–195.
- Williams, D., Tijssen, M., Van Bruggen, G., Bosch, A., Insola, A., Di Lazzaro, V., Mazzone, P., Oliviero, A., Quartarone, A., Speelman, H., et al., 2002. Dopamine-dependent changes in the functional connectivity between basal ganglia and cerebral cortex in humans. *Brain* 125, 1558–1569.

Supplementary

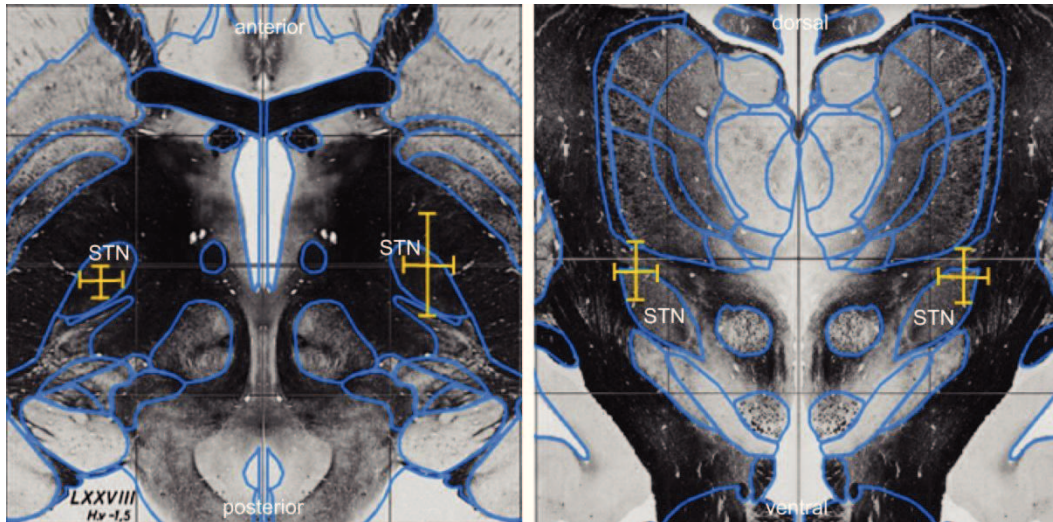


Fig. S1: Average position of DBS electrode contacts.

Stereotactic contact coordinates were normalized with respect to the distance between anterior commissure (AC) and posterior commissure (PC), averaged and projected onto the *Schaltenbrand–Wahren* atlas. **Left:** Axial slice 1.5mm ventral to MCP. **Right:** Coronal slice 3mm caudal to mid-commissural point (MCP). Grid spacing is 9 mm; yellow crosses depict standard deviations. Four subjects used their left hand in the motor task and contributed to the average location in the right hemisphere. Six subjects used their right hand and contributed to the average location in the left hemisphere.

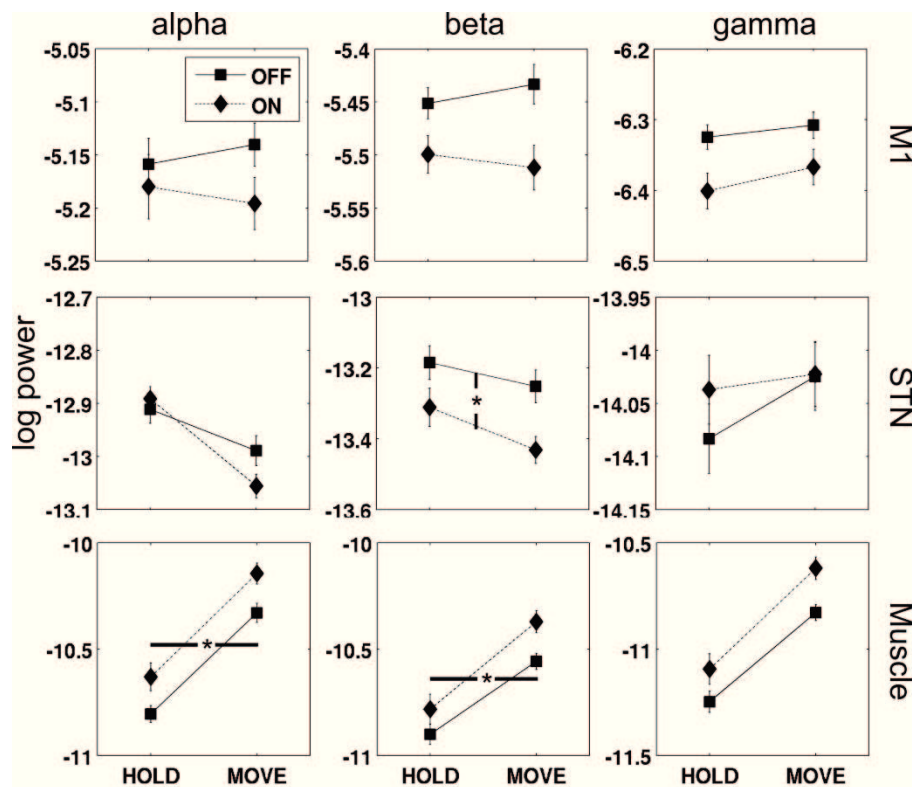


Fig S2: Effects of levodopa and motor task on M1, STN and muscle power. Condition-specific means of M1, STN and muscle power. Power values were log10-transformed and averaged across subjects. Error bars indicate the standard error of the mean (SEM). Asterisks mark significant differences ($p < 0.05$).

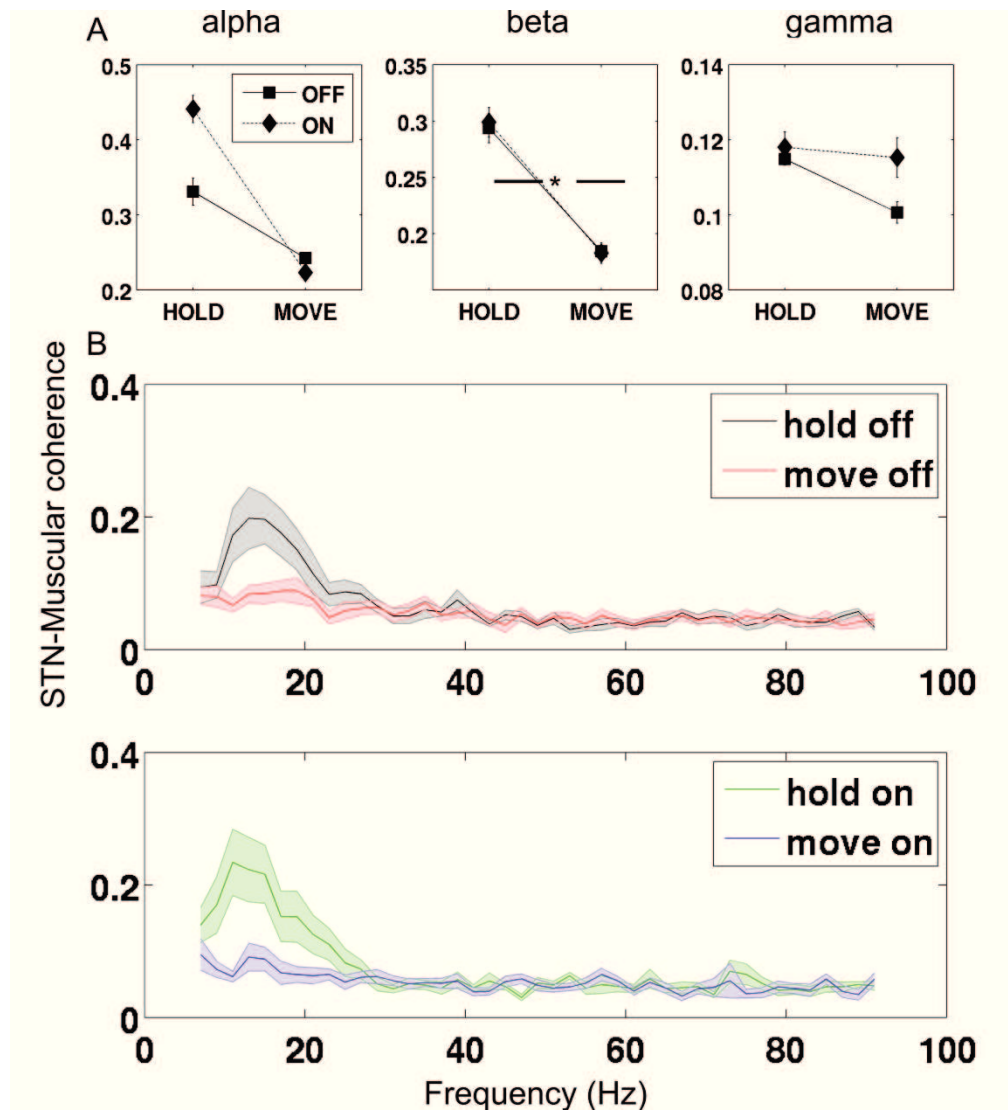


Fig. S3: Movement reduces STN-muscular beta coherence.

A) Condition-specific means of STN-muscular coherence. Coherence values were z-transformed and averaged across subjects. Error bars indicate the standard error of the mean (SEM). Asterisks mark significant differences ($p < 0.05$).

B) Average STN-muscular coherence spectra. Shaded areas indicate SEMs.

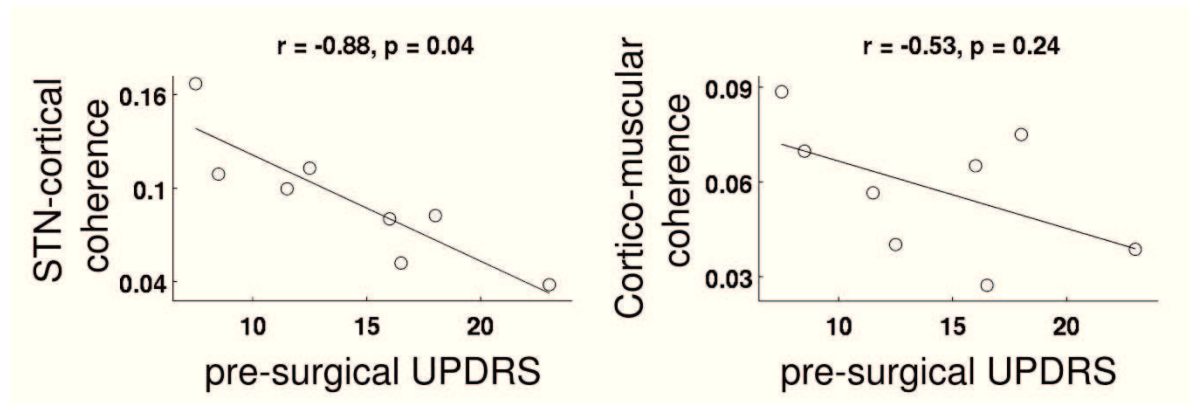


Fig. S4: Correlation between pre-surgical UPDRS and beta coherence in the OFF state. Beta coherence between M1 and STN was negatively correlated with pre-surgical hemibody akinesia/rigidity UPDRS scores in the OFF state. HOLD OFF and MOVE OFF beta coherence were averaged. Pre-surgical UPDRS scores from five days before surgery were available solely for eight of ten subjects.

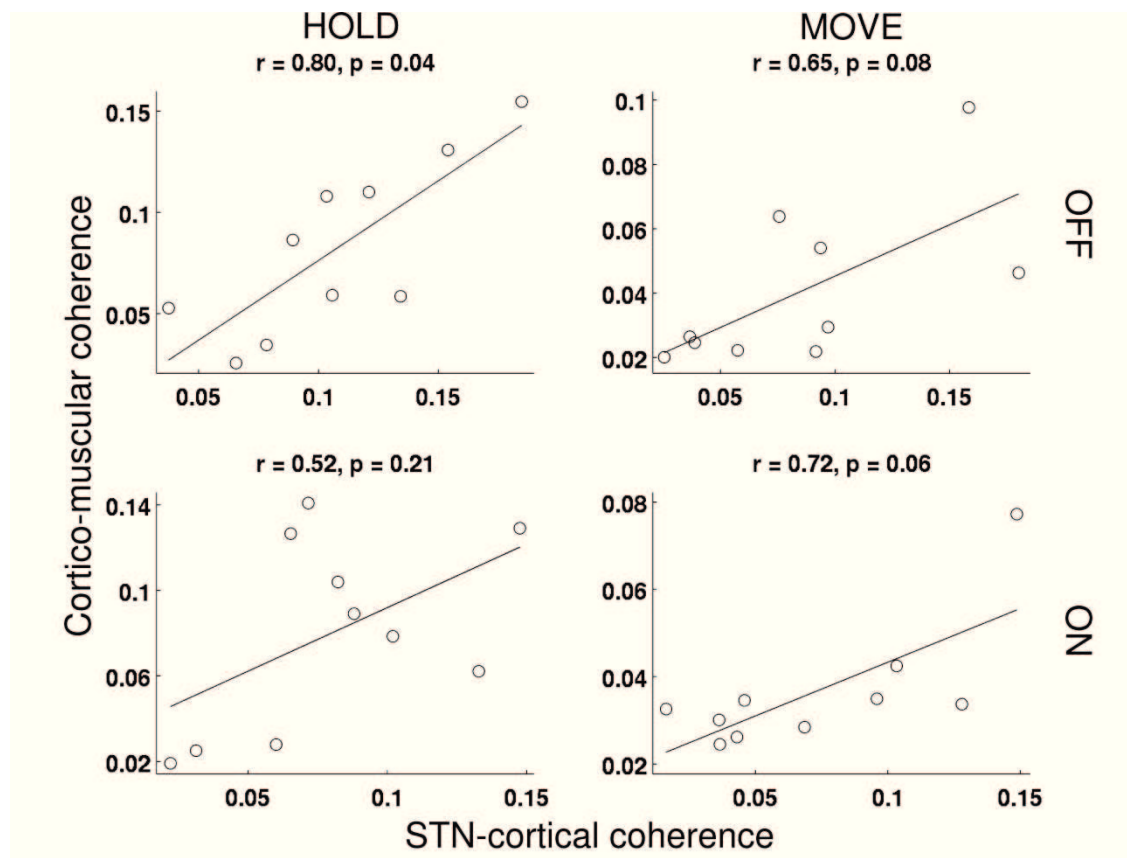


Fig. S5: Correlation between M1-STN and M1-muscular beta coherence. M1-STN and M1-muscular beta coherence were positively correlated in HOLD OFF. Trends for a positive correlation were observed in MOVE OFF and MOVE ON.

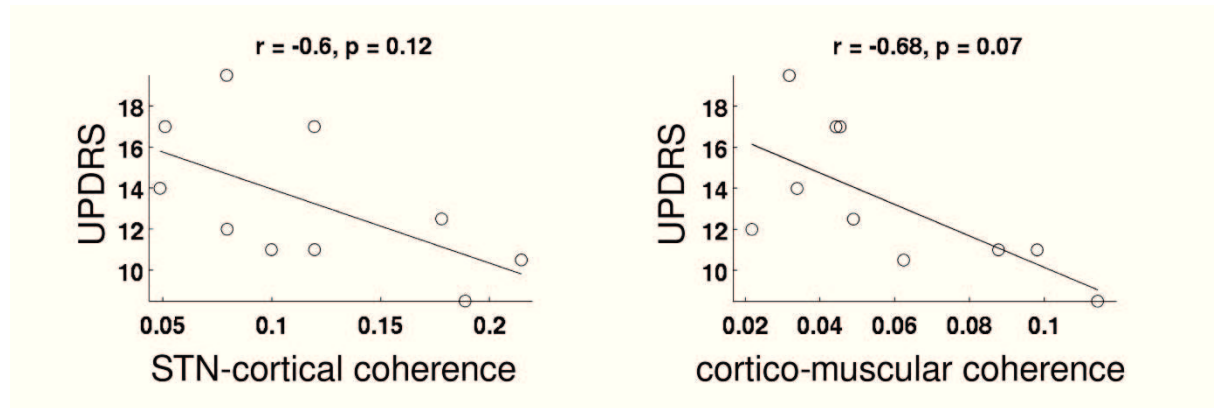


Fig. S6: Correlation between UPDRS and resting state beta coherence in the OFF state. At rest, UPDRS and beta coherence showed the same negative relationship as observed during motor task performance. However, the anti-correlations were not significant.ⁱ

Effect of Spatial Sampling

In order to exclude that spatial under-sampling of the cortical signal confounded the results, we reproduced the main findings of this study with a different definition of the M1 ROI. Instead of a single location, we considered a 2-dimensional grid of points with axial orientation that was centered on the original M1 ROI (5x5 regular grid, 5 mm spacing). For the first test, we averaged coherence over each point in the sensorimotor grid. Notably, the modulations of coherence (Tab. S1, upper row) and the anti-correlation between beta coherence and UPDRS scores in the OFF state (Fig. S7, left column) could be reproduced. For the second test, we chose a location within the sensorimotor grid for each individual subject. In analogy with ROI and reference channel selection in the original analysis, this was the location with maximal STN-cortical beta coherence in REST OFF. Again, we detected exactly the same modulations of coherence as with the original procedure (Tab. S1, lower row). Moreover, the correlation coefficients quantifying the relationship between beta coherence and UPDRS scores were very similar to the ones reported in the main article (Fig. S7, right column). We conclude that the spatial sampling applied in the original analysis was sufficient to capture the dominant activity in the sensorimotor region.

beta coherence M1-STN mean			alpha coherence M1-muscle mean			beta coherence M1-muscle mean		
	F	p		F	p		F	p
<i>medication</i>	15.70	<0.01	<i>medication</i>	1.97	0.19	<i>medication</i>	0.24	0.64
<i>motor task</i>	3.35	0.10	<i>motor task</i>	9.90	0.01	<i>motor task</i>	19.68	<0.01
<i>medication * motor task</i>	3.79	0.08	<i>medication * motor task</i>	0.03	0.87	<i>medication * motor task</i>	0.06	0.81

beta coherence M1-STN max.			alpha coherence M1-muscle max.			beta coherence M1-muscle max.		
	F	p		F	p		F	p
<i>medication</i>	17.76	<0.01	<i>medication</i>	2.67	0.17	<i>medication</i>	0.01	0.92
<i>motor task</i>	2.98	0.12	<i>motor task</i>	11.99	<0.01	<i>motor task</i>	13.17	<0.01
<i>medication * motor task</i>	1.91	0.20	<i>medication * motor task</i>	<0.01	0.97	<i>medication * motor task</i>	0.10	0.76

Tab. S1: Effects of medication and movement on coherence are robust against changes in spatial sampling.

Beta coherence was measured between a reference channel and several locations within a sensorimotor region of interest (ROI). **Upper row:** Beta coherence was averaged over locations within the ROI. **Lower Row:** Beta coherence was extracted from the subject-specific location within the ROI that showed maximal coherence in REST OFF. Significant effects are marked by italics. Only signal pair – frequency band combinations with at least one significant effect are listed.

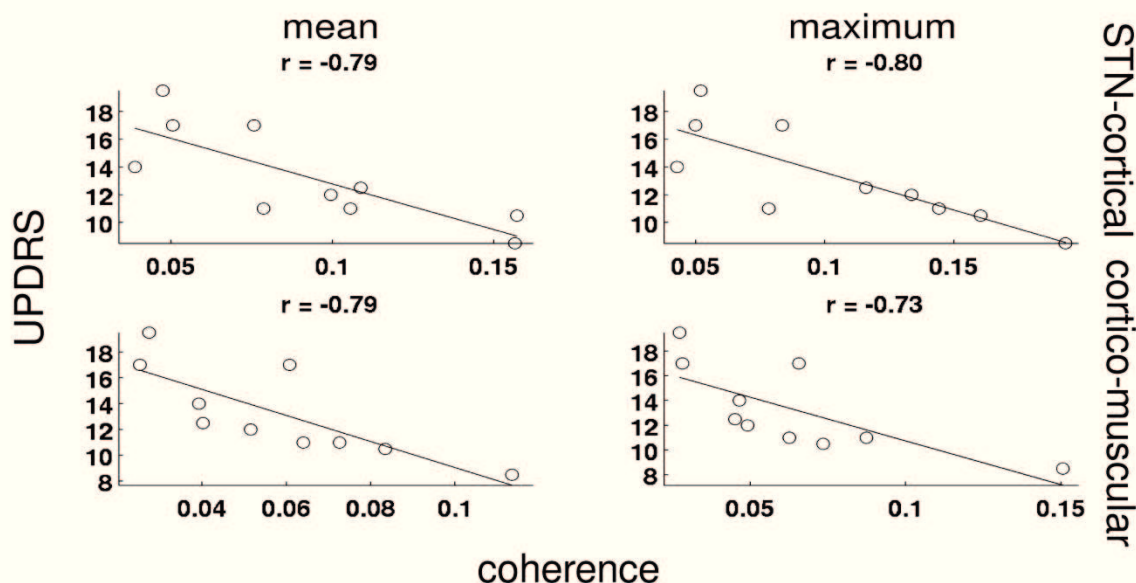


Fig. S7: The anti-correlation between beta coherence and UPDRS is robust against changes in spatial sampling.

The figure shows the relationship between beta coherence during motor task performance (HOLD OFF and MOVE OFF averaged) and UPDRS OFF scores. Beta coherence was measured between a reference channel and several locations within a sensorimotor region of interest (ROI). **Left column:** Beta coherence was averaged over locations within the ROI. **Right column:** Beta coherence was extracted from the subject-specific location within the ROI that showed maximal coherence in REST OFF.ⁱ

ⁱ In the published version x- and y-label are erroneously swapped

A direct relationship between oscillatory subthalamic nucleus–cortex coupling and rest tremor in Parkinson's disease

Jan Hirschmann,^{1,2} Christian J. Hartmann,^{1,2} Markus Butz,^{1,3} Nienke Hoogenboom,^{1,2} Tolga E. Özkurt,⁴ Saskia Elben,^{1,2} Jan Vesper,⁵ Lars Wojtecki^{1,2} and Alfons Schnitzler^{1,2}

- 1 Institute of Clinical Neuroscience and Medical Psychology, Medical Faculty, Heinrich-Heine-University Düsseldorf, Düsseldorf, Germany
- 2 Department of Neurology, University Hospital Düsseldorf, Düsseldorf, Germany
- 3 Sobell Department of Motor Neuroscience and Movement Disorders, Institute of Neurology, University College London, London, UK
- 4 Department of Health Informatics, Informatics Institute, Middle East Technical University, Ankara, Turkey
- 5 Department of Functional Neurosurgery and Stereotaxy, University Hospital Düsseldorf, Düsseldorf, Germany

Correspondence to: Alfons Schnitzler
Institute of Clinical Neuroscience and Medical Psychology
Heinrich-Heine-University Düsseldorf
Universitätsstr. 1
D-40225 Düsseldorf
Germany
E-mail: SchnitzA@med.uni-duesseldorf.de

Electrophysiological studies suggest that rest tremor in Parkinson's disease is associated with an alteration of oscillatory activity. Although it is well known that tremor depends on cortico-muscular coupling, it is unclear whether synchronization within and between brain areas is specifically related to the presence and severity of tremor. To tackle this longstanding issue, we took advantage of naturally occurring spontaneous tremor fluctuations and investigated cerebral synchronization in the presence and absence of rest tremor. We simultaneously recorded local field potentials from the subthalamic nucleus, the magnetoencephalogram and the electromyogram of forearm muscles in 11 patients with Parkinson's disease (all male, age: 52–74 years). Recordings took place the day after surgery for deep brain stimulation, after withdrawal of anti-parkinsonian medication. We selected epochs containing spontaneous rest tremor and tremor-free epochs, respectively, and compared power and coherence between subthalamic nucleus, cortex and muscle across conditions. Tremor-associated changes in cerebro-muscular coherence were localized by Dynamic Imaging of Coherent Sources. Subsequently, cortico-cortical coupling was analysed by computation of the imaginary part of coherency, a coupling measure insensitive to volume conduction. After tremor onset, local field potential power increased at individual tremor frequency and cortical power decreased in the beta band (13–30 Hz). Sensor level subthalamic nucleus-cortex, cortico-muscular and subthalamic nucleus-muscle coherence increased during tremor specifically at tremor frequency. The increase in subthalamic nucleus-cortex coherence correlated with the increase in electromyogram power. On the source level, we observed tremor-associated increases in cortico-muscular coherence in primary motor cortex, premotor cortex and posterior parietal cortex contralateral to the tremulous limb. Analysis of the imaginary part of coherency revealed tremor-dependent coupling between these cortical areas at tremor frequency and double tremor frequency. Our findings demonstrate a direct relationship between the synchronization of cerebral oscillations and tremor manifestation. Furthermore, they suggest the feasibility of tremor detection based on local field potentials and might thus become relevant for the design of closed-loop stimulation systems.

Keywords: Parkinson's disease; tremor; magnetoencephalography; coherence; deep brain stimulation

Abbreviations: DBS = deep brain stimulation; ImCoh = imaginary part of coherency; LFP = local field potential; MEG = magnetoencephalography

Introduction

Parkinson's disease is a debilitating neurological disorder resulting from progressive cell death of dopaminergic neurons in the mid-brain (Lang and Lozano, 1998). Recent research revealed abnormally strong synchronization of rhythmic neuronal activity both in animal models of Parkinson's disease and patients, suggesting that Parkinson's disease is associated with pathologically altered neuronal oscillations (Schnitzler and Gross, 2005; Hammond *et al.*, 2007). Enhanced synchronization was shown to play a role in akinesia and rigidity (Kühn *et al.*, 2006) and was suggested to be involved in parkinsonian tremor.

Tremor occurs in ~75% of patients and may range from mild to severe manifestations (Hoehn and Yahr, 1967; Hughes *et al.*, 1993). Classical parkinsonian tremor occurs at rest, and is attenuated at movement onset (Deuschl *et al.*, 2000). Therefore, it is referred to as rest tremor. The frequency of parkinsonian rest tremor ranges between 3 and 7 Hz.

It is generally agreed that central rather than peripheral mechanisms underlie parkinsonian tremor (Elble, 1996; McAuley and Marsden, 2000; Schnitzler *et al.*, 2006). Currently, two overlapping central networks are considered candidate generators: the cerebello-thalamo-cortical circuit and the basal ganglia-cortical motor loop (Helmich *et al.*, 2012). Tremor-related neural activity occurs in both networks, and lesions and deep brain stimulation (DBS) of structures in either network lead to tremor suppression (Bergman *et al.*, 1990; Benabid *et al.*, 1991; Krack *et al.*, 1997).

Patient recordings from the ventrolateral thalamus revealed coherence between single unit and muscle activity at tremor frequency, suggesting that the thalamus is involved in tremor generation (Lenz *et al.*, 1988; Zirh *et al.*, 1998). Moreover, the ventral intermediate nucleus of the thalamus is considered the most effective DBS target for tremor suppression (Deuschl *et al.*, 2000). As this nucleus receives mainly cerebellar afferents, it was proposed that cerebellar activity also contributes to tremor expression (Stein and Aziz, 1999). In fact, imaging studies demonstrated that DBS of the ventral intermediate nucleus affects cerebellar blood flow and revealed that cerebellar blood oxygenation and metabolic activity are positively correlated with tremor amplitude (Deiber *et al.*, 1993; Helmich *et al.*, 2011; Mure *et al.*, 2011).

Besides the cerebello-thalamic circuit, tremor research has focused on the basal ganglia. Microelectrode recordings in non-human primates (Raz *et al.*, 2000; Heimer *et al.*, 2006) and patients undergoing surgery (Hutchison *et al.*, 1997) revealed so-called tremor cells in the internal globus pallidus. These cells fire bursts at tremor frequency and bursting is, at least transiently, coherent with tremor recordings from the muscle (Hurtado *et al.*, 2005).

Similar observations were made in the subthalamic nucleus. In vervet monkeys, oscillations at tremor frequency and double tremor frequency emerged when the animals began to develop tremor due to 1-methyl-4-phenyl-1,2,3,6-tetrahydropyridine (MPTP) injection (Bergman *et al.*, 1994). Furthermore, power

spectra of subthalamic nucleus local field potentials (LFPs) show peaks at tremor frequency and subthalamic nucleus LFPs are coherent with the EMG at tremor frequency (Levy *et al.*, 2002; Liu *et al.*, 2002; Wang *et al.*, 2005; Reck *et al.*, 2009).

Notably, tremor-related oscillatory activity is not only found in subcortical nuclei and the cerebellum, but also in the cortex. Timmermann *et al.* (2003) studied cerebro-muscular coherence using magnetoencephalography (MEG) and observed significant coupling at tremor frequency and double the tremor frequency in a network including primary motor cortex, premotor cortex, posterior parietal cortex, cerebellum and a diencephalic source that was assumed to be the thalamus. The same network was later shown to underlie voluntary tremor in healthy controls (Pollok *et al.*, 2004), and a similar network was found to be involved in essential tremor (Schnitzler *et al.*, 2009).

In summary, several lines of evidence suggest that tremor manifestation is associated with cerebral oscillations at tremor frequency, indicating that they could serve as a trigger signal in closed-loop DBS (Rosin *et al.*, 2011). The nature of this association, however, remains elusive. Patient studies on subthalamic nucleus single unit activity reported that rhythmic spiking around 5 Hz can be observed in the absence of tremor (Magariños-Ascone *et al.*, 2000; Moran *et al.*, 2008; Shimamoto *et al.*, 2013). These results demonstrate that the presence of spectral peaks at tremor frequency is not sufficient to make inferences on the tremor state. Furthermore, they show that oscillations on the single cell level are not sufficient to elicit tremor, suggesting that tremor manifestation might require coordinated network activity.

In this study, we hypothesized that tremor depends on synchronization within the motor system. Specifically, we aimed at demonstrating that tremor is associated with modulations of subthalamic nucleus power, cortical power, subthalamic nucleus-cortex and cortico-cortical coupling. To this end, we simultaneously recorded subthalamic nucleus LFPs, MEG and the EMG of forearm muscles in tremor-dominant patients with Parkinson's disease. As demonstrated by several recent studies (Hirschmann *et al.*, 2011, 2013; Litvak *et al.*, 2011, 2012; Oswal *et al.*, 2013), this combination of recording techniques is a powerful tool for studying connectivity between subthalamic nucleus, cortex and muscle. We identified epochs of spontaneous rest tremor as well as tremor-free epochs using the EMG recordings and compared oscillatory activity across conditions. The study critically extends our current knowledge about parkinsonian rest tremor by demonstrating the pivotal role of synchronous oscillations in subthalamic nucleus and cortex.

Materials and methods

Patients

Eleven patients with Parkinson's disease who were clinically selected for DBS because of levodopa-induced fluctuations and dyskinesias

Table 1 Clinical details of patients

Subject	Gender	Age (years)	Disease duration (years)	UPDRSIII recording day	Individual tremor frequency (hz)	Side	OFF/OFF upper limb rest tremor subscore	OFF/ON upper limb rest tremor subscore
1	M	65	8	40	4.0	Right Left	1 3	0 2
2	M	69	6	51	3.5	Right Left	3 3	3 2
3	M	68	11	36	3.0	Left	1	0
4	M	59	6	39	4.5	Right Left	3 3	1 0
5	M	68	2	39	4.0	Right Left	1 2	0 1
6	M	52	11	31	6.0	Right Left	2 0	0 0
7	M	67	6	34	6.5	Right Left	m.d. m.d.	m.d. m.d.
8	M	53	12	26	5.0	Left	2	2
9	M	65	4	43	4.5	Right Left	4 4	0 0
10	M	74	7	60	5.0	Right	4	0
11	M	69	12	30	7.0	Right	3	0
Mean		64.45	7.73	39.00	4.82		2.40	0.60
Standard deviation		6.93	3.38	9.75	1.25		1.17	1.07

The column labelled side indicates which body sides were analysed. The last two columns show the effect of deep brain stimulation on upper limb rest tremor as documented in the control assessment of motor symptoms ~3 months after implantation of the stimulation device. OFF/OFF signifies that medication was off and stimulation was on (m.d. = missing data). M = male; UPDRS = Unified Parkinson's Disease Rating Scale.

participated in this study with written informed consent. All subjects suffered from moderate to severe rest tremor that was alleviated by DBS (Table 1). Seven subjects showed bilateral tremor during the recordings so that it was possible to include both hemispheres in the analysis. Four subjects showed unilateral tremor so that we were restricted to one hemisphere. Thus, 18 subthalamic nuclei were analysed in total. Subject 6 had been included in an earlier study on akinesia (Hirschmann *et al.*, 2013). He showed transiently emerging tremor in addition to severe akinesia and rigidity. The study was approved by the local ethics committee (Study no. 3209) and is in accordance with the Declaration of Helsinki.

Surgery

Implantation of electrodes was carried out at the Department of Functional Neurosurgery and Stereotaxy of the University Hospital Düsseldorf. The surgical procedures are described elsewhere (Özkurt *et al.*, 2011). Oral anti-parkinsonian medication was withdrawn the evening before surgery and substituted by subcutaneous apomorphine medication. Eight of 11 subjects were implanted with electrode model 3389 (Medtronic Inc.). Subjects 6, 8 and 9 were implanted with a DBS system by St. Jude Medical Inc. Electrode placement was guided by intraoperative microelectrode recordings, intraoperative stimulation and clinical testing of DBS efficacy.

Electrode contact localization

To reconstruct the final electrode placement, preoperative MRIs and postoperative CT scans were aligned using rigid transformation as provided by the functional magnetic resonance imaging of the Brain Linear Image Registration Tool (Jenkinson *et al.*, 2012). Subsequently, the electrode position was derived from its characteristic artefacts in

CT scans (Hemm *et al.*, 2009). Contacts were labelled in a $0.5 \times 0.5 \times 0.5$ mm mask image in individual MRI space. For group comparison, individual MRI scans were transformed to Montreal Neurological Institute (MNI) space using the symmetric normalization strategy implemented in Advanced Normalisation Tools (Avants *et al.*, 2008). The same transformation was applied to the mask images to obtain contact positions in MNI space.

Recordings

We simultaneously recorded LFPs from the subthalamic nucleus, MEG and the EMG of the extensor digitorum communis and flexor digitorum superficialis muscles of both upper limbs. All recordings were performed using a 306 channel, whole-head MEG system (Elekta Oy). The sampling rate was 2000 Hz. DBS electrodes were connected to the amplifier integrated into the MEG system by non-magnetic extension leads. Online filters were applied to create a passband of 0.03–660 Hz for MEG signals, and a passband of 0.1–660 Hz for LFP and EMG signals. EMG electrodes were referenced to surface electrodes at the muscle tendons. DBS electrodes were referenced to a surface electrode at the left mastoid and rearranged to a bipolar montage offline. Re-referencing was performed by signal subtraction and yielded three bipolar LFP channels per electrode: 0–1 (ventral), 1–2 and 2–3 (dorsal).

Clinical ratings and paradigm

Recordings took place the day after surgery. Two hours before recording apomorphine administration was stopped. The clinical OFF state was quantified by means of the motor score of the Movement Disorder Society Unified Parkinson's Disease Rating Scale immediately before the recording started (Goetz *et al.*, 2008). The rating was performed by an experienced movement disorders specialist. Inside the

shielded room, subjects were instructed to sit as still as possible with eyes open. In the period analysed in this study, there was neither a task nor any kind of stimulus presentation. The duration of the rest recording varied according to the subsequent paradigm. Paradigm 1 (Subjects 1–8) included 10 min of rest in total and is described in detail in Hirschmann *et al.* (2013). Paradigm 2 (Subjects 9–11) included 3 min of rest.

Epoch selection

Raw data were inspected by eye. Epochs were labelled as tremor epochs if continuous 3–7 Hz periodic activity was clearly apparent in the EMG time series of both the upper limb extensor and flexor. Simultaneous tremor on the contralateral body side was not accounted for when determining tremor epochs, i.e. we did not differentiate between bilateral and unilateral tremor. Epochs were labelled as tremor-free only if neither forearm showed any periodic activity. Epochs containing artefacts such as contraction of jaw muscles or coughing were discarded. Data selection yielded 82 s of tremor-free data (range: 17–235 s) and 63 s of tremor data (range: 14–201 s) on average.

Preprocessing

Temporal Signal Space Separation (Taulu and Simola, 2006) was applied using MaxFilter (Elekta Oy) as a means to shield the MEG signal from tremor-related muscle activity. A discrete Fourier transform filter was applied to remove any remaining power line noise (50 Hz) and its first two harmonics (100 and 150 Hz). This processing step and all of the following were performed using Matlab R2012a (The Mathworks) and the FieldTrip toolbox (Oostenveld *et al.*, 2011). EMGs were high-pass filtered at 10 Hz and full-wave rectified. Data were down-sampled to 256 Hz.

Channel selection

A set of 24 gradiometers contralateral to the tremulous limb was selected *a priori* as MEG sensors of interest. The sensors were chosen such that they covered sensorimotor and premotor motor cortex (Fig. 1A). The selection was adapted for each body side individually: in the sensors of interest, power was averaged over the individual tremor frequency band (tremor frequency ± 0.5 Hz) and the first harmonic band (double tremor frequency ± 0.5 Hz) and summed over conditions (tremor and tremor-free episodes). Subsequently, the sensor with maximum power and its six nearest neighbours were selected.

Furthermore, one LFP and one EMG channel were selected for each body side. For each of the three LFP channels contralateral to the tremulous limb, we computed LFP-MEG coherence and averaged across MEG channels of interest, resulting in one spectrum per LFP channel and condition. Coherence spectra from both conditions were summed, and we selected the LFP channel with highest coherence at individual tremor frequency for further analysis. Selection of the EMG channel of interest was performed analogously (either the forearm extensor or the forearm flexor of the tremulous limb was chosen). Fig. 1B shows the positions of selected LFP channels in MNI space together with a probability map of the subthalamic nucleus (Forstmann *et al.*, 2012).

Sensor level analysis

Time-frequency representations

To investigate the dynamics of tremor-related LFP and MEG power at tremor onset, we selected all available tremor epochs with a discernible tremor onset that lasted ≥ 10 s and were separated from the previous tremor epoch of the same limb by ≥ 10 s. Time-frequency representations were produced by Fourier transformation of Hanning-tapered data in a sliding window that was moved in steps of 50 ms. Window length was set to 2 s for 1–4.5 Hz and to seven cycles for 5–30 Hz to obtain a better time resolution.

For statistical analysis, time-frequency representations were aligned to individual tremor frequency and compared to baseline (–9 to 0 s relative to tremor onset) using a non-parametric, cluster-based randomization approach (Maris and Oostenveld, 2007). In case multiple epochs were available for a single subthalamic nucleus, the corresponding time-frequency representations were averaged prior to statistical analysis. In short, a group statistical image was computed and two thresholds were applied. In this case, the thresholds were chosen to be the 0.05 and 0.95 percentiles of the distribution of the ‘activation versus baseline *t*-value’. Following threshold application, values of neighbouring supra-threshold voxels were summed and the cluster sums were stored. Then, subject-specific images were randomly shuffled across conditions, an alternative statistical image was computed and cluster sums were computed as before. By repeating this step 1000 times, an empirical, non-parametric null distribution was constructed to which the original cluster sums were compared. Importantly, this approach effectively controls for multiple comparisons. Please note, however, that it does not account for possible statistical dependencies between hemispheres.

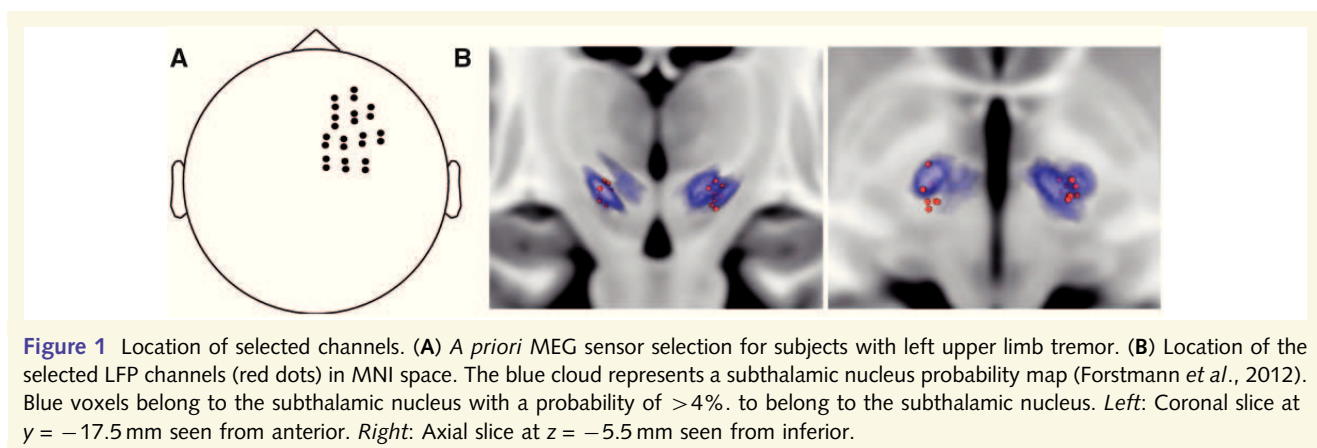


Figure 1 Location of selected channels. (A) *A priori* MEG sensor selection for subjects with left upper limb tremor. (B) Location of the selected LFP channels (red dots) in MNI space. The blue cloud represents a subthalamic nucleus probability map (Forstmann *et al.*, 2012). Blue voxels belong to the subthalamic nucleus with a probability of $>4\%$ to belong to the subthalamic nucleus. *Left*: Coronal slice at $y = -17.5$ mm seen from anterior. *Right*: Axial slice at $z = -5.5$ mm seen from inferior.

Coherence spectra

For coherence analysis, data were divided into half-overlapping segments of 2-s length. Subsequently, data segments were arranged into two separate sets containing tremor and tremor-free episodes, respectively. Segments were convolved with a Hanning taper and coherence was calculated for both conditions. As in the analysis of power, coherence spectra were aligned to individual tremor frequency and compared across conditions using a non-parametric, cluster-based randomization approach. The dependent samples *t*-value served to define the cluster thresholds.

Correlation between EMG power and LFP-MEG coherence was quantified by Pearson's linear correlation coefficient. Power was considered in logarithmic units and coherence was Fisher *z*-transformed. In order to account for peaks at tremor frequency and at its first harmonic, we averaged coherence over the tremor frequency band and the first harmonic band prior to computing correlation.

Source analysis

Source analysis was performed using beamforming, a spatial filtering approach. Importantly, tremor and tremor-free epochs were both projected through a common, real-valued spatial filter that was derived from the joint data from both conditions. This step excludes the possibility that statistical differences between conditions occur due to differences in spatial filters.

Subthalamic nucleus-cortex and cortico-muscular coherence

Estimation of subthalamic nucleus-cortex and cortico-muscular coherence on the source level was realized by Dynamic Imaging of Coherent Sources (Gross *et al.*, 2001). Regularization was set to 5% of the mean of the trace of the channel cross-spectral density matrix. Source orientation was defined as the orientation that maximized power. The forward model was based on a realistic, single shell head model derived from individual T_1 -weighted structural MRIs (Nolte, 2003). The latter were obtained prior to surgery using a Magnetom Trio MRI scanner (Siemens). We made use of regular beamformer grids with 5 mm spacing that were aligned to MNI space (Mattout *et al.*, 2007). All analysed beamformer grid points lay within 1.5 cm from the cortical surface, i.e. we did not consider subcortical structures. Limiting the analysis to cortical areas served to increase statistical power.

Statistical analysis of source level coherence was performed in the same way as for sensor level coherence. The non-parametric randomization approach is suited to analyse one-dimensional input, such as coherence spectra, as well as multi-dimensional input such as volumetric images (Maris and Oostenveld, 2007). A one-sided test was used as we explicitly sought to localize the coherence increases observed in the previous sensor level analysis.

Cortico-cortical coupling

For investigation of cortico-cortical coupling, the time domain activity of selected sources was reconstructed using a Linear Constraint Minimum Variance beamformer (Van Veen and Buckley, 1988). Regularization was set to 20%. To improve the signal-to-noise ratio, we made use of the FieldTrip implementation of the eigenspace beamformer approach (Sekihara *et al.*, 2002). In this approach, a projection onto a subspace of the data covariance matrix is applied to remove noise components. We chose the subspace spanned by the first *N* singular vectors of the sensor covariance matrix with corresponding singular values σ_1 to σ_N , such that $\sigma_i / \sigma_1 > 0.2$ for all $i \in [1, 2, \dots, N]$.

Following reconstruction of source time courses, we calculated coherence and the imaginary part of coherence (ImCoh) for all source pairs.

ImCoh is a coupling measure related to coherence. Unlike coherence, it is unaffected by volume conduction and therefore better suited to investigate cortico-cortical coupling (Nolte *et al.*, 2004). To improve the signal-to-noise ratio, the data were convolved with three Slepian tapers before analysing cortico-cortical coupling (Thomson, 1982).

Cortico-cortical coupling was statistically analysed using a repeated-measures ANOVA. The non-parametric randomization approach was not applied in this case since there is no established procedure to assess the influence of multiple factors. As in correlation analysis, coherence and ImCoh were averaged over the tremor frequency band and the first harmonic band. Coherence was Fisher *z*-transformed and ImCoh was rectified. The latter step ensured that subject-specific ImCoh values did not cancel in the group average. ANOVAs included the factors 'tremor' (no tremor, tremor), 'pair' (source X – source Y, source X – source Z, ...) and 'shuffling' (original, shuffled). In the shuffled condition, one signal in each pair was shifted forward in time by *k* segments (circular shift). *k* was a random integer between 2 and *M* – 1, *M* being the total number of segments. We applied Greenhouse-Geisser correction for non-sphericity where appropriate.

Results

For each subject, we determined the individual tremor frequency. The latter was defined as the frequency of the first clear peak in the EMG power spectrum during tremor. Additional peaks at tremor frequency harmonics were observed in 15 cases. Individual tremor frequencies ranged between 3 and 7 Hz (Table 1). In every subject, individual tremor frequency was consistent across EMGs from different muscles and limbs.

Sensor level power

We investigated changes in MEG and LFP power around tremor onset. Twenty-nine tremor epochs from 17 subthalamic nuclei and 10 subjects were included in this analysis. One subject was excluded because tremor onset could not be determined. For seven subthalamic nuclei, more than one epoch was available (average: 2.7, range: 2–6). In these cases, subject-specific time-frequency representations were averaged prior to statistical analysis (see 'Materials and methods').

Figure 2A shows an example of tremor onset (Subject 2, right subthalamic nucleus). In this case, tremor amplitude did not increase linearly over time. Instead, tremor developed in a staged fashion. Stage transitions were reflected by MEG power decreases in the beta band, followed by beta power increases and increases at tremor frequency. An enhancement of LFP power at tremor frequency occurred only in the last stage, when tremor amplitude was maximal.

Figure 2B depicts the time course of group level MEG and LFP power statistically compared to baseline (–9 to 0 s). Please note that time-frequency representations were aligned to individual tremor frequency (*f*). Following tremor onset, both MEG and LFP power showed a similar pattern: narrow-band power increases at tremor frequency and its first harmonic co-occurred with a decrease in the higher frequencies, corresponding to the beta band (13–30 Hz). For LFP power, the increase at tremor frequency reached significance 4.8 s after tremor onset ($P = 0.01$). MEG power decreased significantly between 10 and 20 Hz relative to tremor frequency in the

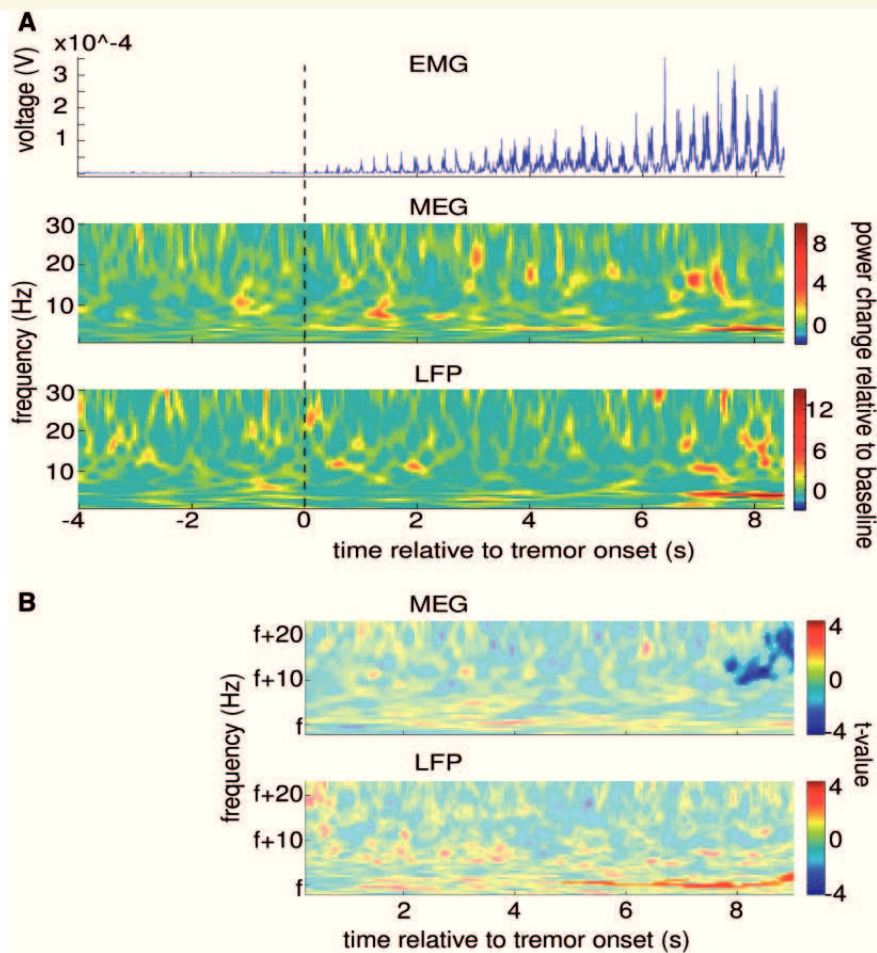


Figure 2 Cortex and subthalamic nucleus showed tremor-related power changes. (A) Exemplary data from a tremor phase in Subject 2. The figure shows the rectified EMG signal (*top*), MEG power (*middle*) and LFP power (*bottom*) around tremor onset (dotted line). MEG power was averaged over the sensors of interest. Time-frequency plots were baseline-corrected (baseline: -4 to 0 s) and the relative power change is colour-coded. Note that sudden increases of tremor amplitude are preceded by MEG beta power decreases and followed by power increases at tremor frequency. (B) Group statistical image of MEG and LFP power showing the contrast between the period from 0 to 9 s and the baseline period (-9 to 0 s). Time-frequency representations were aligned to individual tremor frequency (f) i.e. individual time-frequency representations were shifted along the frequency axis until the individual tremor frequency reached the 0 Hz position. Significant effects are highlighted by increased colour intensity ($P < 0.05$; $n = 17$) and t -values are colour-coded. *Top*: MEG power between 10 and 20 Hz relative to individual tremor frequency ($f + 10 - f + 20$) decreased gradually. The effect was significant between 8 and 9 s after tremor onset. *Bottom*: Starting ~ 1 s after tremor onset, LFP power increased at tremor frequency (f). The effect was significant from 4.8 to 9 s after tremor onset.

period from $8-9$ s after tremor onset ($P < 0.01$). Investigation of the original, non-aligned time-frequency representations revealed a corresponding power decrease between 15 and 25 Hz ($P = 0.01$; data not shown). As depicted in Supplementary Fig. 1, this effect was due to a sustained beta power suppression that began around tremor onset and intensified as tremor continued. Group average LFP beta power decreased between -4 and 0 s and increased transiently at tremor onset (Fig. 2B).

Sensor level coherence

As depicted in Fig. 3A, alignment of coherence spectra to individual tremor frequency revealed tremor-related coherence increases

between all pairs of signals specifically at tremor frequency (LFP-MEG: $P = 0.02$, EMG-MEG: $P < 0.01$, EMG-LFP: $P = 0.04$). Notably, the tremor-induced change in EMG power was positively correlated with the change in LFP-MEG coherence ($r = 0.50$, $P = 0.03$; Fig 3B). We did not test for correlations between EMG power and LFP-EMG or EMG-MEG coherence since in these cases power changes are likely to cause coherence changes, leading to trivial correlations.

Source level coherence

The sensor level results show that coupling at tremor frequency between subthalamic nucleus, cortex and muscle increases

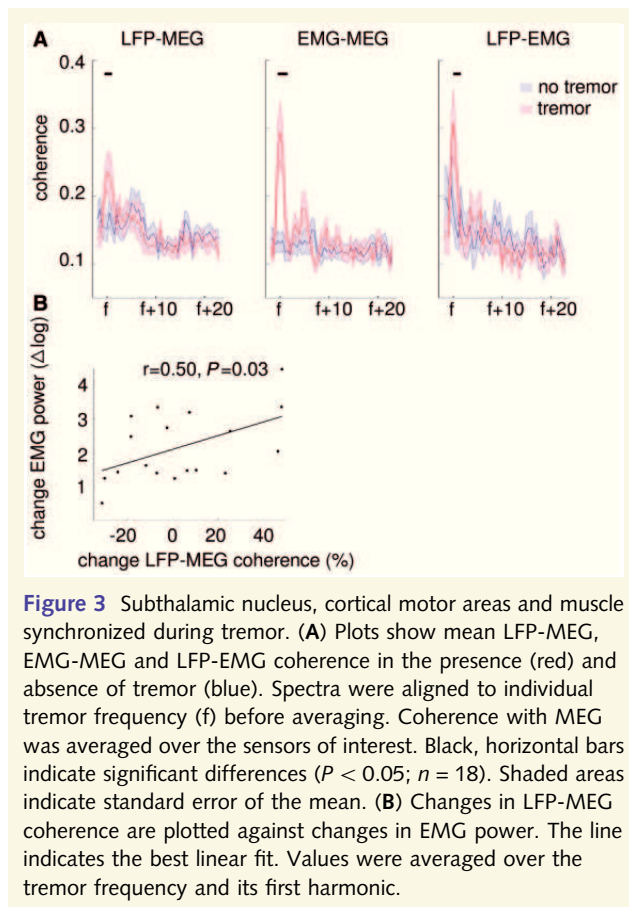


Figure 3 Subthalamic nucleus, cortical motor areas and muscle synchronized during tremor. (A) Plots show mean LFP-MEG, EMG-MEG and LFP-EMG coherence in the presence (red) and absence of tremor (blue). Spectra were aligned to individual tremor frequency (f) before averaging. Coherence with MEG was averaged over the sensors of interest. Black, horizontal bars indicate significant differences ($P < 0.05$; $n = 18$). Shaded areas indicate standard error of the mean. (B) Changes in LFP-MEG coherence are plotted against changes in EMG power. The line indicates the best linear fit. Values were averaged over the tremor frequency and its first harmonic.

when tremor occurs. To identify the brain areas involved in this process, we computed source level coherence at tremor frequency and contrasted tremor and tremor-free epochs. As the quality of spatial filters depends on the amount of data, we included only subthalamic nuclei for which at least 30 s of rest tremor and 30 s of tremor-free episodes were available. The inclusion criterion was met by eight subthalamic nuclei from six subjects.

Source level analysis revealed significant changes in cortico-muscular but not in subthalamic nucleus-cortex coherence. One cluster was found ($P = 0.02$; Fig. 4), which covered several motor and sensory areas contralateral to tremor. By visual inspection, we identified three local maxima that appeared to be distinct sources. They were located in the primary motor cortex (MNI coordinates: $\pm 60, -15, 50$), premotor cortex (MNI coordinates: $\pm 30, 10, 70$) and posterior parietal cortex (MNI coordinates: $\pm 20, -75, 50$). Supplementary Fig. 2 shows the spatial configuration of selected sources in detail.

Cortico-cortical coupling

To test whether the identified cortical sources are themselves coupled, we estimated their time domain activity and computed ImCoh for all source pairs. In line with previous reports (Timmermann *et al.*, 2003; Pollok *et al.*, 2004), we found

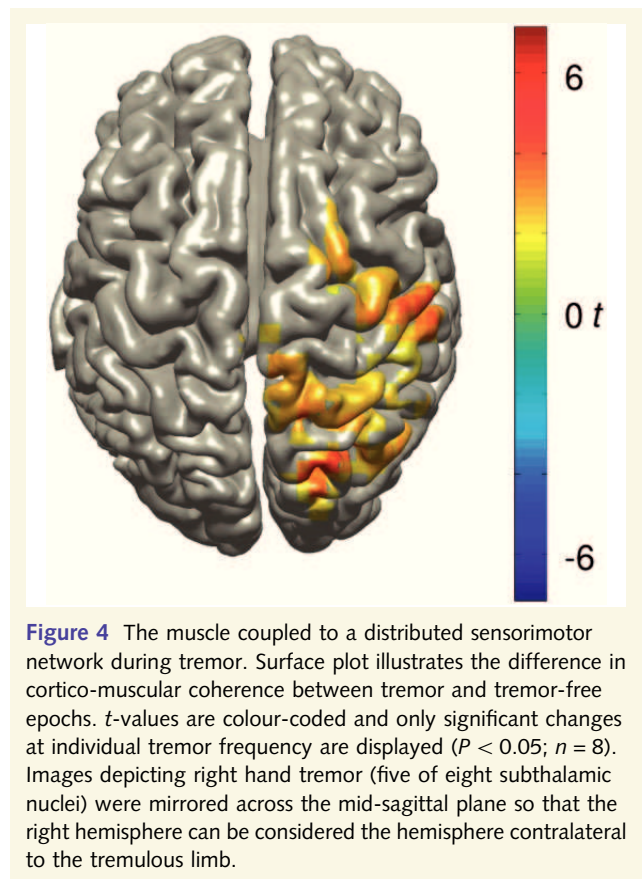


Figure 4 The muscle coupled to a distributed sensorimotor network during tremor. Surface plot illustrates the difference in cortico-muscular coherence between tremor and tremor-free epochs. t -values are colour-coded and only significant changes at individual tremor frequency are displayed ($P < 0.05$; $n = 8$). Images depicting right hand tremor (five of eight subthalamic nuclei) were mirrored across the mid-sagittal plane so that the right hemisphere can be considered the hemisphere contralateral to the tremulous limb.

cortico-cortical coupling to occur not only at tremor frequency, but also and more frequently at double the tremor frequency. Two representative examples of cortico-cortical coupling are shown in Fig. 5.

A repeated-measures ANOVA with factors 'shuffling' and 'pair' revealed that shifting one signal in time destroyed ImCoh at tremor frequency and its first harmonic. A main effect of shuffling was found when considering tremor epochs [$F(1,7) = 5.95$, $P < 0.05$] and a trend was observed for tremor-free epochs [$F(1,7) = 4.65$, $P = 0.07$]. We found neither a main effect of pair [tremor: $F(2,14) = 0.11$, $P = 0.83$; no tremor: $F(2,14) = 0.04$, $P = 0.94$] nor an interaction between shuffling and pair [tremor: $F(2,14) = 0.58$, $P = 0.57$; no tremor: $F(2,14) = 0.19$, $P = 0.78$]. Rather than affecting coupling between specific pairs of cortical areas, shuffling reduced ImCoh between all pairs to a similar degree (Fig. 6A).

Tremor-related changes in cortico-cortical coupling

The fact that 'shuffling' had a slightly stronger effect in the tremor condition might hint at an influence of tremor on ImCoh. This possibility was not investigated further because a conditional change in ImCoh is difficult to interpret. It may be explained either by a change in phase consistency or by alteration of the

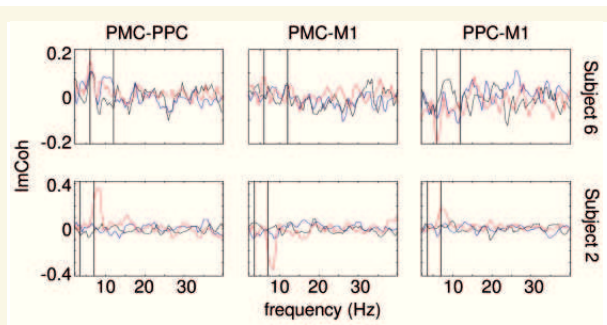


Figure 5 Cortical areas in the tremor network are coupled to one another at tremor frequency and/or double tremor frequency. Plots show examples of ImCoh between pairs of cortical sources from Subject 6 (*top row*) and Subject 2 (*bottom row*). Blue = no tremor; red = tremor; black = shuffled. Vertical lines indicate the tremor frequency and its first harmonic. M1 = primary motor cortex; PPC = parietal cortex; PMC = premotor cortex.

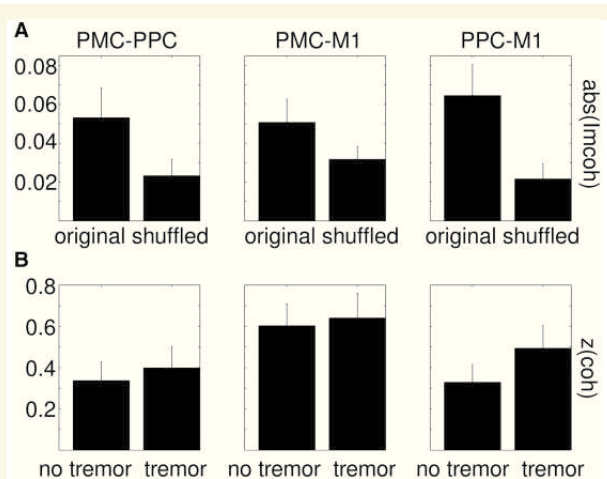


Figure 6 Cortico-cortical coupling increased during tremor. (A) Bars represent mean, absolute ImCoh between pairs of cortical sources during tremor ($n = 8$). (B) Bars represent mean, z-transformed coherence between pairs of cortical sources. Values were averaged over the tremor frequency and its first harmonic. Error bars indicate the standard error of the mean. The y-axis scale is the same for all sub-plots within one row. M1 = primary motor cortex; PPC = parietal cortex; PMC = premotor cortex.

preferred phase difference (Gross *et al.*, 2013). As coherence is unaffected by a change in the preferred phase difference, we used coherence to quantify the difference between tremor and tremor-free epochs.

An ANOVA with factors 'tremor' and 'pair' revealed a main effect of tremor [$F(1,7) = 7.48$, $P = 0.03$] and a main effect of pair [$F(2,14) = 5.65$, $P = 0.04$] but no interaction between tremor and pair [$F(2,14) = 1.0$, $P = 0.36$]. As depicted in Fig. 6B, coherence between all pairs increased in the tremor condition.

The effect of pair was most likely due to volume conduction, as neighbouring areas exhibited higher coherence than distant areas, regardless of the tremor state.

Discussion

We investigated the parkinsonian rest tremor network by means of simultaneous LFP, MEG and EMG recordings and found that cerebral synchronization at tremor frequency increases as tremor becomes manifest. Increases were observed in a network including subthalamic nucleus, primary motor, premotor and posterior parietal cortex contralateral to the tremulous limb. In addition, we demonstrated that the tremor-associated increase in subthalamic nucleus-cortex coherence was positively correlated with the tremor-associated increase in muscle activity.

Methodological considerations

Simultaneous LFP, MEG and EMG recordings provide unique insights into the relationship between subcortical, cortical and muscle activity in humans and enabled recent advances in the characterization of functional connectivity in Parkinson's disease (Hirschmann *et al.*, 2011, 2013; Litvak *et al.*, 2011, 2012; Oswal *et al.*, 2013). Before discussing the results of the current study in detail, we will consider some methodological aspects associated with coherence measurements obtained with this approach.

One of the major concerns in coherence analysis is the possibility that changes in coherence are trivial consequences of changes in power (Schoffelen and Gross, 2009). Although coherence is normalized by power, it is affected by power changes as they result in changes in the signal-to-noise ratio (Palva and Palva, 2012). In tremor analysis, the most drastic power changes occur in the EMG. Therefore, one might expect EMG power changes to cause changes in cortico-muscular coherence. Importantly, group statistical analysis on the source level excluded this potential confound by demonstrating consistent spatial patterns. Changes in cortico-muscular coherence were consistently observed in a limited set of cortical areas contralateral to the tremulous limb. There is no plausible mechanism by which EMG power changes might affect specifically these areas while sparing all others.

Apart from affecting the signal-to-noise ratio, tremulous movement creates rhythmically changing magnetic fields that may in principle be measured by MEG directly, resulting in artefacts and spurious cortico-muscular coherence. A systematic effect of the latter seems unlikely for the same reasons that speak against confounds because of EMG power changes. Artefacts were rarely observed in this study due to the usage of non-magnetic externalization leads and application of temporal signal space separation.

Finally, imprecise determination of tremor onset could have influenced the results on power time courses. As the emergence of tremor was often gradual, it was not always possible to determine the exact moment of tremor onset. This inevitable imprecision diminished the detection probability of transient effects, since detection requires a high degree of temporal overlap across

epochs. Thus, the analysis was biased towards the detection of sustained effects. Moreover, detection probability increased with time after tremor onset, as any jitter in onset times affected the temporal overlap of sustained effects only in the first seconds after tremor onset.

Subthalamic nucleus and cortical power

In line with previous studies (Levy *et al.*, 2002; Liu *et al.*, 2002; Wang *et al.*, 2006; Reck *et al.*, 2009), we observed clear peaks in the subthalamic nucleus LFP power spectra at tremor frequency and double tremor frequency. Moreover, we found a tremor-induced increase of subthalamic nucleus power at individual tremor frequency, as reported in a previous single case study (Wang *et al.*, 2005). Notably, the increase occurred several seconds after tremor onset, at a time when tremor amplitude had reached its maximum. Hence, this power increase cannot be the cause of tremor, but could reflect a gradual entrainment of more and more subthalamic nucleus neurons, e.g. by sustained somatosensory feedback (Wang *et al.*, 2007; Florin *et al.*, 2010). Alternatively, it is conceivable that the detected subthalamic nucleus activity is related to the scale of tremor. Given that the basal ganglia are important for movement scaling (Oliverira *et al.*, 1998; Desmurget and Turner, 2010), strong and sustained subthalamic nucleus oscillations might emerge only when tremor amplitude exceeds a certain threshold, i.e. when a large-scale movement is being executed.

In addition to changes at tremor frequency, we found that cortical beta power was suppressed during continuous tremor. This finding tallies with a study in healthy subjects that reported a sustained decrease of cortical beta power during repetitive, voluntary movement (Erbil and Ungan, 2007). Thus, our results further strengthen the claim that voluntary movement and tremor have a common neurophysiological basis (Pollok *et al.*, 2004; Schnitzler *et al.*, 2006). However, they also provide indications for differences with respect to the dynamics of power. In this study, we did not observe a decrease of cortical beta power before tremor onset, whereas this effect is known to occur before voluntary movement (Pfurtscheller *et al.*, 2003). Further studies are needed to elaborate on these potential differences in cortical activity.

Subthalamic nucleus-cortex coherence

While coherence between subthalamic nucleus and EMG at tremor frequency has been addressed by numerous studies (Wang *et al.*, 2006; Amtage *et al.*, 2008; Reck *et al.*, 2009, 2010), subthalamic nucleus-cortex coupling has rarely been investigated in the context of tremor. Importantly, we demonstrated that subthalamic nucleus-cortex coherence increases in the presence of tremor and correlates with tremor severity, showing that: (i) the subthalamic nucleus is part of the central tremor network; and (ii) it generates input to cortex or receives output from cortex that directly reflects tremor amplitude. These findings are complemented by a recent intraoperative study reporting that phase-locking of subthalamic nucleus spikes to motor cortical 6 Hz oscillations is more common in the presence than in the absence of tremor (Shimamoto *et al.*, 2013).

The paucity of epochs did not allow for localization of the tremor-associated increase in subthalamic nucleus-cortex coherence observed on the sensor level. Many subjects showed either continuous tremor intermitted by short breaks or short episodes of tremor, resulting in limited amounts of data suited for balanced contrasts and spatial filter construction. Although the amount of epochs sufficed to localize the change in cortico-muscular coherence, localization of the weaker change in subthalamic nucleus-cortex coherence likely requires more or longer recordings.

Cortico-muscular and cortico-cortical coherence

In keeping with previous studies (Volkman *et al.*, 1996; Hellwig *et al.*, 2000), we found strong cortico-muscular coherence at tremor frequency and its first harmonic. Coherence increased during epochs of spontaneously emerging rest tremor and the increase could be localized to a set of cortical areas contralateral to the tremulous limb. The fact that increases occurred in both motor and sensory cortical areas suggests that both efferent and afferent rhythmical signalling is enhanced during tremor.

The localization presented in this study closely resembles the tremor network identified in previous MEG (Timmermann *et al.*, 2003; Pollok *et al.*, 2009) and EEG studies (Muthuraman *et al.*, 2012) on parkinsonian tremor. Thus, there is mounting evidence for the existence of a cortical network including primary motor, premotor and posterior parietal cortex that is active during pathological and voluntary tremor (Pollok *et al.*, 2004). Interestingly, a recent study revealed the therapeutic potential of modulating the cortical tremor network (Brittain *et al.*, 2013). The study demonstrated that interfering with cortical oscillations by transcranial alternating current stimulation over motor cortex leads to substantial tremor alleviation.

In line with the aforementioned studies (Timmermann *et al.*, 2003; Pollok *et al.*, 2004, 2009), we found that the cortical areas coherent with muscle activity are also coupled to one another. The current results additionally show that cortico-cortical coupling at tremor frequency is dependent on tremor manifestation and is not a trivial consequence of volume conduction.

Comparison with previous studies

Earlier mappings of tremor-related coherence led to the identification of more areas than reported in this study (Timmermann *et al.*, 2003; Pollok *et al.*, 2004, 2009; Muthuraman *et al.*, 2012). In addition to primary motor, premotor and posterior parietal cortex, significant coherence was observed in the supplementary motor area, secondary somatosensory cortex, cerebellum and thalamus. The different results can be explained by differences in methodology. We restricted the analysis to cortical areas to increase statistical power. Furthermore, we used the EMG as reference signal and localized coherence changes (rather than coherence *per se*) in a single step procedure. Previous studies first identified primary motor cortex as the source of maximum coherence with the muscle. Subsequently, the authors searched for sources coherent with primary motor cortex.

Although the approach applied here is less sensitive than the approach used previously, it provides improved reliability. Association with tremor is not based on coherence peaks at tremor frequency but on the contrast between tremor and tremor-free epochs, allowing for the computation of group statistics controlled for multiple comparisons. Moreover, the method does not require removing the activity of strongly coherent sources from the data prior to detection of weaker couplings (Gross *et al.*, 2001). This analysis step bears caveats, as incomplete removal will lead to the detection of spurious coupling. Finally, it accounts for the effect of volume conduction. Volume conduction, also referred to as spatial leakage, results from suboptimal spatial filtering and may substantially confound analysis of cortico-cortical connectivity (Schoffelen and Gross, 2009; Palva and Palva, 2012).

Clinical relevance

The current study demonstrates a direct relationship between subthalamic nucleus oscillations at tremor frequency and tremor manifestation. Thus, subthalamic nucleus power and/or subthalamic nucleus-cortex coherence might potentially be used by closed-loop DBS systems designed to suppress tremor. Subthalamic nucleus power is a particularly promising parameter for triggering DBS. In contrast to systems that use cortical action potentials as triggers (Rosin *et al.*, 2011), a system using subthalamic nucleus power would not require additional cortical implants and would be robust to slight changes in electrode position. Furthermore, online computation of oscillatory power requires less computational resources than other suggested control parameters, such as phase-amplitude coupling (de Hemptinne *et al.*, 2013).

This study provides important information on how subthalamic nucleus power could be used by closed-loop systems. It suggests that power increases at individual tremor frequency could serve as a trigger signal. To achieve more robust tremor detection, we propose to apply DBS whenever subthalamic nucleus power increases at tremor frequency and its first harmonic and simultaneously decreases in the beta band.

Conclusion

Parkinsonian rest tremor is associated with an increase of cerebral synchronization at tremor frequency and double tremor frequency. The increase occurs in a network including subthalamic nucleus, primary motor cortex, premotor cortex and posterior parietal cortex. These results suggest the feasibility of tremor detection based solely on cerebral oscillations.

Acknowledgements

The authors would like to express their sincere gratefulness to the patients who participated in this study. Furthermore, we are very thankful to Medtronic for providing non-magnetic lead extensions. In addition, we thank Mrs. E. Rädisch for assistance with MRI scans.

Funding

This work was supported by ERA-NET Neuron [Neuron-48-013 to A.S.], by the Deutsche Forschungsgemeinschaft [FOR1328, SCHN 592/3-1 to A.S.] and by the European Commission [Marie Curie Fellowship; FP7-PEOPLE-2009-IEF-253965 to M.B.].

Supplementary material

Supplementary material is available at *Brain* online.

References

- Amtage F, Henschel K, Schelter B, Vesper J, Timmer J, Lücking C, *et al.* Tremor-correlated neuronal activity in the subthalamic nucleus of parkinsonian patients. *Neurosci Lett* 2008; 442: 195–9.
- Avants BB, Epstein CL, Grossman M, Gee JC. Symmetric diffeomorphic image registration with cross-correlation: evaluating automated labeling of elderly and neurodegenerative brain. *Med Image Anal* 2008; 12: 26–41.
- Benabid AL, Pollak P, Gervason C, Hoffmann D, Gao DM, Hommel M, *et al.* Long-term suppression of tremor by chronic stimulation of the ventral intermediate thalamic nucleus. *Lancet* 1991; 337: 403–6.
- Bergman H, Wichmann T, DeLong MR. Reversal of experimental parkinsonism by lesions of the subthalamic nucleus. *Science* 1990; 249: 1436–8.
- Bergman H, Wichmann T, Karmon B, DeLong MR. The primate subthalamic nucleus. II. Neuronal activity in the MPTP model of parkinsonism. *J Neurophysiol* 1994; 72: 507–20.
- Brittain J, Probert-Smith P, Aziz T, Brown P. Tremor suppression by rhythmic transcranial current stimulation. *Curr Biol* 2013; 23: 436–40.
- de Hemptinne C, Ryapolova-Webb ES, Air EL, Garcia PA, Miller KJ, Ojemann JG, *et al.* Exaggerated phase–amplitude coupling in the primary motor cortex in Parkinson disease. *Proc Natl Acad Sci USA* 2013; 110: 4780–5.
- Deiber MP, Pollak P, Passingham R, Landais P, Gervason C, Cinotti L, *et al.* Thalamic stimulation and suppression of parkinsonian tremor. Evidence of a cerebellar deactivation using positron emission tomography. *Brain* 1993; 116 (Pt 1): 267–79.
- Desmurget M, Turner RS. Motor sequences and the basal ganglia: kinematics, not habits. *J Neurosci* 2010; 30: 7685–90.
- Deuschl G, Raethjen J, Baron R, Lindemann M, Wilms H, Krack P. The pathophysiology of parkinsonian tremor: a review. *J Neurol* 2000; 247: V33–48.
- Elble RJ. Central mechanisms of tremor. *J Clin Neurophysiol* 1996; 13: 133–44.
- Erbil N, Ungan P. Changes in the alpha and beta amplitudes of the central EEG during the onset, continuation, and offset of long-duration repetitive hand movements. *Brain Res* 2007; 1169: 44–56.
- Florin E, Gross J, Reck C, Maarouf M, Schnitzler A, Sturm V, *et al.* Causality between local field potentials of the subthalamic nucleus and electromyograms of forearm muscles in Parkinson's disease. *Eur J Neurosci* 2010; 31: 491–8.
- Forstmann BU, Keuken MC, Jahfari S, Bazin P-L, Neumann J, Schäfer A, *et al.* Cortico-subthalamic white matter tract strength predicts inter-individual efficacy in stopping a motor response. *Neuroimage* 2012; 60: 370–5.
- Goetz CG, Tilley BC, Shaftman SR, Stebbins GT, Fahn S, Martinez-Martin P, *et al.* Movement Disorder Society-sponsored revision of the Unified Parkinson's Disease Rating Scale (MDS-UPDRS): scale presentation and clinimetric testing results. *Mov Disord* 2008; 23: 2129–70.

- Gross J, Baillet S, Barnes GR, Henson R, Hillebrand A, Jensen O, et al. Good practice for conducting and reporting MEG research. *Neuroimage* 2013; 65: 349–63.
- Gross J, Kujala J, Hamalainen M, Timmermann L, Schnitzler A, Salmelin R. Dynamic imaging of coherent sources: studying neural interactions in the human brain. *Proc Natl Acad Sci USA* 2001; 98: 694–9.
- Hammond C, Bergman H, Brown P. Pathological synchronization in Parkinson's disease: networks, models and treatments. *Trends Neurosci* 2007; 30: 357–64.
- Heimer G, Rivlin-Etzion M, Bar-Gad I, Goldberg JA, Haber SN, Bergman H. Dopamine replacement therapy does not restore the full spectrum of normal pallidal activity in the 1-methyl-4-phenyl-1,2,3,6-tetra-hydropyridine primate model of Parkinsonism. *J Neurosci* 2006; 26: 8101–14.
- Hellwig B, Häussler S, Lauk M, Guschlbauer B, Köster B, Kristeva-Feige R, et al. Tremor-correlated cortical activity detected by electroencephalography. *Clin Neurophysiol* 2000; 111: 806–9.
- Helmich RC, Hallett M, Deuschl G, Toni I, Bloem BR. Cerebral causes and consequences of parkinsonian resting tremor: a tale of two circuits? *Brain* 2012; 135: 3206–26.
- Helmich RC, Janssen MJR, Oyen WJG, Bloem BR, Toni I. Pallidal dysfunction drives a cerebellothalamic circuit into Parkinson tremor. *Ann Neurol* 2011; 69: 269–81.
- Hemm S, Coste J, Gabrillargues J, Ouchchane L, Sarry L, Caire F, et al. Contact position analysis of deep brain stimulation electrodes on post-operative CT images. *Acta Neurochir* 2009; 151: 823–9.
- Hirschmann J, Özkurt TE, Butz M, Homburger M, Elben S, Hartmann CJ, et al. Distinct oscillatory STN-cortical loops revealed by simultaneous MEG and local field potential recordings in patients with Parkinson's disease. *Neuroimage* 2011; 55: 1159–68.
- Hirschmann J, Özkurt TE, Butz M, Homburger M, Elben S, Hartmann CJ, et al. Differential modulation of STN-cortical and cortico-muscular coherence by movement and levodopa in Parkinson's disease. *Neuroimage* 2013; 68: 203–13.
- Hoehn MM, Yahr MD. Parkinsonism: onset, progression and mortality. *Neurology* 1967; 17: 427–42.
- Hughes AJ, Daniel SE, Blankson S, Lees AJ. A clinicopathologic study of 100 cases of Parkinson's disease. *Arch Neurol* 1993; 50: 140–8.
- Hurtado JM, Rubchinsky LL, Sigvardt KA, Wheelock VL, Pappas CTE. Temporal Evolution of Oscillations and Synchrony in GPI/Muscle Pairs in Parkinson's Disease. *J Neurophysiol* 2005; 93: 1569–84.
- Hutchison WD, Lozano AM, Tasker RR, Lang AE, Dostrovsky JO. Identification and characterization of neurons with tremor-frequency activity in human globus pallidus. *Exp Brain Res* 1997; 113: 557–63.
- Jenkinson M, Beckmann CF, Behrens TEJ, Woolrich MW, Smith SM. FSL. *Neuroimage* 2012; 62: 782–90.
- Krack P, Pollak P, Limousin P, Benazzouz A, Benabid AL. Stimulation of subthalamic nucleus alleviates tremor in Parkinson's disease. *Lancet* 1997; 350: 1675.
- Kühn AA, Kupsch A, Schneider G-H, Brown P. Reduction in subthalamic 8-35 Hz oscillatory activity correlates with clinical improvement in Parkinson's disease. *Eur J Neurosci* 2006; 23: 1956–60.
- Lang AE, Lozano AM. Parkinson's disease. Second of two parts. *N Engl J Med* 1998; 339: 1130–43.
- Lenz FA, Tasker RR, Kwan HC, Schnider S, Kwong R, Murayama Y, et al. Single unit analysis of the human ventral thalamic nuclear group: correlation of thalamic 'tremor cells' with the 3-6 Hz component of parkinsonian tremor. *J Neurosci* 1988; 8: 754–64.
- Levy R, Ashby P, Hutchison WD, Lang AE, Lozano AM, Dostrovsky JO. Dependence of subthalamic nucleus oscillations on movement and dopamine in Parkinson's disease. *Brain* 2002; 125: 1196–209.
- Litvak V, Eusebio A, Jha A, Oostenveld R, Barnes G, Foltynie T, et al. Movement-related changes in local and long-range synchronization in Parkinson's disease revealed by simultaneous magnetoencephalography and intracranial recordings. *J Neurosci* 2012; 32: 10541–53.
- Litvak V, Jha A, Eusebio A, Oostenveld R, Foltynie T, Limousin P, et al. Resting oscillatory cortico-subthalamic connectivity in patients with Parkinson's disease. *Brain* 2011; 134: 359–74.
- Liu X, Ford-Dunn H, Hayward G, Nandi D, Miall R, Aziz TZ, et al. The oscillatory activity in the parkinsonian subthalamic nucleus investigated using the macro-electrodes for deep brain stimulation. *Clin Neurophysiol* 2002; 113: 1667–72.
- Magariños-Ascone CM, Figueiras-Mendez R, Riva-Meana C, Córdoba-Fernández A. Subthalamic neuron activity related to tremor and movement in Parkinson's disease. *Eur J Neurosci* 2000; 12: 2597–607.
- Maris E, Oostenveld R. Nonparametric statistical testing of EEG- and MEG-data. *J Neurosci Methods* 2007; 164: 177–90.
- Mattout J, Henson RN, Friston KJ. Canonical source reconstruction for MEG. *Comput Intell Neurosci* 2007; 2007: 1–10.
- McAuley JH, Marsden CD. Physiological and pathological tremors and rhythmic central motor control. *Brain* 2000; 123 (Pt 8): 1545–67.
- Moran A, Bergman H, Israel Z, Bar-Gad I. Subthalamic nucleus functional organization revealed by parkinsonian neuronal oscillations and synchrony. *Brain* 2008; 131: 3395–409.
- Mure H, Hirano S, Tang CC, Isaías IU, Antonini A, Ma Y, et al. Parkinson's disease tremor-related metabolic network: characterization, progression, and treatment effects. *Neuroimage* 2011; 54: 1244–53.
- Muthuraman M, Heute U, Arning K, Anwar AR, Elble RJ, Deuschl G, et al. Oscillating central motor networks in pathological tremors and voluntary movements. What makes the difference? *NeuroImage* 2012; 60: 1331–9.
- Nolte G. The magnetic lead field theorem in the quasi-static approximation and its use for magnetoencephalography forward calculation in realistic volume conductors. *Phys Med Biol* 2003; 48: 3637–52.
- Nolte G, Bai O, Wheaton L, Mari Z, Vorbach S, Hallett M. Identifying true brain interaction from EEG data using the imaginary part of coherence. *Clin Neurophysiol* 2004; 115: 2292–307.
- Oliverira RM, Gurd JM, Nixon P, Marshall JC, Passingham RE. Hypometria in Parkinson's disease: automatic versus controlled processing. *Mov Disord* 1998; 13: 422–7.
- Oostenveld R, Fries P, Maris E, Schoffelen J-M. FieldTrip: open source software for advanced analysis of MEG, EEG, and invasive electrophysiological data. *Comput Intell Neurosci* 2011; 2011: 1–9.
- Oswal A, Brown P, Litvak V. Movement related dynamics of subthalamic cortical alpha connectivity in Parkinson's disease. *Neuroimage* 2013; 70: 132–42.
- Özkurt TE, Butz M, Homburger M, Elben S, Vesper J, Wojtecki L, et al. High frequency oscillations in the subthalamic nucleus: a neurophysiological marker of the motor state in Parkinson's disease. *Exp Neurol* 2011; 229: 324–31.
- Palva S, Palva JM. Discovering oscillatory interaction networks with M/EEG: challenges and breakthroughs. *Trends Cogn Sci (Regul Ed)* 2012; 16: 219–30.
- Pfurtscheller G, Graimann B, Huggins JE, Levine SP, Schuh LA. Spatiotemporal patterns of beta desynchronization and gamma synchronization in corticographic data during self-paced movement. *Clin Neurophysiol* 2003; 114: 1226–36.
- Pollok B, Gross J, Dirks M, Timmermann L, Schnitzler A. The cerebral oscillatory network of voluntary tremor. *J Physiol (Lond)* 2004; 554: 871–8.
- Pollok B, Makhlofi H, Butz M, Gross J, Chaieb L, Wojtecki L, et al. Levodopa affects functional brain networks in parkinsonian resting tremor. *Mov Disord* 2009; 24: 91–8.
- Raz A, Vaadia E, Bergman H. Firing patterns and correlations of spontaneous discharge of pallidal neurons in the normal and the tremulous 1-methyl-4-phenyl-1,2,3,6-tetrahydropyridine vervet model of parkinsonism. *J Neurosci* 2000; 20: 8559–71.
- Reck C, Florin E, Wojtecki L, Krause H, Groiss S, Voges J, et al. Characterisation of tremor-associated local field potentials in the subthalamic nucleus in Parkinson's disease. *Eur J Neurosci* 2009; 29: 599–612.

- Reck C, Himmel M, Florin E, Maarouf M, Sturm V, Wojtecki L, et al. Coherence analysis of local field potentials in the subthalamic nucleus: differences in parkinsonian rest and postural tremor. *Eur J Neurosci* 2010; 32: 1202–14.
- Rosin B, Slovik M, Mitelman R, Rivlin-Etzion M, Haber SN, Israel Z, et al. Closed-loop deep brain stimulation is superior in ameliorating parkinsonism. *Neuron* 2011; 72: 370–84.
- Schnitzler A, Gross J. Normal and pathological oscillatory communication in the brain. *Nat Rev Neurosci* 2005; 6: 285–96.
- Schnitzler A, Müns C, Butz M, Timmermann L, Gross J. Synchronized brain network associated with essential tremor as revealed by magnetoencephalography. *Mov Disord* 2009; 24: 1629–35.
- Schnitzler A, Timmermann L, Gross J. Physiological and pathological oscillatory networks in the human motor system. *J Physiol Paris* 2006; 99: 3–7.
- Schoffelen J-M, Gross J. Source connectivity analysis with MEG and EEG. *Hum Brain Mapp* 2009; 30: 1857–65.
- Sekihara K, Nagarajan SS, Poeppel D, Marantz A, Miyashita Y. Application of an MEG eigenspace beamformer to reconstructing spatio-temporal activities of neural sources. *Hum Brain Mapp* 2002; 15: 199–215.
- Shimamoto SA, Ryapolova-Webb ES, Ostrem JL, Galifianakis NB, Miller KJ, Starr PA. Subthalamic nucleus neurons are synchronized to primary motor cortex local field potentials in Parkinson's disease. *J Neurosci* 2013; 33: 7220–33.
- Stein JF, Aziz TZ. Does imbalance between basal ganglia and cerebellar outputs cause movement disorders? *Curr Opin Neurol* 1999; 12: 667–9.
- Taulu S, Simola J. Spatiotemporal signal space separation method for rejecting nearby interference in MEG measurements. *Phys Med Biol* 2006; 51: 1759–68.
- Thomson DJ. Spectrum estimation and harmonic analysis. *Proc IEEE* 1982; 70: 1055–96.
- Timmermann L, Gross J, Dirks M, Volkmann J, Freund H-J, Schnitzler A. The cerebral oscillatory network of parkinsonian resting tremor. *Brain* 2003; 126: 199–212.
- Van Veen BD, Buckley KM. Beamforming: a versatile approach to spatial filtering. *IEEE ASSP Mag* 1988; 5: 4–24.
- Volkmann J, Joliot M, Mogilner A, Ioannides AA, Lado F, Fazzini E, et al. Central motor loop oscillations in parkinsonian resting tremor revealed magnetoencephalography. *Neurology* 1996; 46: 1359–9.
- Wang S, Aziz TZ, Stein JF, Bain PG, Liu X. Physiological and harmonic components in neural and muscular coherence in parkinsonian tremor. *Clin Neurophysiol* 2006; 117: 1487–1498.
- Wang S, Aziz TZ, Stein JF, Liu X. Time–frequency analysis of transient neuromuscular events: dynamic changes in activity of the subthalamic nucleus and forearm muscles related to the intermittent resting tremor. *J Neurosci Methods* 2005; 145: 151–8.
- Wang S, Chen Y, Ding M, Feng J, Stein JF, Aziz TZ, et al. Revealing the dynamic causal interdependence between neural and muscular signals in parkinsonian tremor. *J Franklin Ins* 2007; 344: 180–195.
- Zirh TA, Lenz FA, Reich SG, Dougherty PM. Patterns of bursting occurring in thalamic cells during parkinsonian tremor. *Neuroscience* 1998; 83: 107–21.

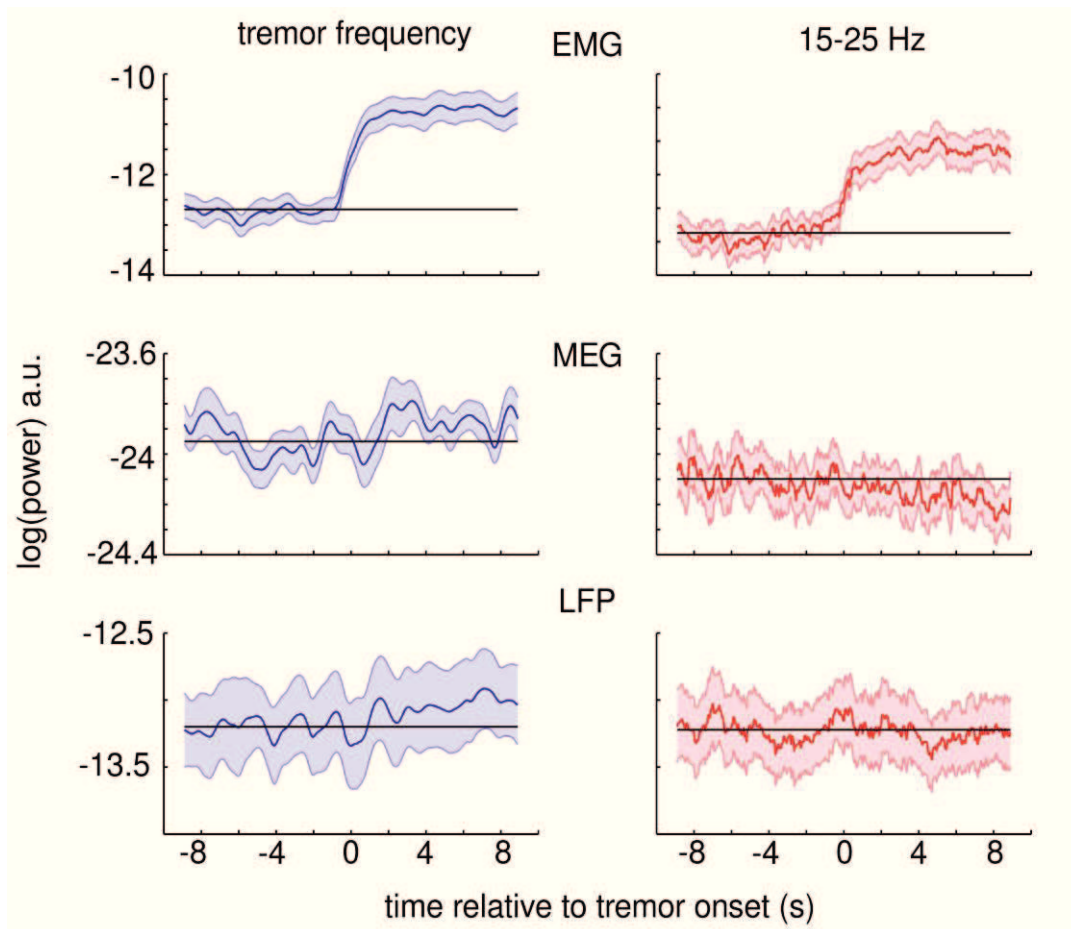


Fig. S1: Time course of power before and after tremor onset.

The figure shows the dynamics of group average EMG (upper row), MEG (middle row) and LFP power (lower row). Black horizontal lines indicate mean baseline power (-9 to 0 s) and shaded areas depict the standard error of the mean. Left column: Power at individual tremor frequency ± 0.5 Hz. Right column: Power at 20 Hz ± 5 Hz. Please note that LFP power at tremor frequency started to fluctuate around a higher mean value after tremor onset. LFP beta power decreased between -4 to 0 s, followed by a transient increase at tremor onset and another transient decrease. MEG beta power had similar dynamics, but the power decrease intensified gradually as tremor continued.

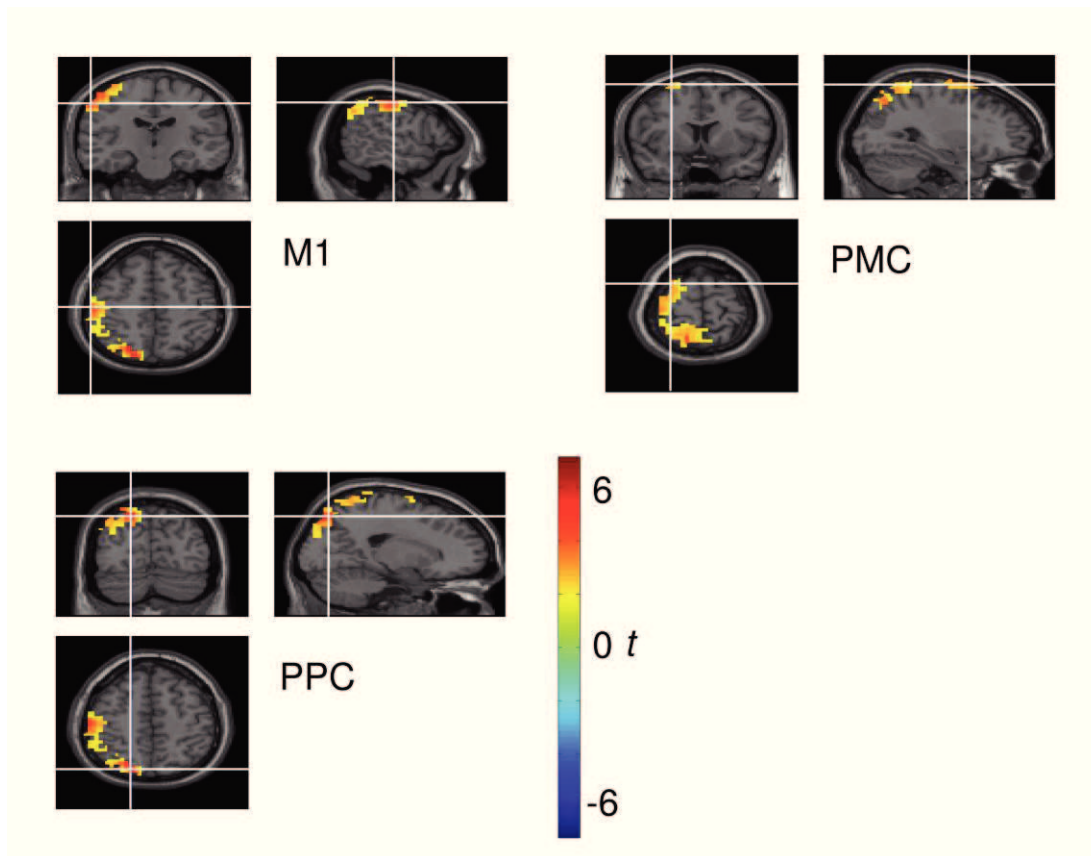
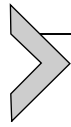


Fig. S2: Tremor-related changes in cortico-muscular coherence occurred in spatially separated cortical areas.

Cortical areas that showed significant increases in cortico-muscular coherence during tremor are displayed ($p < 0.05$; $N = 8$). All of these areas belonged to a single cluster, i.e. they were interconnected in space by super-threshold voxels. However, distinct local maxima within that cluster were clearly distinguishable. Cross hairs mark the regions of interest from which time series were reconstructed. M1 = primary motor cortex; PPC = parietal cortex; PMC = premotor cortex.



Magnetoencephalography and Neuromodulation

Alfons Schnitzler^{*,†,1}, Jan Hirschmann^{*,†}

^{*}Institute of Clinical Neuroscience and Medical Psychology, Medical Faculty, Heinrich-Heine-University Düsseldorf, Düsseldorf, Germany

[†]Department of Neurology, University Hospital Düsseldorf, Düsseldorf, Germany

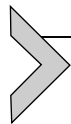
¹Corresponding author: e-mail address: SchnitzA@med.uni-duesseldorf.de

Contents

1. Introduction	121
2. MEG and TMS	122
2.1 MEG informs TMS	122
2.2 MEG characterizes TMS effects	124
3. MEG and Transcranial Direct or Alternate Current Stimulation	125
4. MEG and DBS	125
4.1 Simultaneous MEG and local field potential recordings in PD patients	126
4.2 MEG characterizes DBS effects	130
5. Conclusions and Outlook	132
References	133

Abstract

Magnetoencephalography (MEG) is a noninvasive method which allows recordings of human brain activity with excellent temporal and good spatial resolution. In this chapter, we review applications of MEG in neuromodulation. We provide an overview of studies which used MEG to optimize parameters for neuromodulation and to characterize the electrophysiological effects of brain stimulation. In particular, we discuss how MEG may be employed to study deep brain stimulation. In this context, we describe the problems arising from stimulation artifacts and present approaches to solve them.

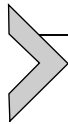


1. INTRODUCTION

Magnetoencephalography (MEG) is one of the most widely used techniques to measure brain activity noninvasively in humans. Based on superconducting interference device technology, MEG is able to detect the extremely small magnetic fields resulting from joint activity of several thousand neurons (Hämäläinen, Hari, Ilmoniemi, Knuutila, & Lounasmaa, 1993).

Modern MEG systems are equipped with hundreds of sensors which sample brain activity with a frequency of several thousand Hertz. Due to recent advances in source reconstruction methodology, task-related or spontaneous activity can be localized with sub-centimeter spatial resolution (Barnes, Hillebrand, Fawcett, & Singh, 2004). Thus, MEG has excellent temporal and good spatial resolution and is therefore ideally suited to study the effects of neuromodulation in humans.

MEG provides helpful information at all stages of neuromodulation research. It may be used (i) to identify the anatomical targets and the appropriate timing of brain stimulation, (ii) to characterize immediate and lasting neurophysiological effects of intervention, and (iii) to acquire basic knowledge about the pathophysiological mechanisms which make therapeutic neuromodulation necessary. In this chapter, we will review recent applications of MEG in neuromodulation. In the first part, we will give an overview of studies combining MEG with transcranial magnetic stimulation (TMS). In the second part, we will provide a short outlook on prospective applications of MEG in combination with transcranial current stimulation. Finally, we will discuss in detail how MEG studies may contribute to the understanding and improvement of deep brain stimulation (DBS) and give examples of studies combining these two techniques.



2. MEG AND TMS

TMS is a noninvasive brain stimulation technique which is used to study casual relationships between brain activity and behavior (Pascual-Leone, Bartres-Faz, & Keenan, 1999). Moreover, TMS is applied for therapeutic purposes (Barr et al., 2011; Croarkin, Wall, & Lee, 2011; Corti, Patten, & Triggs, 2012). In TMS, a current is produced in a coil which is positioned above the target brain area. The current induces a strong and focal magnetic field which in turn induces a secondary current in the targeted brain area. The induced current interferes with local processing and may result in an observable change in behavior.

2.1. MEG informs TMS

Naturally, the outcome of TMS depends on the specific target. A study by Raj et al. (2008) showed how MEG may be employed to obtain knowledge about the appropriate stimulation target. The authors measured somatosensory-evoked fields (SEFs) by means of MEG and identified individual SEF latencies and the underlying generator sources. Subsequently, they combined median nerve stimulation, electroencephalography (EEG)

and TMS and let each somatosensory stimulus be followed by a single TMS pulse. The pulse was targeted at the region functionally identified as secondary somatosensory cortex (S2) in the previous MEG experiment. Subjects were instructed to react to each somatosensory stimulus as fast as possible. The authors found that a TMS pulse delivered 15–40 ms after somatosensory stimulation decreased reaction times and shifted the 140 ms component of the evoked potential forward in time, suggesting that S1 → S2 reciprocal pathways were facilitated by TMS of S2.

Another example of how MEG may be used to inform TMS protocols is given by a recent study by [Thut et al. \(2011\)](#). In this study, MEG was recorded to obtain information on brain target area and frequency of stimulation. The authors recorded the MEG of subjects performing a visual attention task. Using frequency analysis and MEG source reconstruction techniques, they identified the alpha frequency and parietal brain region which showed the strongest modulation by attention in each individual subject ([Fig 6.1A](#)). In a subsequent session, they applied TMS at the individual alpha frequency over the individual alpha generator in a combined

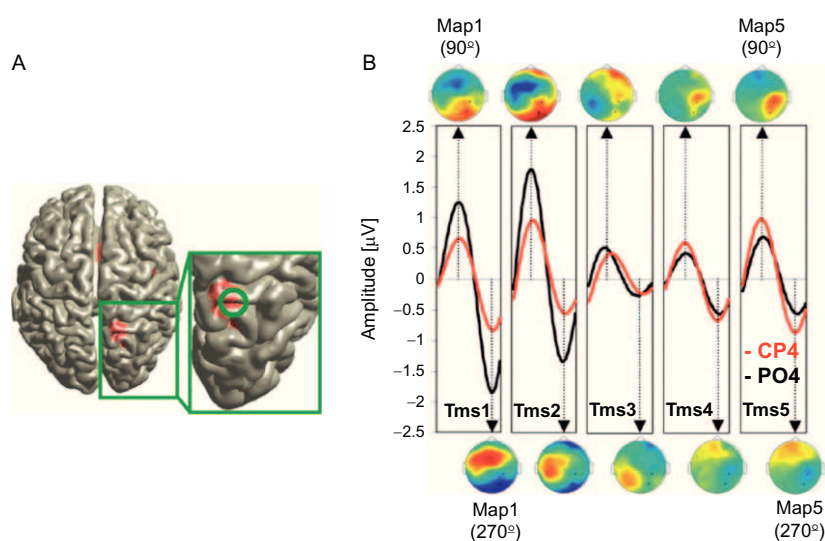


Figure 6.1 MEG-informed rhythmic TMS entrains endogenous alpha oscillations. (A) Beamformer reconstruction of the alpha source showing the strongest modulation by attention in the MEG experiment. The source was localized using group average data. (B) Sensor waveforms from EEG electrodes CP4 (red) and PO4 (black) evoked by each of five TMS pulses (TMS 1–5) delivered at individual alpha frequency. Heat maps show the topography of evoked activity at 90 °C (upper row) and 270 °C (lower row) of the alpha cycle. *From Thut et al. (2011).*

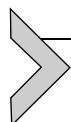
EEG–TMS experimental setup. They were able to show that on-going alpha oscillations can be externally entrained by rhythmic TMS (Fig 6.1B). This result is of importance as it points toward a new approach in neuromodulation which aims at modulating endogenous, on-going oscillatory activity.

The two studies reviewed above nicely demonstrate the advantages and limitations of MEG in combination with stimulation. Both studies used MEG to obtain individually adjusted stimulation parameters but then applied EEG to measure the immediate electrophysiological effects of TMS. In contrast to EEG, MEG allows high-density measurements with little preparation time, making MEG an optimal tool to perform quick localizer experiments. Moreover, MEG is often preferred over EEG for source localization because its localization accuracy depends to a lesser extent on the accuracy and complexity of the forward model (Leahy, Mosher, Spencer, Huang, & Lewine, 1998). However, the greatest strength of MEG is also its greatest drawback when used in combination with TMS. Simultaneous MEG–TMS recordings are rendered impossible by the extreme sensitivity of MEG to magnetic fields. Characterization of immediate TMS effects must therefore be performed by less sensitive devices. Combined EEG–TMS recordings have lately emerged as a powerful tool for this purpose (Thut & Miniussi, 2009).

2.2. MEG characterizes TMS effects

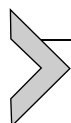
As discussed in the previous section, MEG is not suitable to evaluate the immediate neurophysiological effects of TMS. However, the lasting effects of repetitive TMS (rTMS) can be characterized by means of MEG. Depending on the frequency of stimulation, rTMS either decreases (1 Hz) or increases (≥ 5 Hz) cortical excitability (Siebner & Rothwell, 2003). The effect can outlast stimulation by several minutes (Peinemann et al., 2004). While motor evoked potentials are the standard output measure of excitability in the TMS literature, MEG studies have additionally investigated modulations of oscillatory activity. Tamura et al. (2005) found the postmovement rebound of motor cortical beta oscillations to be reduced after 1 Hz rTMS. Another study made use of intermittent theta burst TMS (iTBS), an excitability enhancing protocol (Hsu et al., 2011). Complementary to the results by Tamura et al., the study reported iTBS to increase postmovement beta synchronization. The same approach was used to study therapeutic effects of TMS. Lorenz, Müller, Schlee, Langguth, and Weisz (2010) recorded the

MEG of tinnitus patients after treatment by rTMS. They found the auditory steady state response to be reduced along with perceived tinnitus loudness.



3. MEG AND TRANSCRANIAL DIRECT OR ALTERNATE CURRENT STIMULATION

Characterization of lasting effects of neuromodulation by MEG is not limited to TMS. For example, MEG has been used to investigate the neurophysiological after-effects of transcutaneous electrical nerve stimulation (Hoshiyama & Kakigi, 2000; Murakami et al., 2010). Moreover, the approach will likely play an important role in unveiling the mechanisms by which both transcranial direct current stimulation (tDCS) and transcranial alternating current stimulation (tACS) modulate behavior. In particular, it may help to clarify whether and to what extent tACS affects endogenous oscillations. Currently, there is both evidence for (Marshall, Helgadóttir, Mölle, & Born, 2006; Kirov, Weiss, Siebner, Born, & Marshall, 2009; Zaehle, Rach, & Herrmann, 2010) and against (Antal et al., 2008) the notion that tACS can modulate brain oscillations to an extent that it affects behavior. In the future, tACS may be used with individually tailored parameters which may be provided by MEG recordings. This procedure may enable researchers to not only impose a rhythm on the stimulated areas but also to selectively enhance or reduce specific components of on-going oscillatory activity, much like rhythmic TMS (Thut et al., 2011). In this form, tACS might become a powerful therapeutic tool for the treatment of disorders which are characterized by abnormal synchronization, such as schizophrenia, epilepsy, or Parkinson's disease (PD; Schnitzler & Gross, 2005).



4. MEG AND DBS

DBS is an invasive electrical brain stimulation intervention routinely applied to treat symptoms of PD, essential tremor, dystonia, and several pain syndromes (Perlmutter & Mink, 2006). Further, it is being tested as a potential treatment for a variety of other disorders, such as depression, obsessive compulsive disorder, and Tourette syndrome. In DBS, macroelectrodes are implanted into the target area. The electrodes deliver current pulses generated by a subcutaneously implanted stimulator. Target area and stimulation parameters depend on the disorder which is treated. For treatment of PD,

the most common target is the subthalamic nucleus (STN), which is typically stimulated with a frequency of 130 Hz.

Despite intensive research, the mechanisms of action by which DBS alleviates PD symptoms are not finally understood. Invasive recordings in animal models and humans have identified inhibitory and excitatory effects of DBS as well as complex polysynaptic responses (Kringelbach, Jenkinson, Owen, & Aziz, 2007). Given that the clinical effect of DBS is similar to the effect of lesioning the STN (Bergman, Wichmann, & DeLong, 1990), it is often hypothesized that DBS acts by disrupting pathological activity. In fact, there is growing evidence that PD symptoms are correlated with or caused by pathological oscillatory activity which can be recorded in the STN and other basal ganglia nuclei (Brown, 2003). Further, it was shown that symptom-associated synchronization is not restricted to the basal ganglia but can be found within a wider network of cortical and subcortical areas (Timmermann et al., 2003; Pollok et al., 2008). Not surprisingly, growing interest in synchronized networks has motivated MEG studies addressing cortical synchronization with basal ganglia oscillations and combination of MEG and DBS.

4.1. Simultaneous MEG and local field potential recordings in PD patients

Much has been learned about PD pathophysiology by studying local field potentials (LFPs) recorded by DBS electrodes. It was revealed that STN activity of PD patients is characterized by strong beta oscillations (13–35 Hz) which are modulated by movement and dopaminergic medication (Brown et al., 2001; Kühn et al., 2004; Priori et al., 2004). Beta oscillations are phase–amplitude coupled to high frequency oscillations (>200 Hz) which are themselves dopamine responsive (López-Azcárate et al., 2010; Özkurt et al., 2011). Despite their substantial contribution to PD research, the insights gained through LFP recordings are limited. DBS electrodes record from only a small fraction of the spatially distributed motor network. In order to gain insights into network connectivity, LFP recordings need to be combined with multisensor recording techniques, such as whole head MEG or high-density EEG.

4.1.1 STN–cortical coupling

Several studies investigated STN–cortical coupling in PD patients selected for therapeutic DBS. Most of them analyzed coherence, a frequency-domain measure of similarity. Coherence measures the degree of linear

dependency between two signals. It quantifies to what degree two signals have a stable phase and amplitude relation over time. Coherence may arise when membrane potential fluctuations in two distant neuronal populations *A* and *B* are coordinated in time, for example, such that incoming action potentials from *A* reach *B* at the time of maximum excitability (Fries, 2005). In this case, population *A* would have maximum gain on population *B*. Note, however, that coherence analysis may yield the very same value when timing is such that action potentials from *A* reach *B* at the time of minimum excitability, as it merely captures the presence of any coordination in time.

EEG studies investigating coupling between STN LFPs and cortical activity showed that beta coherence is reduced by movement (Cassidy et al., 2002; Lalo et al., 2008) and found indications for a modulation by dopaminergic medication (Williams et al., 2002). Further, it was demonstrated that STN–cortical coherence has a frequency-dependent topography on the sensor level (Fogelson et al., 2006). However, the limited number of EEG channels precluded localization of coherence on the source level. Recently, localization of coherent sources was achieved by simultaneous recordings of LFPs and MEG (Hirschmann et al., 2011; Litvak et al., 2011). In two independent studies, Hirschmann et al. and Litvak et al. recorded PD patients at rest after withdrawal of dopaminergic medication and independently reported the same frequency-dependent spatial distribution of coherence (Fig. 6.2). STN–cortical beta coherence was found in medial sensorimotor and premotor cortex ipsilateral to the recorded STN. In contrast, alpha coherence localized to areas in ipsilateral temporal cortex and brainstem. In contrast to alpha coherence with temporal cortex, beta coherence with sensorimotor cortex was restricted to one or two bipolar contacts of the DBS electrode, suggesting a focal origin of coherent beta oscillations within the recording area of the electrode (Hirschmann et al., 2011). In summary, these studies revealed two distinct functional connections involving the STN which operate in distinct frequency bands. The results may hint at a general mechanism in communication between distant brain areas: Simultaneously on-going interactions involving the same anatomical structures might be distinguished by frequency.

Litvak et al. extended their analysis of MEG–LFP resting state coherence beyond the description of its spatial distribution (Litvak et al., 2011, 2012). They investigated causal interactions between STN and cortex and found motor cortex to drive STN in the beta band, in agreement with previous studies (Williams et al., 2002; Lalo et al., 2008). Thus, enhanced STN

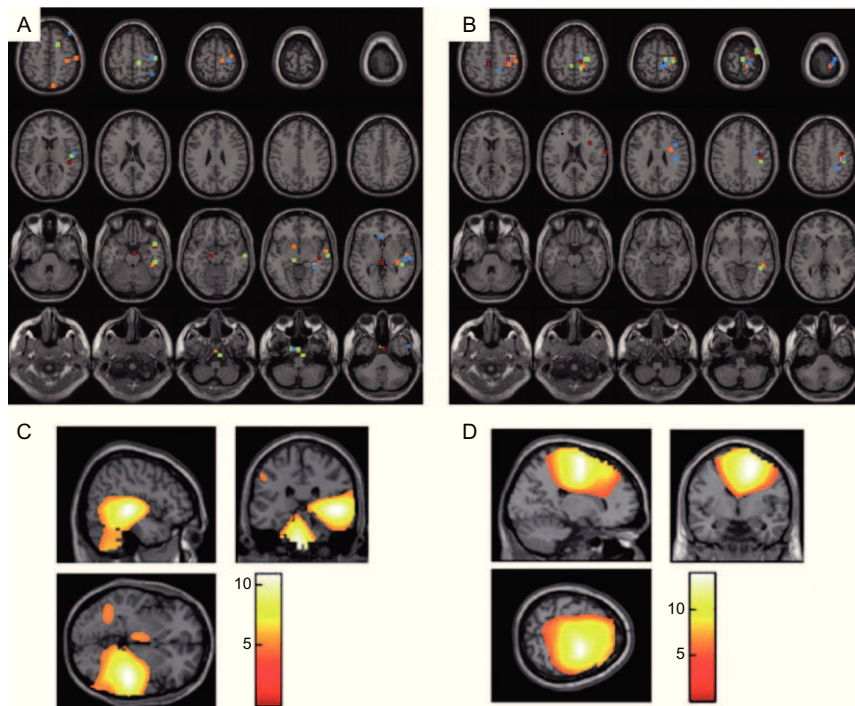


Figure 6.2 The spatial distribution of STN–cortical coherence is frequency dependent. *Upper row:* Distribution of spatial maxima of significant coherent sources. (A) Spatial maxima of alpha coherent sources from a group of eight bilateral implanted Parkinson's diseases patients. (B) Spatial maxima of beta coherent sources. Sources coherent to the left STN have been mirrored across the midsagittal plane. Colors code electrode contact pairs recording local field potentials, that is, the reference signal for coherence computations. Blue = channel 01 (most ventral), green = channel 12, orange = channel 23, and red = channel 03. From [Hirschmann et al. \(2011\)](#). *Lower row:* Statistical parametric maps (SPMs) showing the relative distribution of alpha and beta STN–cortical coherence. (C) SPM showing regions where alpha coherence is significantly higher than beta coherence. (D) SPM showing regions where beta coherence is significantly higher than alpha coherence. Color bars indicate t -statistic. From [Litvak et al. \(2011\)](#).

beta activity may have its origin in the cortex. In fact, high frequency optical stimulation of STN afferents from primary motor cortex (M1) was shown to effectively ameliorate motor symptoms in the rat model of PD ([Gradinaru, Mogri, Thompson, Henderson, & Deisseroth, 2009](#)), demonstrating the importance of STN–cortical pathways in PD pathophysiology. However, 20 Hz stimulation of STN afferents did not worsen PD symptoms,

suggesting that motor cortical input at beta frequencies may not be the cause of symptoms. On the contrary, a recent MEG–LFP study in PD patients found M1–STN beta coherence to be anticorrelated with akinesia, meaning that the highest coherence was found in patients with the least akinesia (Hirschmann et al., 2012). These results suggest that M1–STN beta coherence may be of physiological nature or serve compensation, rather than reflecting or causing slowing of movement. In combination, the studies summarized above indicate that the STN receives rhythmic input at beta frequencies from motor cortex. This input may not be pathological *per se*, but may be unusually amplified in the basal ganglia of PD patients, possibly due to increased circuit resonance resulting from dopamine depletion (Eusebio et al., 2009).

4.1.2 Modulation of STN–cortical coupling

To better understand the role of STN–cortical coupling in normal and impaired motor function, it is important to study its modulation by dopaminergic medication and voluntary movement. Recent research indicates that these two factors strongly interact. While administration of levodopa was reported to have no effect on STN–cortical coherence at rest (Litvak et al., 2011), it was found to modulate coupling during movement (Hirschmann et al., 2012; Litvak et al., 2012). Litvak et al. investigated the effect of levodopa administration on movement-related changes in M1–STN–cortical coherence (Litvak et al., 2012). They reported a short-lived increase of gamma band coherence at movement onset, which was intensified by administration of dopaminergic medication. The effect of medication was positively correlated with improvement of PD motor symptoms. Hirschmann et al. measured baseline levels of M1–STN coherence while subjects performed two different motor tasks and found coherence to be suppressed by levodopa in the beta band (Hirschmann et al., 2012). Thus, levodopa administration may specifically affect movement-related oscillatory coupling. Moreover, the studies discussed above provide further evidence for the antagonistic relationship between movement-related beta and gamma oscillations (Brown, 2003): Gamma activity is enhanced by movement and dopaminergic medication while beta activity is reduced.

4.1.3 Concluding remarks on simultaneous MEG and LFP recordings

The results reviewed above demonstrate how simultaneous LFP–MEG recordings can extend our knowledge about basic motor system neurophysiology and its pathological alterations. The interplay between DBS surgery and

MEG recordings is a good example of how basic research may profit from applied neuromodulation. In turn, neuromodulation relies on basic research. For example, LFP–MEG coherence analysis provides information on the functional connectivity of the DBS target. This information may help to explain some of the effects and side-effects of DBS and might contribute to the identification of new and better stimulation targets.

4.2. MEG characterizes DBS effects

In the studies discussed above, MEG has been combined with recordings from DBS electrodes. Other studies aimed at investigating the immediate neurophysiological effects of DBS and applied high frequency stimulation while recording MEG. As the magnetic fields induced by DBS may exceed physiological magnetic fields by several orders of magnitude, this experimental approach requires tools for artifact suppression. So far, two methods have been employed: beamforming and temporal signal space separation (tSSS).

4.2.1 DBS artifact suppression by beamforming

The term beamforming refers to the application of a spatial filter which lets activity from a selected location pass while blocking all other signals (Van Veen & Buckley, 1988). Over the past few years, beamforming has become an established method for source reconstruction in MEG research (Hillebrand, Singh, Holliday, Furlong, & Barnes, 2005). As it is designed to cancel interfering signals, beamforming provides implicit protection against artifacts. This property has previously been exploited to suppress artifacts which can arise in simultaneous LFP–MEG recordings (Litvak et al., 2010).

Early MEG–DBS studies made use of a beamforming variant called synthetic aperture magnetometry to study the effects of DBS in a small number of chronic pain patients (Kringelbach et al., 2007; Ray et al., 2007, 2009). These studies demonstrated the feasibility of measuring MEG during DBS and reported modulations of power in areas involved in pain sensation. Recently, the authors of this pioneering work refined their source reconstruction methodology by modifying the beamformer formulation to obtain a so-called null-beamformer (Mohseni et al., 2012). In null-beamforming, the constraints on spatial filtering are extended by the requirement to force output to zero for signals originating from a selected location (Van Veen & Buckley, 1988). Based on the observation that the entry points of DBS electrodes into the skull are a source of artifacts, the

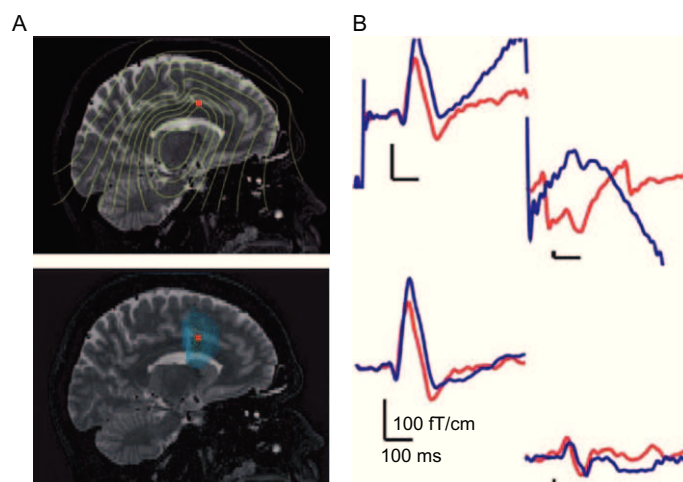


Figure 6.3 Methods for artifact suppression in MEG-DBS recordings. (A) The null-beamformer (lower row) provides better localization of a known source than a conventional beamformer (upper row) in MEG-DBS experiments. The red dot marks the location of the DBS electrode contact producing the 130 Hz activity which was localized for evaluation purposes. Contours indicate 130 Hz power. From [Mohseni et al. \(2012\)](#). (B) Auditory-evoked fields (AEFs) in two MEG sensors recorded during DBS ON (blue) and DBS OFF (red). The upper row shows AEFs before application of tSSS. The lower row shows AEFs in the same sensors after application of tSSS. From [Airaksinen et al. \(2011\)](#).

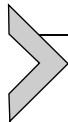
authors chose to suppress signals originating from burr holes. Using the null-beamformer, they analyzed data from a chronic pain patient implanted with electrodes for stimulation of the anterior cingulate cortex (ACC). They found the null-beamformer to be superior to conventional beamforming when localizing the source of high frequency stimulation for evaluation purposes ([Fig. 6.3A](#)). Further, they reported that DBS decreased theta power in caudal ACC, an area involved in pain sensation. Notably, the stimulation-induced power decrease in ACC was less strong when the experiment was repeated after 12 months, suggesting that chronic DBS triggered plasticity changes.

4.2.2 DBS artifact suppression by tSSS

Other studies have employed tSSS to suppress DBS artifacts. In contrast to beamforming, tSSS is not a source reconstruction method but a preprocessing procedure serving artifact suppression. tSSS is the temporal extension of signal space separation, a commercial algorithm which separates

the MEG signal into two subspaces: one for the sources inside the sensor array and one for interfering sources outside the array (Taulu & Kajola, 2005; Taulu & Simola, 2006). When the signal is reconstructed the latter are left out, resulting in suppression of external artifacts (Fig. 6.3B).

Mäkelä, Taulu, Pohjola, Ahonen, and Pekkonen (2007) first applied tSSS to analyze the effects of STN stimulation on MEG activity in a PD patient. They reported that DBS suppressed spontaneous sensorimotor activity in the 3–10 Hz range. This pilot experiment was followed by two group studies investigating the effects of DBS in PD patients (Airaksinen et al., 2011, Airaksinen et al., 2012). In the first study, subjects received auditory and somatosensory stimulations during DBS OFF and DBS ON (Airaksinen et al., 2011). It was found that DBS increased auditory-evoked fields ipsilateral to auditory stimulation. In the second study, the authors analyzed changes in oscillatory activity and correlated the latter to clinical ratings of PD motor symptom severity (Airaksinen et al., 2012). They reported that alpha and beta power in pericentral areas correlated positively with rigidity scores only when DBS was on, suggesting that DBS affects the behavioral relevance of oscillatory activity in sensorimotor cortex. However, patients were medicated in this study, so that the observed effects could not be attributed uniquely to DBS.



5. CONCLUSIONS AND OUTLOOK

We have provided several examples of how MEG may be used to inform and to evaluate different brain stimulation techniques, such as TMS or DBS. We have elaborated on the strengths of MEG but also discussed the artifacts which complicate combinations of MEG and stimulation. The future role of MEG in neuromodulation research will depend to a large extent on the development of methods for artifact suppression. Fortunately, much progress has been made. Algorithms such as tSSS and null-beamforming provide a promising basis for future research.

Provided that artifacts are handled efficiently, one of the greatest contributions of MEG to neuromodulation research will continue to be the analysis of stimulation effects on source level network activity. Although it is not trivial to reconstruct numerous simultaneously active sources based on MEG sensor data, MEG remains the best available, noninvasive method for investigation of synchronized networks in humans. In the future, network studies addressing coupling between all voxels in the brain will become more frequent and will provide important insights into large-scale connectivity

patterns (Schoffelen & Gross, 2011; Hillebrand, Barnes, Bosboom, Berendse, & Stam, 2012; Hipp, Hawellek, Corbetta, Siegel, & Engel, 2012). As a large body of evidence supports the importance of synchronized networks in normal and pathological brain function, it must be expected that effective brain stimulation, be it invasive or noninvasive, modifies these networks. Future studies will uncover such modifications and thereby extend our knowledge about the mechanisms of action of targeted brain stimulation. Most likely, MEG studies will make a significant contribution.

REFERENCES

- Airaksinen, K., Butorina, A., Pekkonen, E., Numminen, J., Taulu, S., Ahonen, A., et al. (2012). Somatomotor mu rhythm amplitude correlates with rigidity during deep brain stimulation in Parkinsonian patients. *Clinical Neurophysiology*, *123*, 2010–2017.
- Airaksinen, K., Mäkelä, J. P., Taulu, S., Ahonen, A., Nurminen, J., Schnitzler, A., et al. (2011). Effects of DBS on auditory and somatosensory processing in Parkinson's disease. *Human Brain Mapping*, *32*, 1091–1099.
- Antal, A., Boros, K., Poreisz, C., Chaieb, L., Terney, D., & Paulus, W. (2008). Comparatively weak after-effects of transcranial alternating current stimulation (tACS) on cortical excitability in humans. *Brain Stimulation*, *1*, 97–105.
- Barnes, G. R., Hillebrand, A., Fawcett, I. P., & Singh, K. D. (2004). Realistic spatial sampling for MEG beamformer images. *Human Brain Mapping*, *23*, 120–127.
- Barr, M. S., Farzan, F., Wing, V. C., George, T. P., Fitzgerald, P. B., & Daskalakis, Z. J. (2011). Repetitive transcranial magnetic stimulation and drug addiction. *International Review of Psychiatry*, *23*, 454–466.
- Bergman, H., Wichmann, T., & DeLong, M. R. (1990). Reversal of experimental parkinsonism by lesions of the subthalamic nucleus. *Science*, *249*, 1436–1438.
- Brown, P. (2003). Oscillatory nature of human basal ganglia activity: Relationship to the pathophysiology of Parkinson's disease. *Movement Disorders*, *18*, 357–363.
- Brown, P., Oliviero, A., Mazzone, P., Insola, A., Tonali, P., & Di Lazzaro, V. (2001). Dopamine dependency of oscillations between subthalamic nucleus and pallidum in Parkinson's disease. *The Journal of Neuroscience*, *21*, 1033–1038.
- Cassidy, M., Mazzone, P., Oliviero, A., Insola, A., Tonali, P., Di Lazzaro, V., et al. (2002). Movement-related changes in synchronization in the human basal ganglia. *Brain*, *125*, 1235–1246.
- Corti, M., Patten, C., & Triggs, W. (2012). Repetitive transcranial magnetic stimulation of motor cortex after stroke: A focused review. *American Journal of Physical Medicine & Rehabilitation*, *91*, 254–270.
- Croarkin, P. E., Wall, C. A., & Lee, J. (2011). Applications of transcranial magnetic stimulation (TMS) in child and adolescent psychiatry. *International Review of Psychiatry*, *23*, 445–453.
- Eusebio, A., Pogosyan, A., Wang, S., Averbek, B., Gaynor, L. D., Cantiniaux, S., et al. (2009). Resonance in subthalamo-cortical circuits in Parkinson's disease. *Brain*, *132*, 2139–2150.
- Fogelson, N., Williams, D., Tijssen, M., van Bruggen, G., Speelman, H., & Brown, P. (2006). Different functional loops between cerebral cortex and the subthalamic area in Parkinson's disease. *Cerebral Cortex*, *16*, 64–75.

- Fries, P. (2005). A mechanism for cognitive dynamics: Neuronal communication through neuronal coherence. *Trends in Cognitive Sciences*, 9, 474–480.
- Gradinaru, V., Mogri, M., Thompson, K. R., Henderson, J. M., & Deisseroth, K. (2009). Optical deconstruction of Parkinsonian neural circuitry. *Science*, 324, 354–359.
- Hämäläinen, M., Hari, R., Ilmoniemi, R. J., Knuutila, J., & Lounasmaa, O. V. (1993). Magnetoencephalography—Theory, instrumentation, and applications to noninvasive studies of the working human brain. *Reviews of Modern Physics*, 65, 413–497.
- Hillebrand, A., Barnes, G. R., Bosboom, J. L., Berendse, H. W., & Stam, C. J. (2012). Frequency-dependent functional connectivity within resting-state networks: An atlas-based MEG beamformer solution. *NeuroImage*, 59, 3909–3921.
- Hillebrand, A., Singh, K. D., Holliday, I. E., Furlong, P. L., & Barnes, G. R. (2005). A new approach to neuroimaging with magnetoencephalography. *Human Brain Mapping*, 25, 199–211.
- Hipp, J. F., Hawellek, D. J., Corbetta, M., Siegel, M., & Engel, A. K. (2012). Large-scale cortical correlation structure of spontaneous oscillatory activity. *Nature Neuroscience*, 15, 884–890.
- Hirschmann, J., Özkurt, T. E., Butz, M., Homburger, M., Elben, S., Hartmann, C. J., et al. (2011). Distinct oscillatory STN-cortical loops revealed by simultaneous MEG and local field potential recordings in patients with Parkinson's disease. *NeuroImage*, 55, 1159–1168.
- Hirschmann, J., Özkurt, T. E., Butz, M., Homburger, M., Elben, S., Hartmann, C. J., et al. (2012). Differential modulation of STN-cortical and cortico-muscular coherence by movement and levodopa in Parkinson's disease. In Press.
- Hoshiyama, M., & Kakigi, R. (2000). After-effect of transcutaneous electrical nerve stimulation (TENS) on pain-related evoked potentials and magnetic fields in normal subjects. *Clinical Neurophysiology*, 111, 717–724.
- Hsu, Y.-F., Liao, K.-K., Lee, P.-L., Tsai, Y.-A., Yeh, C.-L., Lai, K.-L., et al. (2011). Intermittent theta burst stimulation over primary motor cortex enhances movement-related beta synchronisation. *Clinical Neurophysiology*, 122, 2260–2267.
- Kirov, R., Weiss, C., Siebner, H. R., Born, J., & Marshall, L. (2009). Slow oscillation electrical brain stimulation during waking promotes EEG theta activity and memory encoding. *PNAS*, 106, 15460–15465.
- Kringelbach, M. L., Jenkinson, N., Green, A. L., Owen, S. L. F., Hansen, P. C., Cornelissen, P. L., et al. (2007). Deep brain stimulation for chronic pain investigated with magnetoencephalography. *Neuroreport*, 18, 223–228.
- Kringelbach, M. L., Jenkinson, N., Owen, S. L. F., & Aziz, T. Z. (2007). Translational principles of deep brain stimulation. *Nature Reviews. Neuroscience*, 8, 623–635.
- Kühn, A. A., Williams, D., Kupsch, A., Limousin, P., Hariz, M., Schneider, G.-H., et al. (2004). Event-related beta desynchronization in human subthalamic nucleus correlates with motor performance. *Brain*, 127, 735–746.
- Lalo, E., Thobois, S., Sharott, A., Polo, G., Mertens, P., Pogosyan, A., et al. (2008). Patterns of bidirectional communication between cortex and basal ganglia during movement in patients with Parkinson disease. *The Journal of Neuroscience*, 28, 3008–3016.
- Leahy, R., Mosher, J., Spencer, M., Huang, M., & Lewine, J. (1998). A study of dipole localization accuracy for MEG and EEG using a human skull phantom. *Electroencephalography and Clinical Neurophysiology*, 107, 159–173.
- Litvak, V., Eusebio, A., Jha, A., Oostenveld, R., Barnes, G., Foltynie, T., et al. (2012). Movement-related changes in local and long-range synchronization in Parkinson's disease revealed by simultaneous magnetoencephalography and intracranial recordings. *The Journal of Neuroscience*, 32, 10541–10553.
- Litvak, V., Eusebio, A., Jha, A., Oostenveld, R., Barnes, G. R., Penny, W. D., et al. (2010). Optimized beamforming for simultaneous MEG and intracranial local field potential recordings in deep brain stimulation patients. *NeuroImage*, 50, 1578–1588.

- Litvak, V., Jha, A., Eusebio, A., Oostenveld, R., Foltynie, T., Limousin, P., et al. (2011). Resting oscillatory cortico-subthalamic connectivity in patients with Parkinson's disease. *Brain*, *134*, 359–374.
- López-Azcárate, J., Tainta, M., Rodríguez-Oroz, M. C., Valencia, M., González, R., Guridi, J., et al. (2010). Coupling between beta and high-frequency activity in the human subthalamic nucleus may be a pathophysiological mechanism in Parkinson's disease. *The Journal of Neuroscience*, *30*, 6667–6677.
- Lorenz, I., Müller, N., Schlee, W., Langguth, B., & Weisz, N. (2010). Short-term effects of single repetitive TMS sessions on auditory evoked activity in patients with chronic tinnitus. *Journal of Neurophysiology*, *104*, 1497–1505.
- Mäkelä, J. P., Taulu, S., Pohjola, J., Ahonen, A., & Pekkonen, E. (2007). Effects of subthalamic nucleus stimulation on spontaneous sensorimotor MEG activity in a Parkinsonian patient. *International Congress Series*, *1300*, 345–348.
- Marshall, L., Helgadóttir, H., Mölle, M., & Born, J. (2006). Boosting slow oscillations during sleep potentiates memory. *Nature*, *444*, 610–613.
- Mohseni, H. R., Smith, P. P., Parsons, C. E., Young, K. S., Hyam, J. A., Stein, A., et al. (2012). MEG can map short and long-term changes in brain activity following deep brain stimulation for chronic pain. *PLoS One*, *7*, e37993.
- Murakami, T., Takino, R., Ozaki, I., Kimura, T., Iguchi, Y., & Hashimoto, I. (2010). High-frequency transcutaneous electrical nerve stimulation (TENS) differentially modulates sensorimotor cortices: An MEG study. *Clinical Neurophysiology*, *121*, 939–944.
- Özkurt, T. E., Butz, M., Homburger, M., Elben, S., Vesper, J., Wojtecki, L., et al. (2011). High frequency oscillations in the subthalamic nucleus: A neurophysiological marker of the motor state in Parkinson's disease. *Experimental Neurology*, *229*, 324–331.
- Pascual-Leone, A., Bartres-Faz, D., & Keenan, J. P. (1999). Transcranial magnetic stimulation: Studying the brain-behaviour relationship by induction of "virtual lesions" *Philosophical Transactions of the Royal Society of London. Series B, Biological Sciences*, *354*, 1229–1238.
- Peinemann, A., Reimer, B., Löer, C., Quartarone, A., Münchau, A., Conrad, B., et al. (2004). Long-lasting increase in corticospinal excitability after 1800 pulses of subthreshold 5 Hz repetitive TMS to the primary motor cortex. *Clinical Neurophysiology*, *115*, 1519–1526.
- Perlmutter, J. S., & Mink, J. W. (2006). Deep brain stimulation. *Annual Review of Neuroscience*, *29*, 229–257.
- Pollok, B., Makhlofi, H., Butz, M., Gross, J., Timmermann, L., Wojtecki, L., et al. (2008). Levodopa affects functional brain networks in Parkinsonian resting tremor. *Movement Disorders*, *24*, 91–98.
- Priori, A., Foffani, G., Pesenti, A., Tamma, F., Bianchi, A. M., Pellegrini, M., et al. (2004). Rhythm-specific pharmacological modulation of subthalamic activity in Parkinson's disease. *Experimental Neurology*, *189*, 369–379.
- Raj, T., Karhu, J., Kicić, D., Lioumis, P., Julkunen, P., Lin, F.-H., et al. (2008). Parallel input makes the brain run faster. *NeuroImage*, *40*, 1792–1797.
- Ray, N. J., Jenkinson, N., Kringelbach, M. L., Hansen, P. C., Pereira, E. A., Brittain, J. S., et al. (2009). Abnormal thalamocortical dynamics may be altered by deep brain stimulation: Using magnetoencephalography to study phantom limb pain. *Journal of Clinical Neuroscience*, *16*, 32–36.
- Ray, N., Kringelbach, M., Jenkinson, N., Owen, S., Davies, P., Wang, S., et al. (2007). Using magnetoencephalography to investigate brain activity during high frequency deep brain stimulation in a cluster headache patient. *Biomedical Imaging and Intervention Journal*, *3*, e25.
- Schnitzler, A., & Gross, J. (2005). Normal and pathological oscillatory communication in the brain. *Nature Reviews. Neuroscience*, *6*, 285–296.

- Schoffelen, J.-M., & Gross, J. (2011). Improving the interpretability of all-to-all pairwise source connectivity analysis in MEG with nonhomogeneous smoothing. *Human Brain Mapping, 32*, 426–437.
- Siebner, H., & Rothwell, J. (2003). Transcranial magnetic stimulation: New insights into representational cortical plasticity. *Experimental Brain Research, 148*, 1–16.
- Tamura, Y., Hoshiyama, M., Nakata, H., Hiroe, N., Inui, K., Kaneoke, Y., et al. (2005). Functional relationship between human rolandic oscillations and motor cortical excitability: An MEG study. *The European Journal of Neuroscience, 21*, 2555–2562.
- Taulu, S., & Kajola, M. (2005). Presentation of electromagnetic multichannel data: The signal space separation method. *Journal of Applied Physics, 97*, 124905–124910.
- Taulu, S., & Simola, J. (2006). Spatiotemporal signal space separation method for rejecting nearby interference in MEG measurements. *Physics in Medicine and Biology, 51*, 1759–1768.
- Thut, G., & Miniussi, C. (2009). New insights into rhythmic brain activity from TMS–EEG studies. *Trends in Cognitive Sciences, 13*, 182–189.
- Thut, G., Veniero, D., Romei, V., Miniussi, C., Schyns, P., & Gross, J. (2011). Rhythmic TMS causes local entrainment of natural oscillatory signatures. *Current Biology, 21*, 1176–1185.
- Timmermann, L., Gross, J., Dirks, M., Volkman, J., Freund, H.-J., & Schnitzler, A. (2003). The cerebral oscillatory network of parkinsonian resting tremor. *Brain, 126*, 199–212.
- Van Veen, B. D., & Buckley, K. M. (1988). Beamforming: A versatile approach to spatial filtering. *IEEE ASSP Magazine, 5*, 4–24.
- Williams, D., Tijssen, M., Van Bruggen, G., Bosch, A., Insola, A., Di Lazzaro, V., et al. (2002). Dopamine-dependent changes in the functional connectivity between basal ganglia and cerebral cortex in humans. *Brain, 125*, 1558–1569.
- Zaehle, T., Rach, S., & Herrmann, C. S. (2010). Transcranial alternating current stimulation enhances individual alpha activity in human EEG. *PloS One, 5*, e13766.